Functional Analysis of the Zebrafish Dorsal Organizer

Maria Leonor Tavares Saúde

Thesis submitted to the University of London

for the degree of Doctor of Philosophy

National Institute for Medical Research

The Ridgeway, Mill Hill

London NW7 1AA

April 2001

ProQuest Number: 10014904

All rights reserved

INFORMATION TO ALL USERS
The quality of this reproduction is dependent upon the quality of the copy submitted.

In the unlikely event that the author did not send a complete manuscript
and there are missing pages, these will be noted. Also, if material had to be removed,
a note will indicate the deletion.
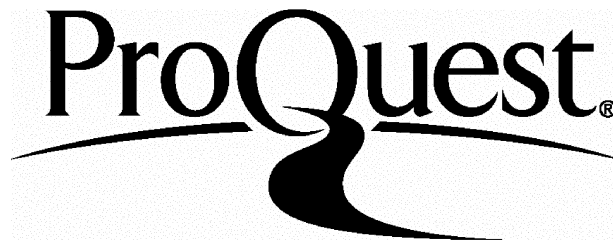
ProQuest 10014904

Published by ProQuest LLC(2016). Copyright of the Dissertation is held by the Author.

ProQuest LLC
789 East Eisenhower Parkway
P.O. Box 1346
Ann Arbor, MI 48106-1346

Abstract

The Spemann's organizer is a region of the amphibian gastrula that will induce a second body axis when transplanted to ventral or lateral regions of a host embryo. The organizer can dorsalise mesoderm, induce convergent extension movements and specify neuroectoderm. Functional equivalents of the Spemann's organizer have been identified in other vertebrates by transplantation experiments. A region of the fish gastrula called the embryonic shield is thought to function as the dorsal organizer. Using a novel surgical method, I showed that the morphological shield can induce complete secondary axes when transplanted into the ventral germ ring of a host embryo. In induced secondary axes, the donor shield contributed to hatching gland, prechordal plate, notochord, floor plate and hypochord. When explanted shields were divided into deep and superficial fragments and separately transplanted, I found that deep tissue can induce ectopic axes with heads but lacking posterior tissues. I found that when only the morphological shield was removed, embryos recovered and were completely normal by 24 hours-post-fertilisation. Ablation of the morphological shield does not remove all *goosecoid-* and *floating head*-expressing cells, suggesting that the morphological shield does not comprise the entire organizer region. Removal of the morphological shield plus adjacent marginal tissue, however, led to loss of all shield derivatives, a cyclopean head, loss of floor plate and primary motorneurons and disrupted somite patterning. Embryos from which only the morphological shield was removed still had some *goosecoid-* and *floating head*-expressing cells. I have tested whether these residual shield cells were sufficient to form all shield derivatives or, alternatively, if adjacent non-shield tissues could be recruited to shield fate. After morphological shield removal, I found no increase in cell proliferation. Transplantation studies indicated, however, that non-shield tissue may be recruited to a shield fate. Finally, I have employed the shield removal and transplantation method to study two mutations: *sneezy* and *silberblick/wnt11*. Transplantation results indicate that *sneezy* acts autonomously within the shield derivatives. By contrast, *silberblick/wnt11* acts non-autonomously in paraxial tissues to drive the convergent extension movement of axial mesoderm.

À Rosinha, ao Joaquim, ao Raúl e ao António

Acknowledgements

First and foremost, I would like to thank my supervisor, Derek Stemple, for his guidance, encouragement and constant good humour throughout my time in Mill Hill.

Thank you Ben Feldman, Mike Parsons, Carl-Philipp Heisenberg, Pedro Coutinho, Isabel Campos, Richard Gibbons, Steve Pollard and Albert Geishauser for your help and advice and for making the laboratory a great and fun place to work.

To Josh Brickman, Juan Pedro Martinez-Barbera, Masa Tada and Jonathan Cooke I wish to thank for the interest in my research and their critical advice.

I am grateful to Ben Feldman, Carl-Philipp Heisenberg, Pedro Domingos, Pedro Coutinho, Rita de Sousa Nunes and above all to Mike Parsons for critical reading parts of this manuscript.

I am indebted to the Fundação para a Ciência e Tecnologia – Programa Praxis XXI for the financial support and to the National Institute for Medical Research for the excellent working conditions.

Table of Contents

List of Figures

List of Tables

Publications

The work described in this thesis contributed to the following publications:

Saúde L., Woolley K., Martin P., Driever W. and Stemple D. L (2000). Axis-Inducing Activities and Cell Fates of the Zebrafish Organizer. Development *127*, 3407-17.

Heisenberg C-P., Tada M., Rauch G-J., Saúde L., Concha M. L., Geisler R., Stemple D. L., Smith J. C. and Wilson S. W (2000). Silberblick/Wnt11 Mediates Convergent Extension Movements During Zebrafish Gastrulation. Nature *405*, 76 – 81.

Chapter 1

General Introduction

Here, I review studies which address early stages of zebrafish, *Xenopus*, chick and mouse development, in particular the formation of the dorsal organizer and its involvement in neural induction and patterning. The study of several model organisms offers complementary embryological, molecular and genetic approaches, allowing a more comprehensive understanding of mechanisms of development. For example, the *Xenopus* embryo is particularly useful to analyse the effects of over-expression of a gene, antisense oligonucleotides and dominant-negative proteins. The large and flat chick embryo allows position-specific surgical manipulations. The genetics of mouse and zebrafish give researchers a powerful tool to analyse the effects of loss of gene function and interactions among genes. The studies reviewed here reveal that despite the high degree of conservation at the genetic level throughout evolution, different vertebrates display remarkable differences in the timing of developmental processes and expression patterns of their regulatory genes.

1.1. Gastrulation, a conserved process in vertebrates

Before gastrulation begins, embryos from various vertebrate species are physically very different (Fig. 1.1A). The overall form of a vertebrate embryo is determined by a variety of factors, such as the amount of yolk in the egg or the development of specialised structures to facilitate nutrient exchange. Zebrafish and chick embryos sit on top of a large yolk, which apparently makes no cellular contribution to the embryo proper. By contrast, every cell of a pre-gastrula *Xenopus* embryo carries some amount of yolk. Embryonic mice do not possess yolk, instead are surrounded by extraembryonic tissues such as the placenta, the umbilical cord and the yolk sac (reviewed in Wolpert, 1998).
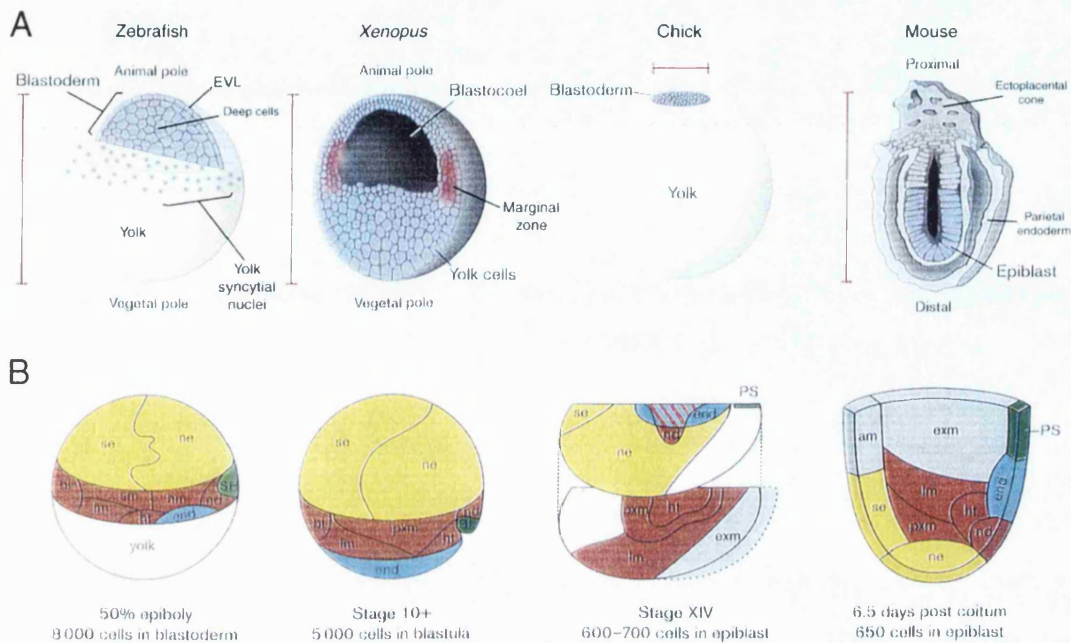
Fig. 1.1. (A) Morphology and size of vertebrate model organisms before gastrulation. Scale bars: zebrafish, 800-900 μm; *Xenopus*, 1-2 mm; chick, 2-3 mm; mouse, 700 μm. **(B) Fate maps of vertebrate model systems at early gastrulation.** Zebrafish and *Xenopus* embryos are represented with dorsal to the right. Chick and mouse embryos are represented with posterior to the right. The representation of the chick embryo shows separate images of the different overlaying layers of the blastoderm. There are differences in the proportion of tissues assigned to the various tissue types, in particular the neural tissues. The overlap of tissue types also varies between the vertebrate model organisms, for example the endoderm precursors. Ectoderm, yellow; mesoderm, red; endoderm, blue; organizer, green; extraembryonic tissues, grey. SH, embryonic shield; BL, blastopore lip; PS, early primitive streak. Ectodermal tissues: ne, neuroectoderm; se, surface ectodem. Mesodermal tissues: pxm, paraxial mesoderm; hm, head mesoderm; sm, somites; lm, lateral mesoderm; nd, notochord; ht, heart; bl, blood. Endodermal tissues: end, gut endoderm. Extraembryonic tissues: am, amnion ectoderm; exm, extraembryonic mesoderm. After Tam and Quilan, 1996.

Fate map studies illustrate the complexity of gastrulation movements. Such studies have revealed variations among vertebrate species (Fig. 1.1B). Nevertheless, the fate of cells in equivalent embryonic positions following gastrulation is similar, thus strengthening the idea that body patterning is conserved in vertebrate species (reviewed in Tam and Quilan, 1996). The morphogenetic movements that occur during gastrulation transform the epithelial monolayered embryo into a multilayered one, consisting of three germ layers, the ectoderm, the mesoderm and the endoderm. In general terms, the ectoderm will form epidermis and neural tissue, the mesoderm will give rise to muscle, bone and vasculature and the endoderm will make the gut. The cell movement strategy employed by the embryos of different vertebrate species varies from inward migration of cells along the entire periphery of the blastoderm in zebrafish and the blastopore in *Xenopus*, to cells ingressing into the primitive streak in chick and mouse (reviewed in Tam and Quilan, 1996). Independent of the gastrulation strategy used, cell movements and rearrangements will position cells to the correct place to receive the appropriate signals at the right time.

1.1.1. The zebrafish embryo

In zebrafish, the mid-blastula transition (MBT) begins approximately 4 hours-post-fertilisation (hpf) and marks the onset of zygotic transcription. At that stage, three cell populations can be distinguished (Fig. 1.1A). The yolk syncytial layer (YSL), the enveloping layer (EVL) and the deep cells. The YSL is formed between the ninth to the tenth cell cycle, when nuclei from the leading edge of the blastoderm collapse into the yolk cell, creating a ring of nuclei just beneath the blastoderm. The EVL is an epithelial sheet of one cell thick in the most superficial part of the blastoderm. The EVL will form a protective cover called the periderm, an extraembryonic structure that will disappear later in development. The deep cells are located between the YSL and the EVL and will give rise to the embryo proper (reviewed in Kimmel et al., 1995; Solnica-Krezel et al., 1995).
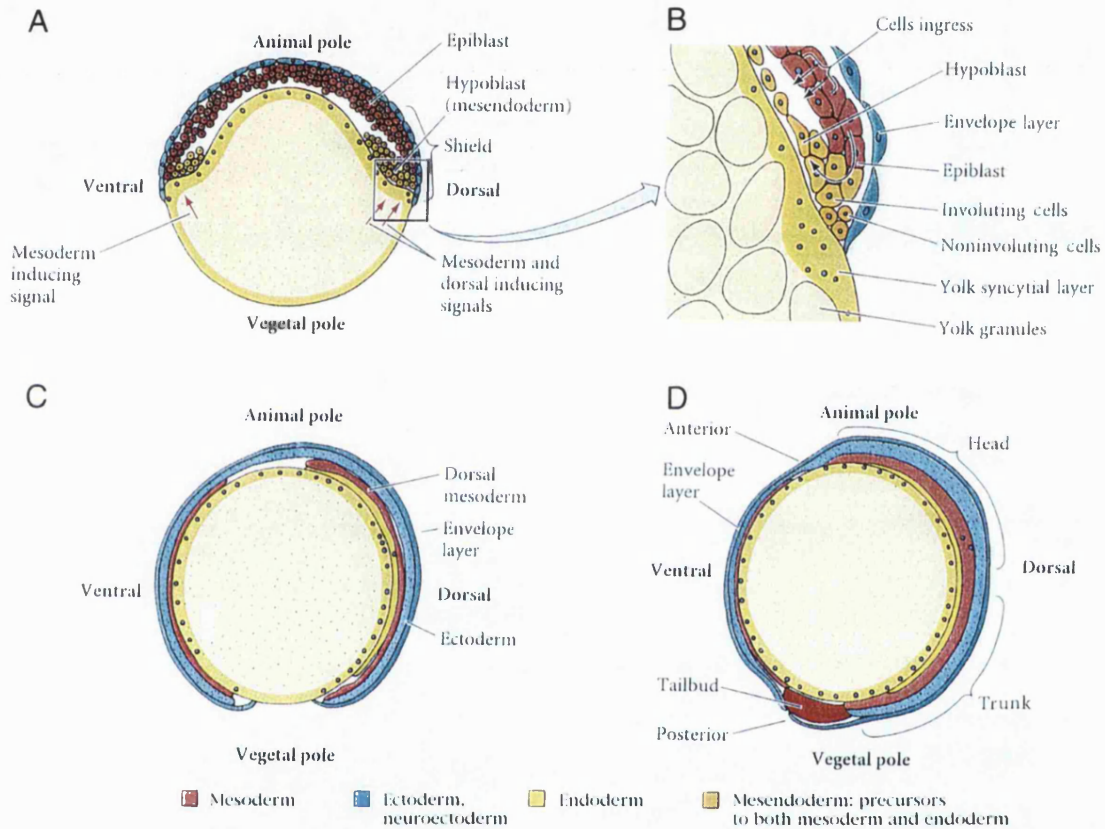
Fig. 1.2. Gastrulation in the zebrafish embryo. (A) When the embryo reaches 50% epiboly, the hypoblast forms by involution of cells at the margin of the blastoderm. **(B)** Close-up of the dorsal marginal region where the embryonic shield forms. **(C)** At 90% epiboly the mesoderm layer has migrated anteriorly and is located between the ectoderm and the endoderm. Epiboly movements bring the embryo layers towards the vegetal pole. **(D)** Gastrulation is completed at the tailbud stage. After Gilbert, 2000.

There are four gastrulation movements that occur in zebrafish embryos, epiboly, involution, convergence and extension. Epiboly is a process in which the blastoderm spreads along the yolk cell towards the vegetal pole. Epiboly continues until the entire yolk cell is covered. Involution starts at 50% epiboly (approximately at 5 hpf), when the blastoderm has covered half of the yolk cell (Fig. 1.2). At this point, cells at the leading edge of the blastoderm move inwards over the yolk cell along the entire margin, forming the germ ring. Hence, the germ ring is composed of two layers. The upper layer is known as the epiblast and the inner layer is called the hypoblast. The hypoblast will give rise to mesoderm and endoderm, while the non-involuted epiblast cells will form ectoderm. Cells in both layers converge to the future dorsal side of the embryo, forming a local thickening called the embryonic shield. As cells converge to the midline they also undergo mediolateral intercalation. The combination of convergence with mediolateral intercalation results in the extension of the embryo along an anterior-posterior direction. Gastrulation is essentially complete by 10 hpf when the embryo reaches the tailbud stage (reviewed in Kimmel et al., 1995; Solnica-Krezel et al., 1995).

1.1.2. The *Xenopus* embryo

Xenopus gastrulation is first visible at stage 10, when a group of marginal endoderm cells, the bottle cells, invaginate forming the dorsal blastopore (Fig. 1.3). This occurs at the future dorsal side of the embryo, just below the equator, in the region called the dorsal marginal zone. Bottle cells constitute the leading edge of a newly formed cavity, the archenteron. Led by the bottle cells, the prospective endodermal surface leaves the blastopore and migrates into a cavity, the blastocoel, just beneath the surface ectoderm. This movement is followed by the involution of mesodermal precursors through the blastopore lip. The most dorsal marginal zone cells involute first and will give rise to axial mesoderm and then the ventral marginal zone cells involute last from more lateral to ventral positions. Convergence and extension movements in
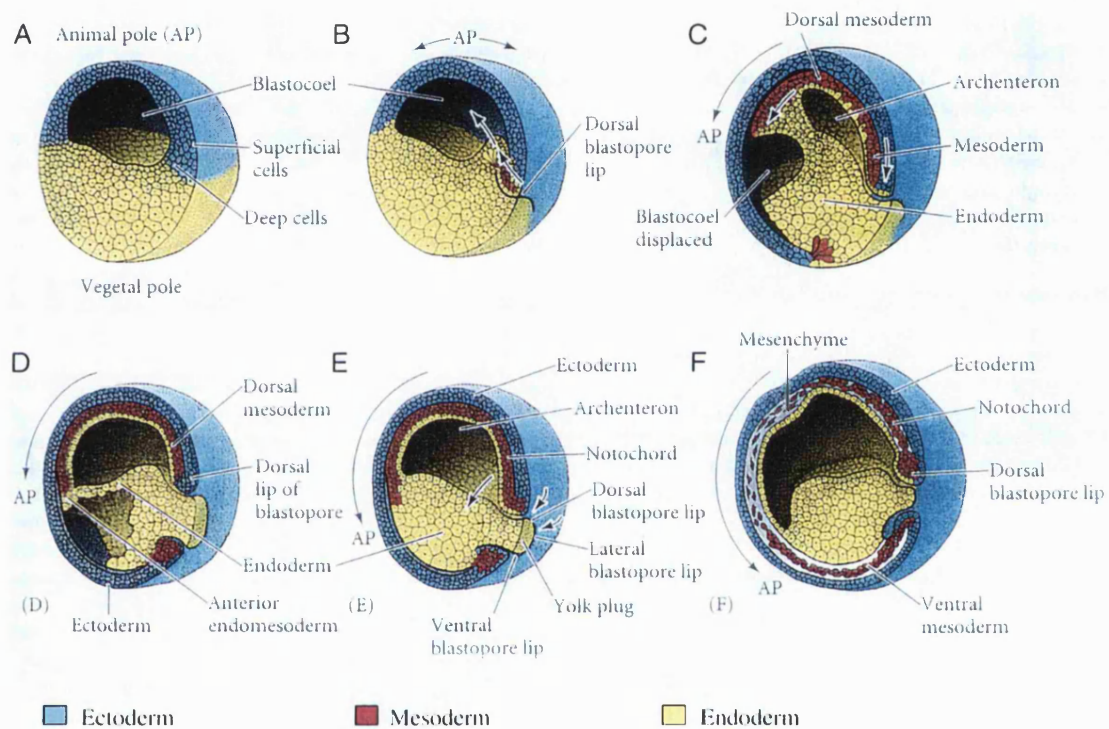
Fig. 1.3. Cell movements during *Xenopus* gastrulation. (A, B) Early gastrulation stages. The bottle cells move inside the embryo and the dorsal lip forms. The mesodermal precursors move under the roof of the blastopore. (C, D) Mid-gastrulation stages. Cells migrate from the lateral and ventral lips of the blastopore into the embryo. Cells of the animal pole migrate towards the vegetal pole. (E, F) The blastocoel disappears, the embryo is surrounded by ectoderm, the endoderm is internalised and the mesoderm is located between the ectoderm and the endoderm. After Gilbert, 2000.

the dorsal side of the embryo reorganise the marginal zone cells along the dorsal midline. The mediolateral intercalation of these cells causes elongation of the dorsal midline, in a direction perpendicular to the movement of individual cells. The extension of the dorsal midline drives the archenteron forward towards the future anterior end of the embryo and drives the blastopore lip backwards over the yolk mass. The animal cap and the non-involuting marginal zone cells will give rise to the ectoderm and by the end of gastrulation (stage 12) would have covered the entire embryo through a process called epiboly (reviewed in Gilbert, 2000; Sive et al., 2000).

1.1.3. The chick embryo

Before gastrulation, the chick blastoderm is a flat circular disc of cells consisting of an inner *area pellucida* and an outer *area opaca* (Fig. 1.4). Most of the cells in the *area pellucida* remain at the surface and form the epiblast, while other cells delaminate and migrate into the subgerminal cavity to form islands of primary hypoblast at stage X (Eyal-Giladi et al., 1992). The cells of these islands are then joined by cells that migrate anteriorly from the posterior margin of the blastoderm (posterior marginal zone and Koller's sickle), thus forming the secondary hypoblast at stage XII (Pasteels, 1945). The avian embryo originates from the epiblast, while the hypoblast will later be swept to the periphery and will not contribute to the embryo proper.

The first visible sign of gastrulation in the chick is the formation of the primitive streak, which could be regarded as the equivalent of the amphibian blastopore (Fig. 1.4). This structure is first visible as a thickened region consisting of mesenchymal cells ventral to the epiblast, just anterior to Koller's sickle . The thickening is the result of ingression of endodermal precursors into the blastocoel and the migration of lateral cells in the posterior epiblast towards the centre. As the cells enter the primitive streak, it elongates towards the future head region. When the primitive streak is formed, some of the epiblast cells start to migrate laterally, between non-ingressed epiblast and the secondary hypoblast, to form the lateral plates. At the same time, cells in the anterior primitive

8
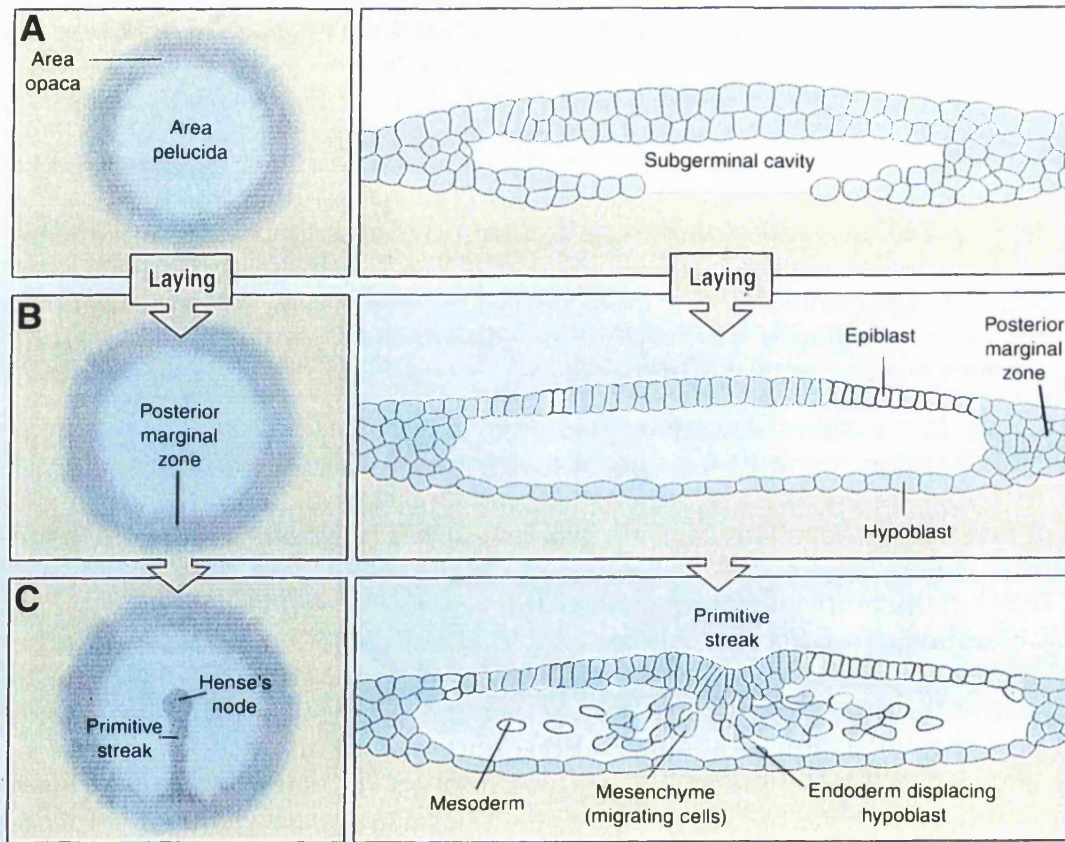
Fig. 1.4. Gastrulation in the chick embryo. (A) The blastoderm that overlies the subgerminal cavity is called area pellucida and the marginal region is called the area opaca. **(B)** The primary hypoblast forms from cells that migrate from the posterior marginal zone. **(C)** Gastrulation starts with the formation of the primitive streak. Future mesoderm and endoderm cells ingress through the primitive streak into the interior of the blastoderm. After Wolpert, 1998.

streak ingress, displacing the secondary hypoblast, and give rise to the definitive endoderm. As the primitive streak elongates anteriorly, a regional thickening of cells, defined as Hensen's node, forms at the tip of the primitive streak. Simultaneously, prospective prechordal plate mesendoderm and notochord cells start to leave this area, forming the head process (HH stage 4+; Hamburger and Hamilton, 1951). Next, the primitive streak stars to regress, leaving behind somitic, intermediate and lateral mesodermal precursors (reviewed in Bellairs and Osmond, 1998; Gilbert, 2000).

1.1.4. The mouse embryo

Prior to implantation, the mouse embryo consists of two cell types, which together form the blastocyst. An outer layer, called the trophoectoderm, surrounds a spherical cavity called the blastocoel. On the inside of the trophoectoderm resides the inner cell mass (ICM). These cells are pluripotent and will give rise to all embryonic tissues. At about the time of implantation, the visceral endoderm differentiates from the blastocoelic surface of the ICM and will contribute to the extraembryonic visceral yolk sac. After implantation, the ICM grows rapidly and fills the blastocoelic cavity. Then it epithelialises into a layer of epiblast cells surrounding the proamniotic cavity. The mouse embryo acquires a cup shape consisting of two layers, the inner epiblast and the outer visceral endoderm (Fig. 1.5). Prior to gastrulation, the visceral endoderm cells located at the distal tip of the egg cylinder move to the future anterior of the embryo to overlay the region of the epiblast fated to form the anterior neuroectoderm.

Gastrulation begins with the formation of the primitive streak (Fig. 1.5). The primitive streak arises on the future posterior side of a 6.5 days-post-coitum (dpc) embryo, at the junction between embryonic and extraembryonic tissues. During gastrulation, the primitive streak elongates and extends to the distal tip of the egg cylinder. As in chick, the epiblast cells in the primitive streak region undergo an epithelial to mesenchymal transformation, thus delaminating, ingressing and moving away to form new mesoderm and endoderm layers. The cells emerging from the posterior part of the streak give rise
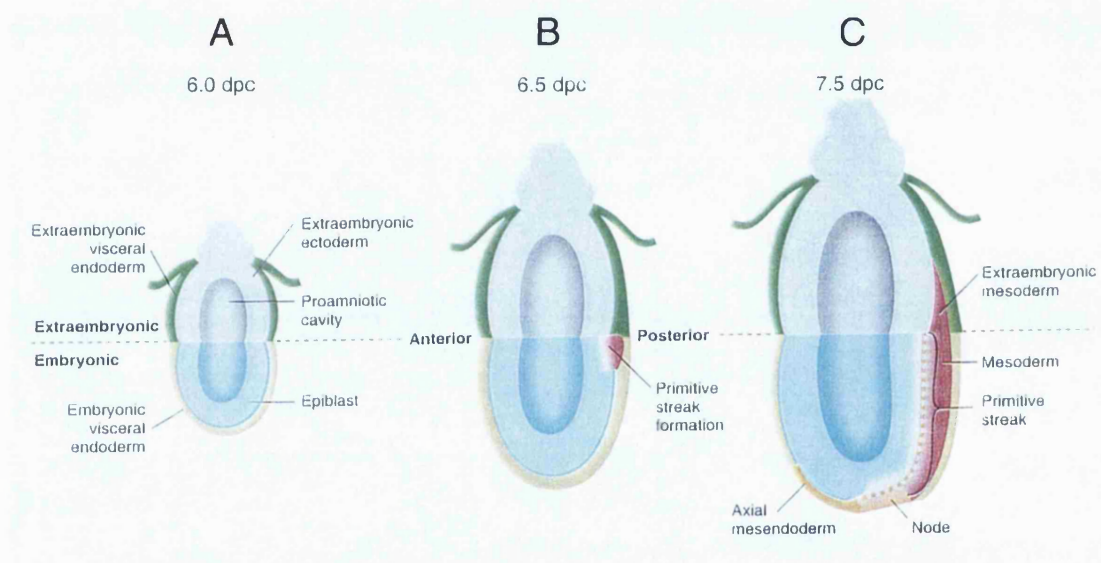
Fig. 1.5. Gastrulation in the mouse embryo. (A) The cup-shape mouse embryo consists of embryonic and extraembryonic tissues. **(B)** The primitive streak is visible at 6.5 dpc. **(C)** The streak elongates to the tip of the egg cylinder and the node, which gives rise to the axial mesendoderm, forms at the anterior end of the streak. After Beddington, 1998.

to extraembryonic mesoderm and the cells coming out of the intermediate streak will form lateral plate mesoderm and paraxial mesoderm. The node forms at the anterior end of the primitive streak. The node is the source of axial mesendoderm cells that will populate axial mesoderm structures (prechordal plate and notochord) and definitive gut endoderm (reviewed in Beddington and Robertson, 1999; Hogan et al., 1994).

1.2. The dorsal organizer

Communication between different cell populations is an essential process of metazoan development. A classical example of such intercellular communication is induction, in which a group of cells produces a signal that influences the development of adjacent tissue. The existence of a specific group of gastrula cells with inductive properties was first reported in 1924 by Spemann and Mangold following grafting experiments between non-pigmented (*Triturus cristatus*) and darkly pigmented (*Triturus taeniatus*) amphibian species. These investigators found that the dorsal blastopore lip of a *T. cristatus* embryo induced the formation of a secondary axis when transplanted to the ventral side of a *T. taeniatus* embryo, a region fated to became non-neural ectoderm and ventral mesoderm. In the induced axis, the donor tissue differentiated into notochord and other mesodermal structures that would normally develop from the dorsal lip. The dorsal lip of the blastopore was named the organizer, since it was able to change the fate of host ventral tissue into neural tissue and dorsal mesoderm and organise host and donor tissues to form a secondary body axis. Spemann proposed that during normal development, the role of the dorsal lip cells and its derivatives is to organise the embryonic cells to form a body axis (reviewed in Hamburger, 1988).

In the years that followed, the axis-inducing assay was used to identify functional equivalents of Spemann's organizer in other vertebrate species. The dorsal blastopore lip of the amphibian *Xenopus laevis* (Gimlich and Cooke, 1983; Smith and Slack, 1983), the embryonic shield of fish embryos (Oppenheimer, 1936; Shih and Fraser, 1996),

12

Hensen's node in the chick embryo (Waddington, 1932) and the node of the mouse embryo (Beddington, 1994) share the ability to organise a body axis in transplantation experiments.

Several heterotopic embryological experiments reinforce the idea that signals underlying the inductive activity of the dorsal organizer are conserved throughout vertebrate evolution. For example, zebrafish blastula halves, when transplanted into the blastocoel of the amphibian *Triturus torosus*, differentiated into notochord and were able to induce a localised portion of neural tissue (Oppenheimer, 1936). While chick Hensen's nodes are unable to differentiate in recombination experiments, they will induce neural tissue in *Xenopus* animal cap explants (Kintner and Dodd, 1991). Hensen's node transplanted into the ventral side of a gastrula zebrafish embryo does not differentiate but induces a secondary axis (Hatta and Takahashi, 1996). The anterior tip of the primitive streak of a 6.75 dpc mouse embryo is able to induce a cement gland when transplanted into the blastocoel of *Xenopus* embryos (Blum et al., 1992).

Apart from the capacity to induce secondary axes, all vertebrate organizers exhibit several other characteristics not shared with other regions of the gastrula embryo. First, when the organizer cells are challenged in transplantation experiments, they still give to the structures they where fated to become in a normal embryo. This means that the organizer cells are not only specified but committed to such fates by early gastrula stages (reviewed in Smith and Schoenwolf, 1998). Second, fate map analysis shows that the organizer contains progenitor cells for axial mesoderm and floor plate, as well as other tissues such as gut endoderm and paraxial mesoderm. Contribution to axial mesoderm is a feature common to all organizers (Camus and Tam, 1999) (for details see Table 1.1). Third, organizer cells express a subset of transcription factors and secreted molecules. The known activities of these molecules suggest that organizer action is indeed a composite of inductive and antagonistic signals (for details see Table 1.2). Finally, there is an emerging view that the organizer is not a static population of cells but rather a dynamic entity. This concept is based on fate map studies and node regeneration experiments in the chick embryo. These studies showed that cells acquire

13

Table 1.1 Embryonic fate of the cells that populate the vertebrate organizer

Organism	Organizer	Embryo stage	Tissue contribuition			
			Neurectoderm	Axial mesoderm	Paraxial mesoderm	Endoderm
Zebrafish	Embryonic shield	50% epiboly	Floor plate	Prechordal plate Notochord	Somites	No contribuition
Xenopus	Dorsal lip	Stage 10	No contribuition	Prechordal plate Notochord	Head mesenchyme Somites	Pharyngeal endoderm
Chick	Hensen's node	Stage 3-3+	Floor plate	Prechordal plate Notochord	Somites	Foregut and midgut endoderm
		Stage 5-9	Floor plate	Notochord	Somites	No contribuition
Mouse	EGO	Early-streak	Floor plate	Prechordal plate Notochord Node	Head mesenchyme Heart Somites	Foregut and trunk endodem
	Node	Late-streak	Floor plate	Notochord	Somites	Trunk endoderm

EGO = Early Gastrula Organizer

After Camus and Tam, 1999

Table 1.2. Genes expressed in the vertebrate organizer

	Transcription factors			Secreted factors		
	Homeodomain	Forkhead domain	Lim domain	BMP inhibitors	Wnt inhibitors	Nodal related
Zebrafish	*gsc* [1] *flh* [2] * [3] *otx1* [4] *ntl* [5]	*axial* [6]	*lim1* [7]	*chordin* [8] *noggin* [9] * [10]	*dkk1* [11] unknown	*cyclops* [13] *squint* [14]
Xenopus	*gsc* [15] *Xnot* [16] *Xanf* [17] *otx2* [18] *Xbra* [19]	*pintallavis* [20]	*lim1* [21]	*chordin* [22] *noggin* [23] *follistatin* [24]	*dkk1* [25] *frzb1* [26]	*Xnr1* [27] *Xnr2* [28]
Chick	*gsc* [29] *Cnot* [30] *Ganf* [31] *otx2* [32] *Ch-T* [33]	*hnf3β* [34]	*lim1* [35]	*chordin* [36] * [37] *follistatin* [38]	* [39] * [40]	* [41]
Mouse	*gsc* [42] unknown * [44] *otx2* [45] *T* [46]	*hnf3β* [47]	*lim1* [48]	*chordin* [49] *noggin* [50] * [51]	*dkk1* [52] * [53]	*nodal* [54]

* = The homologue gene is not expressed in the organizer

Zebrafish:1(Stachel et al., 1993)2(Talbot et al., 1995)3, 17, 31(Kazanskaya et al., 1997)4(Li et al., 1994)5(Schulte-Merker et al., 1994)6(Strahle et al., 1993)7(Toyama et al., 1995)
8(Schulte-Merker et al., 1997)9(Furthauer et al., 1999)10(Bauer et al., 1998)11(Hashimoto et al., 2000)13(Sampath et al., 1998)14(Erter et al., 1998)
Xenopus:15(Cho et al., 1991)16(Gont et al., 1996)18(Pannese et al., 1995)19(Smith et al., 1991)20(Ruiz i Altaba and Jessell, 1992)21(Taira et al., 1992)22(Sasai et al., 1994)23(Smith and Harland, 1992)24(Hemmati-Brivanlou et al., 1994)25(Glinka et al., 1998)26(Wang et al., 1997)27, 28(Jones et al., 1995)
Chick: 29(Izpisua-Belmonte et al., 1993)30(Stein and Kessel, 1995)32(Bally-Cuif et al., 1995)33(Kispert et al., 1995)34, 41(Levin et al., 1995)36(Streit et al., 1998)
37(Connolly et al., 1997)38(Levin, 1998)39(Foley et al., 2000)40(Baranski et al., 2000)
Mouse:42(Rivera-Perez et al., 1995)44(Thomas and Beddington, 1996)45(Simeone et al., 1992)46(Herrmann et al., 1990)47(Ang et al., 1993)48(Barnes et al., 1994)49, 50(Bachiller et al., 2000)
51(Albano et al., 1994)52(Glinka et al., 1998)53(Hoang et al., 1998)54(Zhou et al., 1993)

and lose organizer features as they step in and out of the organizer region (Joubin and Stern, 1999).

1.3. Formation of the organizer and the concept of the Nieuwkoop centre

The classical model for the formation of the dorsal organizer arises from amphibian experimental embryology. According to the model, organizer formation involves two discrete steps. The first step is the microtubule-dependent cortical rotation, leading to the transport of dorsal determinants from the vegetal pole to the prospective dorsal blastomeres. This creates a first organising centre, called the Nieuwkoop centre, within the dorsal-vegetal blastomeres. The second step is the action of the Nieuwkoop centre on overlying dorsal blastomeres to induce Spemann's organizer (reviewed in Moon and Kimelman, 1998).

1.3.1. The Nieuwkoop centre can induce the organizer

It is believed that cortical rotation leads to dorsal accumulation of β-catenin (Larabell et al., 1997). *Xenopus* embryos in which *β-catenin* transcripts were depleted with antisense oligonucleotides fail to form dorsal structures (Heasman et al., 1994). This experiment showed that β-catenin is required for the formation of the dorsal axis. β-catenin is a target of the Wnt signalling transduction pathway and is negatively regulated by glycogen-synthase-kinase-3 (Gsk3) (Dominguez et al., 1995; He et al., 1995; Pierce and Kimelman, 1995; Yost et al., 1996). In the ventral side of the embryo, Gsk3 targets β-catenin for degradation. On the dorsal side, however, the activity of Gsk3 is blocked by Disheveled (Dsh), thereby preventing the degradation of β-catenin (Miller et al., 1999; Sokol, 1996; Sokol et al., 1995). β-catenin is then translocated into

the nucleus where it probably forms a complex with members of the lymphoid enhancer factor/T-cell factor (Lef/Tcf) family of transcription factors to activate target genes (Molenaar et al., 1996). When β-catenin is ectopically expressed in the ventral side of the *Xenopus* embryo it can induce a secondary axis (Guger and Gumbiner, 1995). Several members of the Wnt family (*wnt1, wnt2, wnt3* and *wnt8*) can induce secondary axes when overexpressed in the ventral blastomeres, the same being true for *dsh* and dominant-negative version of *gsk3* (Dominguez et al., 1995; He et al., 1995; Sokol et al., 1995). Despite the ability of injected Wnts and components of the Wnt pathway to induce secondary axes, it is not clear whether an endogenous Wnt protein is involved in establishing the primary axis of *Xenopus*. The only known maternally expressed Wnt gene that can induce a secondary axis is *wnt8*. However, *wnt8* is not vegetally localised, which is where the dorsalising signal is predicted to originate based on transplantation experiments. In addition, injection of dominant-negative *wnt8* does not affect the development of the primary axis (Hoppler et al., 1996). The same being true for dominant-negative *dsh* (Sokol, 1996). These results lead Moon and collaborators to propose that, at early steps of axis specification, the Wnt signalling pathway might be activated downstream of Dsh by an unrelated Wnt molecule (Moon et al., 1997).

Xenopus Siamois and Twin, related homeodomain transcription factors, appear to be targets of the Tcf/β-catenin complex and may be considered as the link between the maternal and zygotic mechanisms controlling axis formation. Siamois appears to play an important role in the Nieuwkoop centre by activating the expression of organizer genes such as *goosecoid* (*gsc*) in overlying dorsal equatorial cells (Fan and Sokol, 1997; Kessler, 1997). Twin, a protein closely related to Siamois, is likely to regulate the same target genes (Laurent et al., 1997).

In zebrafish, the dorsal YSL may be the source of signals responsible for the induction of the embryonic shield and thus be the functional equivalent of the amphibian Nieuwkoop centre. In fact, the yolk cell is able to ectopically induce mesoderm, endoderm and organizer gene expression in the blastoderm (Long, 1983; Mizuno et al., 1996; Ober and Schulte-Merker, 1999; Rodaway et al., 1999) and nuclear β-catenin is

accumulated in the dorsal YSL by vesicular transport (Schneider et al., 1996). No homologue of *siamois* was identified in zebrafish. Instead, a homeobox gene called *bozozok* (*boz*), which is expressed where maternal β-catenin has been localised (Koos and Ho, 1998; Yamanaka et al., 1998), contains several consensus binding sites for Tcf cofactor in its promoter region (Yamanaka et al., 1998). Deletion and point mutation studies showed that these Tcf/β-catenin binding sites are required to drive the expression of *boz* (Ryu et al., 2001). The fact that activation of the Wnt signalling pathway and nuclear accumulation of β-catenin can lead to the induction of a secondary axis on the ventral side of a zebrafish embryo (Kelly et al., 1995), suggest some degree of conservation of the molecular mechanisms for organizer induction between zebrafish and frog. It seems, however, that Boz does not mediate the full spectrum of β-catenin activities. In fact, *boz* mutants lack the derivatives of the organizer, prechordal plate and notochord, but still possess organizer activity, since a neural axis is induced (Fekany et al., 1999). In addition, the injection of *boz* RNA in zebrafish embryos has poor ectopic axis induction, contrasting with *siamois* RNA in *Xenopus*, where the induced complete secondary axis is indistinguishable from a *β-catenin*-induced axis (Koos and Ho, 1998; Lemaire et al., 1995; Yamanaka et al., 1998).

1.3.2. Is the Nieuwkoop centre required to induce the dorsal organizer?

It is clear that the *Xenopus* Nieuwkoop centre and the zebrafish YSL are sufficient to induce the dorsal organizer. However, if they are required for this induction has been a question debated for some time (Kodjabachian and Lemaire, 1998). In a 32-cell stage *Xenopus* embryo, the dorsal-vegetal blastomeres will give rise to the Nieuwkoop centre while the dorsal-marginal blastomeres will form the Spemann's organizer. Removal of either these blastomeres does not prevent axis development (Gimlich, 1986; Kageura, 1995). These experiments revealed that all dorsal blastomeres may share a common dorsalising potential and can act redundantly to specify dorsal development. The specific ablation of the zebrafish YSL has not been done, since it is technically difficult

to carry out this experiment without seriously compromising further development. However, by injecting RNase into the yolk cell, Chen and colleagues were able to specifically eliminate gene expression in the YSL. This study revealed that dorsal mesoderm can be induced and β-catenin can be stabilised in the dorsal-marginal blastomeres, independently of YSL signals (Chen and Kimelman, 2000).

If the Nieuwkoop centre in *Xenopus* and the YSL in zebrafish are not required for axial development, how is the dorsal organizer induced? In *Xenopus*, protein localisation analysis revealed that β-catenin is detected in nuclei within a large dorsal region including vegetal, marginal and animal blastomeres (reviewed in Moon and Kimelman, 1998). Expression of *siamois* is detected in the progeny of dorsal-margin blastomeres isolated at the 32-cell stage, suggesting that it can also be expressed in the dorsal organizer (Ding et al., 1998). In zebrafish, *β-catenin* is found in nuclei in the dorsal blastoderm as well in the dorsal YSL (Schneider et al., 1996). In addition, *squint*, a Nodal-related gene (Erter et al., 1998; Feldman et al., 1998; Rebagliati et al., 1998) and *boz* (Fekany et al., 1999; Koos and Ho, 1998; Yamanaka et al., 1998), which are necessary and sufficient to induce dorsal mesoderm, are not only expressed in the dorsal YSL but also in dorsal-marginal blastomeres. These data support the idea that the dorsal-marginal blastomeres, both in *Xenopus* and zebrafish, contain sufficient information to induce dorsal mesoderm, without the contribution from the Nieuwkoop centre or the dorsal YSL. Taken together, these results challenge the notion that the Nieuwkoop centre induces the dorsal organizer in a non-cell-autonomous manner.

1.3.3. The formation of the organizer requires the combined action of different signalling pathways

The induction of the organizer is part of the process that leads to mesendoderm induction. β-catenin can be seen as a local dorsal signal that needs to be supplemented for the organizer to form. Inhibition of transforming growth factor-β (TGF-β) signalling prevents axis formation in *Xenopus*, but has no effect in the regulation of β-catenin

levels (Fagotto et al., 1997; Hemmati-Brivanlou and Melton, 1992). Taken together with the importance of β-catenin, this result suggests that the formation of the organizer requires the coordination between both Wnt/β-catenin and TGF-β pathways. Evidence for this is the fact that organizer genes like *gsc*, *chordin* and *siamois* are sensitive to dominant-negative TGF-β receptor (Brannon and Kimelman, 1996; Crease et al., 1998). In addition, the promoter region of the organizer gene *gsc* has responsive elements for both Wnt and TGF-β (Watabe et al., 1995).

In *Xenopus*, a maternal T-box transcription factor, called VegT, is required for the specification of mesoderm and endoderm (Zhang et al., 1998). VegT activates the TGF-β superfamily members *derrière*, and Nodal-related genes *Xnr1*, *Xnr2* and *Xnr4* (Kofron et al., 1999). In the dorsal side of the embryo, the presence of β-catenin increases the levels of expression of *Xnr1* and *Xnr2* relative to the ventral side in the late blastula (Agius et al., 2000). This difference in regulation between the ventral and the dorsal side seems to be important for the proper specification of the organizer. It is not known at present what signal activates factors that will induce mesoderm and endoderm in zebrafish, since the *vegT* orthologue, *spadetail*, is not maternally expressed (Griffin et al., 1998). In zebrafish, Nodal signalling is required for induction of mesoderm and endoderm. Mutant fish lacking both Nodal-related *squint* and *cyclops* genes products fail to form mesoderm and endoderm, except for a small amount of tail mesoderm (Feldman et al., 1998). A model for mesoderm induction in zebrafish has been proposed in which β-catenin promotes the dorsal expression of *squint* and *cyclops*. Squint and Cyclops are then necessary for the formation of dorsal mesoderm and endoderm and for the involution of all mesoderm (Kimelman and Griffin, 2000).

1.4. Neural induction and the organizer

1.4.1. The default model in *Xenopus*

Following the landmark experiment of Spemann and Mangold in 1924, it was thought that signals form the dorsal blastopore lip directed ectoderm to form neural tissue (reviewed in Hamburger, 1988). Ectodermal cells on the ventral side do not receive these signals and as a consequence form epidermis. For this reason, it was postulated that epidermis was the default state of the ectoderm. It was later found that *Xenopus* animal cap cells when dissociated, differentiate into neural tissue, whereas normally an intact animal cap will differentiate into epidermis (Godsave and Slack, 1989; Gunz and Tacke, 1989; Sato and Sargent, 1989). This lead to the notion that neural differentiation is the default state of the ectoderm. The default model postulates that a signal produced by the animal cap promotes differentiation of epidermis and dissociation dilutes the signal causing cells to differentiate as neural tissue.

Molecular support for the default model came from the discovery of molecules that can induce epidermis in the dissociated cell assay. Several proteins belonging to bone morphogenetic protein (BMP) subgroup of the TGF-β family, namely Bmp2, Bmp4 and Bmp7, where shown to be epidermal inducers (Suzuki et al., 1997; Wilson and Hemmati-Brivanlou, 1995). Normal expression of *bmp2*, *bmp4* and *bmp7* is also compatible with their proposed epidermal inducing function. They are expressed in the entire ectoderm at the start of gastrulation and then down regulated from the presumptive neural plate by the time the organizer appears (Chang and Hemmati-Brivanlou, 1999; Hawley et al., 1995; Hemmati-Brivanlou and Thomsen, 1995).

Induction of epidermis in cell dissociation experiments can also be achieved by over-expression of downstream effectors of the BMP signalling pathway. Namely, over-expression of activated forms of type I BMP receptors (*Alk2*, *Alk3* and *Alk6*), of receptor-regulated mediators of BMP signalling (*smad1* and *smad5*) and of *msx1*, an immediate response gene to BMP signalling (reviewed in Weinstein and Hemmati-

Brivanlou, 1999). Further support for the default model came from experiments showing that not only BMPs induce epidermal fate *in vitro*, but also inhibition of endogenous BMP signalling neuralises intact ectodermal explants. Animal caps cut from embryos injected with RNA encoding for a dominant-negative BMP receptor (Sasai et al., 1995; Suzuki et al., 1995; Xu et al., 1995), a dominant-negative (non-cleavable) *bmp4* and *bmp7* (Hawley et al., 1995) or antisense *bmp4* RNA (Sasai et al., 1995) adopt a neural fate instead of an epidermal one. Epidermal induction by BMP signalling is mediated by several transcription factors such as Vent1 and Vent2. Dominant-negative versions of these molecules neuralise animal caps (Onichtchouk et al., 1998).

Molecules with direct neural inducing abilities that act by inhibiting BMPs have been identified. Noggin, Chordin, Follistatin, *Xenopus* Nodal-related-3 (Xnr3) and Cerberus are secreted proteins expressed in the organizer and its derivatives. They can induce neural tissue in animal cap explants without inducing mesoderm (Bouwmeester et al., 1996; Hansen et al., 1997; Hemmati-Brivanlou et al., 1994; Lamb et al., 1993; Sasai et al., 1995). Noggin, Chordin and Follistatin have been shown to bind directly to BMP proteins, preventing them from interacting with their receptors (Fainsod et al., 1997; Piccolo et al., 1996; Zimmerman et al., 1996). It was also shown that Cerberus and BMP proteins can bind directly (Piccolo et al., 1999). A direct interaction between Xnr3 and BMP proteins is not known, however neural inducing activity of Xnr3 can be inhibited by over-expression of *bmp4*. This suggests that Xnr3, a divergent TGF-β family member, may competitively bind to BMP receptors, inhibiting BMP signalling (Hansen et al., 1997). The results from the *Xenopus* experiments indicate that BMP inhibition has a role in neural induction *in vivo*.

1.4.2. The default model in other vertebrates

Work done in *Xenopus* provides strong evidence that neural induction depend on the regulation of BMPs by antagonists secreted by the organizer. However, results from

other organisms, particularly chick, suggest that the default model may be too simplistic and that neural induction may involve co-operation of different classes of signals (reviewed in Streit and Stern, 1999). Mis-expression of either Chordin or Noggin in extraembryonic tissue does not induce ectopic neural cells (Streit et al., 1998; Streit and Stern, 1999). A 5-hour exposure of non-neural ectoderm to a node graft is not sufficient to induce a neural plate. However, if the node graft is replaced by Chordin-secreting cells, expression of the pan-neural marker *sox3* is stabilised in non-neural ectoderm (Streit et al., 1998). Taken together, these results suggest that BMP inhibition is not sufficient for neural induction in the chick. Another possibility is that BMP antagonists may have a role in maintaining rather then inducing neural fate.

The expression pattern of BMPs and their inhibitors in other organisms have been used to argue that they may have different roles from the ones proposed in *Xenopus*. The chick and mouse *bmp2*, *bmp4* and *bmp7* are not expressed in the prospective neural plate at early primitive streak stage, at the time neural induction is most likely to begin (Schultheiss et al., 1997; Streit et al., 1998; Winnier et al., 1995). Chick *noggin* and *follistatin* are weakly expressed in the node during gastrulation (Connolly et al., 1997; Levin, 1998). The gene *follistatin* was never reported to be expressed in the mouse node (Albano et al., 1994). Zebrafish *follistatin* is not expressed at blastula or early gastrula stages, when the organizer signalling is occurring (Bauer et al., 1998; Furthauer et al., 1999).

Loss of function studies in mouse and zebrafish failed to provide a strong evidence to the default model for neural induction. Mutant *noggin* mice develop a fairly normal neural plate and show patterning defects only at later stages (McMahon et al., 1998). Also, *noggin/chordin* double mutant embryos have a neural axis, although they do show defects in the forebrain (Bachiller et al., 2000). Null mutants *bmp2* and *bmp7* have no early neural phenotypes (Dudley et al., 1995; Matzuk et al., 1995; Zhang and Bradley, 1996). The few mutants lacking *bmp4* that survive to early limb stages do not appear to have an enlarged nervous system or absence of epidermis (Winnier et al., 1995). A zebrafish mutant called *dino* has a disruption in *chordino*, the fish homologue of *chordin*

23

(Hammerschmidt et al., 1996; Schulte-Merker et al., 1997). In *dino* mutant embryos, the neural plate has a reduced size, however these embryos possess neural tissue. In addition to *dino*, *ogo* mutant embryos have a reduced neural plate and dorsal mesoderm (Hammerschmidt et al., 1996; Miller-Bertoglio et al., 1999). The molecular identity of *ogo* is not known, suggesting that other dorsalising activities have not been identified. However, *dino/ogo* double mutants have a more ventralised phenotype than the single mutants, but still have a patterned neural tube (Miller-Bertoglio et al., 1999).

The analysis of mouse and zebrafish mutants did not give so far a clear proof for the involvement of BMPs and their antagonists in neural induction. This could be a result of functional overlap of families of genes. The mutants, however, support the idea that proper regulation of BMP signalling is important for dorsal-ventral patterning of the mesoderm and neuroectoderm. For example, ventral patterning of the posterior neural tube and somite differentiation are affected in *noggin* mutant mice (McMahon et al., 1998). In the *noggin/chordin* double mutants this type of defects became more severe (Bachiller et al., 2000). In addition to a reduction in neuroectoderm, zebrafish *dino* mutants show an expansion of ventral and lateral mesodermal fates (Hammerschmidt et al., 1996; Schulte-Merker et al., 1997). The development of dorsal-most tissue types such as anterior notochord and prechordal plate is not dramatically affected in *dino* mutants suggesting that *chordin* is primarily required for the repression of ventral fates in lateral regions. The zebrafish mutant *swirl* is caused by a null mutation in *bmp2* (Kishimoto et al., 1997; Martinez-Barbera et al., 1997; Nikaido et al., 1997). *swirl* mutant embryos are partially dorsalised, and have an excess of neural plate and dorsal mesoderm (Hammerschmidt et al., 1996; Mullins et al., 1996). A similar phenotype is observed in *snailhouse* (*bmp7*) and *somitabun* (*smad5*) mutant embryos. *dino/swirl* and *dino/snailhouse* double mutant embryos have phenotypes identical to *swirl* or *snailhouse* single mutants, showing that *swirl* and *snailhouse* are epistatic to *dino* (Dick et al., 2000; Hammerschmidt et al., 1996). Studies in zebrafish (Blader et al., 1997) and *Xenopus* (Piccolo et al., 1997) established that Tolloid homologues cleave Chordin and release active BMP from the BMP-Chordin complexes. The discovery that *mini fin* is a mutation disrupting *tolloid* constitutes genetic evidence for the role of this

metalloproteinase in dorsal-ventral pattern formation in zebrafish embryos (Connors et al., 1999). The fact that all these molecules are involved in mesoderm patterning makes it is difficult to establish if the neural phenotypes observed are direct or due to the primary loss of mesoderm structures.

1.4.3. Other signals involved in neural induction

Whether or not fibroblast growth factors (FGFs) can act as direct neural inducers or as posteriorising factors of existing anterior neural tissue or both is not yet clear. Nevertheless, there is some evidence that FGFs can induce neural tissue both in *Xenopus* and chick embryos. In *Xenopus*, FGF can directly induce posterior neural markers in ectoderm (Kengaku and Okamoto, 1995; Lamb and Harland, 1995). Animal caps treated with a dominant-negative type-1 FGF receptor (XFD) were found to be unresponsive to *noggin* or to signals from the organizer (Launay et al., 1996). *chordin* or *noggin* will normally induce endoderm and neural tissue formation. In the absence of FGF signalling, *chordin* or *noggin* will induce only endoderm (Sasai et al., 1996). These experiments show that the neuralising activity of *chordin* and *noggin* in animal caps requires FGF signalling pathway, suggesting that FGFs may render ectoderm competent to respond to neural inducers. There are however a series of reports that suggest that FGF is not necessary for the induction of neural tissue both in explants and in the embryo. Animal caps co-injected with XFD and *noggin* expressed anterior neural markers (McGrew et al., 1997). In addition, the analysis of transgenic *Xenopus* embryos ubiquitously expressing XFD after the onset of zygotic transcription revealed that, even though mesoderm differentiation was blocked, no disruption in neural induction was observed (Kroll and Amaya, 1996). In chick, implantation of FGF-soaked beads in embryonic or extraembryonic positions leads to the formation of ectopic posterior neural structures (Alvarez et al., 1998; Storey et al., 1998).

In the chick, it was shown that *ERNI*, the earliest neural marker to be induced in response to signals from the Hensen's node, can be induce by Fgf8-coated beads but not

by mis-expression of *chordin* or *noggin* (Streit et al., 2000). A recent study revealed that neural induction in the chick occurs *in utero*, i.e. a much earlier time than the formation of the Hensen' node (Wilson et al., 2000). This study showed that early epiblast cells do express *bmp4* and *bmp7* in prospective neural tissue. The down-regulation of these genes requires FGF signalling and correlates with the acquisition of neural character. The role of FGF signalling in neural induction in the chick epiblast might be similar to the role of Wnt signalling in *Xenopus* or zebrafish embryos. In *Xenopus*, Wnt signalling at blastula stages has been implicated in the suppression of *bmp4* expression, which is sufficient to induce neural markers (Baker et al., 1999). This suggests that an early Wnt signal might predispose the dorsal ectoderm to a neural fate. In zebrafish, it was shown that Boz, a target of the Wnt pathway, may be sufficient to suppress BMP expression (Fekany-Lee et al., 2000; Koos and Ho, 1999).

1.5. Anterior-posterior patterning and the organizer

1.5.1. Vertical versus planar signals

During gastrulation the physical interactions between cell populations change, in particular the mesoderm and endoderm layers become positioned beneath the ectoderm. In 1938, Spemann proposed two alternative ways in which neural patterning signals coming from the organizer could reach the ectoderm. One was via vertical signals coming from the derivatives of the dorsal blastopore lip (prechordal plate and notochord) and acting in the overlying ectoderm. The second was via planar signals travelling horizontally from the dorsal blastopore lip through the plane of the ectoderm (reviewed in Doniach, 1993). It has been shown that neural induction and patterning can occur by both vertical and planar signals. However, the extent to which they operate *in vivo* is still unclear.

Evidence for vertical signalling comes from studies of Mangold in 1933, using the *Einsteck* method. He found that four successive pieces of involuted dorsal mesoderm from different AP levels of an early neurula stage *Triturus* induce neural tissue with different regional morphological characteristics when inserted into the blastocoel cavity of an early gastrula embryo. The AP level of the induced neural tissue roughly corresponded to that of the inserted mesoderm (reviewed in Doniach, 1993). Vertical signals are likely to play a role in patterning anterior neural tissue in the mouse, as suggested by the apposition of the AVE relative to the ectoderm in the early embryo (reviewed in Beddington and Robertson, 1998). However, vertical signalling can not account for all aspects of neural induction and patterning since mutant zebrafish and mouse embryos that lack axial mesendoderm structures, such as double *squint/cyclops* (Feldman et al., 1998), *oep* (Schier et al., 1997) and *hnf3β* (Dufort et al., 1998), have neural tissue with apparently normal AP pattern.

The molecular evidence for planar signalling comes from the work of (Kintner and Melton, 1987). These investigators found that exogastrulae embryos, in which there is no involution of the dorsal mesoderm, and therefore no contact with the ectoderm, express the specific neural marker *N-CAM*, suggesting that planar signals derived from the dorsal lip are sufficient to elicit neural induction of the ectoderm. The induced neural tissue also expresses several AP markers in the correct order. Subsequent work using *Keller* explants, in which dorsal ectoderm and dorsal mesoderm are cultured in the same plane, contacting with each other only in one edge, also showed that neural markers were expressed in the correct AP order (Keller and Daniltchick, 1988). However, in exogastrulae and Keller sandwiches AP patterning is not complete since eyes do not form. This raises the question of whether complete neural pattern requires co-operation between planar and vertical signals. In fact, when prechordal plate mesoderm is placed in contact with ectoderm from exogastrulae and Keller sandwiches, eyes do form (Dixon and Kintner, 1989; Ruiz i Albata, 1992). In zebrafish, the evidence that planar signals play a role in AP patterning of the ectoderm comes from experiments in which it was shown that prior to gastrulation (therefore, before any vertical signals) *opl* and *fkh5* are expressed in specific domains of the presumptive forebrain and that

removal of the blastula organizer prevents the expression of these genes (Grinblat et al., 1998).

1.5.2. Activation-transformation model

Initially designed to test planar induction of AP pattern, Nieuwkoop performed a series of fold experiments that led him to propose a model for AP neural patterning involving two sets of inducer signals (Nieuwkoop, 1952). The experiments consisted in inserting folded flaps of competent ectoderm perpendicularly into the presumptive neural plate of early gastrula embryos at different AP positions. A consistent pattern of results was obtained. First, the grafts showed posterior to anterior neural pattern along their proximal to distal axis. Second, anterior most CNS regions were obtained in the graft at any level along the AP axis of the host neural plate. Third, the proximal part of the graft always adopted the AP value of the host neural plate region with which it was in direct contact. Finally, the distal part of the graft always developed into the anterior-most CNS region. In general, the more posterior the implantation of the competent gastrula ectoderm was performed along the AP axis of the host neural plate, the more the proximal part of the graft differed from its distal part. From these experiments, Nieuwkoop concluded that an initial activator signal present in all organizer mesoderm, induces neural tissue with anterior character. A second transformer signal present in a gradient with a high point in the posterior mesoderm, then progressively posteriorises the neural plate to generate the remaining regions of the CNS. He argued that the transformer is dominant over the activator, since the proximal part of the graft developed with a more posterior character, even though it must have experienced both factors.

The discovery of molecules, such as Noggin and Chordin that can induce neural tissue expressing anterior neural markers in *Xenopus* animal caps gave support to the activation-transformation model. In addition, three classes of signals, FGFs, Wnt and retinoic acid (RA) have been shown to posteriorise neural tissue, making them candidates for the transformer signal (reviewed in Doniach and Musci, 1995; Sasai and

28

De Robertis, 1997). Grafting experiments have shown that posterior non-axial mesoderm, but not axial mesoderm derived from the organizer, can have a posteriorising influence on forebrain regions (Ang and Rossant, 1993; Bang et al., 1997; Muhr et al., 1997; Sagerstrom et al., 1996; Woo and Fraser, 1997). These results obtained in zebrafish, chick and mouse suggest that other regions, and possibly other molecules, may also be involved in posteriorisation of the neural ectoderm.

As discussed previously, the involvement of FGF signalling in neural induction is controversial. However, the role of FGF molecules in posterior specification of the neural tissue is supported by several experiments. FGF is expressed in the posterior mesoderm of *Xenopus* embryos, therefore being a candidate molecule for a posteriorising signal (reviewed in Gamse and Sive, 2000). In *Xenopus*, FGF gives posterior character to anterior neural tissue *in vitro* (Cox and Hemmati-Brivanlou, 1995). Over-expression of XFD in Keller explants inhibits posterior neural markers but not anterior or pan-neural markers (Holowacz and Sokol, 1999). Evidence in both zebrafish and chick indicate that FGFs can posteriorise the paraxial mesoderm, however they are unlikely to constitute the posteriorising signal that passes between the paraxial mesoderm and the neural plate (Muhr et al., 1997; Woo and Fraser, 1997; Koshida, 1998).

There is evidence that Wnt family members are candidates for the posterior transformation signal during gastrulation (Wodarz, 1998). In *Xenopus* embryos, *wnt3a* and *wnt8* are expressed in posterior dorsal, lateral and ventral mesoderm. *wnt3a* can enhance posterior neural markers in *Xenopus* animal caps explants mis-expressing *noggin* and *follistatin* (McGrew et al., 1995). *wnt8* mis-expression in *Xenopus* gastrula embryos leads to loss of anterior structures (Fredieu et al., 1997), while a dominant-negative form of *wnt8* that partially blocks Wnt signalling has the opposite effect, preventing induction of posterior neural markers in neuralised ectoderm (Bang et al., 1997). The zebrafish *wnt8* is expressed in lateral marginal cells of gastrula embryos and is excluded from the dorsal marginal cells (Ho et al., 1999; Kelly et al., 1995).

Therefore, *wnt8*-expressing cells are close to the cells fated to form hindbrain and spinal cord and more distant from the cells fated to became midbrain and hindbrain.

In *Xenopus*, it was shown that low concentrations of RA cause a reduction in forebrain and midbrain structures (Durston et al., 1989; Sive et al., 1990). Additional effects are also seen in the hindbrain, where anterior rhombomeres are reduced or compressed (Papalopulu et al., 1991). In addition, microinjection of constitutively active RA receptors reduce anterior neural tissue, while dominant-negative RA receptors leads to loss of posterior markers (Blumberg et al., 1997). Although causing a reduction of anterior rhombomeres, the RA treatment of zebrafish and chick embryos does not affect forebrain and midbrain development (Hill et al., 1995; Muhr et al., 1997), suggesting that global effects of RA on neural structures are unique to *Xenopus*, and that a more conserved function of RA is restricted to the patterning of the hindbrain.

1.5.3. Head and trunk organizers

Transplantation experiments in *Xenopus* and chick embryos showed that AP patterning of the nervous system can be a direct consequence of the age of the dorsal lip and therefore be dependent on the type of precursors it contains. Early organizer grafts induced complete axes duplications, including heads. Conversely, grafts of later organizers induced only partial axes containing just trunk (Gerhart et al., 1991; Storey et al., 1992). These findings were first observed by Spemann in 1931 and led to the idea of separable head and trunk organizer activities (Doniach, 1993; Harland and Gerhart, 1997). The discovery of head inducing molecules and the study of their mode of action gave new insights into the way head and trunk organizers may work.

Over-expression of the BMP antagonists, Noggin, Chordin and Follistatin, leads to the induction of secondary axes consisting predominantly of trunk structures (reviewed in Niehrs, 2001). The first head inducer discovered was Cerberus, a protein structurally related to the cystine-knot secreted family (Bouwmeester et al., 1996). The gene that

encodes Cerberus is expressed in the anterior endoderm of *Xenopus* gastrula embryos. Radial injection of *cerberus* RNA leads to loss of trunk/tail structures, such as somites or notochord. Moreover, injection of *cerberus* into a single blastomere induces a secondary head with one eye plus a second heart and liver (Bouwmeester et al., 1996). It was shown that Cerberus acts as an antagonist and contains independent domains to bind directly to BMP, Wnt and Nodal molecules, suggesting that it might be able to antagonise the three signalling pathways at the same time (Glinka et al., 1997; Piccolo et al., 1999). This suggested that for head induction to occur it is necessary to inhibit all three signalling pathways (Piccolo et al., 1999). It is possible that Cerberus interacts with the BMPs in a different way as Noggin and Chordin, since Cerberus inhibits trunk and tail formation and can not dorsalise mesoderm (Bouwmeester et al., 1996). In the mouse embryo, a *cerberus*-related gene (*cerl*) is expressed in the anterior visceral endoderm and in the anterior definitive endoderm (Belo et al., 1997; Shawlot et al., 1998). The pattern of expression of *cerl*, plus the fact that *cerl* expression is severely compromised in head-truncated *Lim1* mutant mice, suggested a conserved role of *cerl* in anterior neural induction. However, *cerl* mutant mice survive and have apparently normal development (Simpson et al., 1999). Since there is a family of *cerberus*-related genes in the mouse, it is possible that *cerl* is not the true orthologue of *Xenopus cerberus*. These two genes are only 26% identical and *cerl* is not able to induce ectopic heads when injected into the ventral side of a *Xenopus* embryo (Belo et al., 1997).

Further support to the idea that head induction is possible after co-inhibition of BMP and Wnt signalling pathways came with the discovery of two other Wnt antagonists, Dickkopf-1 (Dkk1) (Glinka et al., 1998) and Frizzled-b-1 (Frzb1) (Leyns et al., 1997; Wang et al., 1997). Dkk1 is a member of a new family of cysteine-rich proteins. In *Xenopus, dkk1* is expressed in the anterior endoderm as well in the prospective prechordal plate. Over-expression of *dkk1* does not induce secondary axes. But co-injection of *dkk1* with a dominant-negative *bmp2/4* receptor (*tBR*) induces a complete axis with a head possessing two eyes and a short trunk (Glinka et al., 1998). Injection of inhibitory antibodies to Dkk1 leads to the formation of embryos with microcephaly and cyclopia and in some cases to complete absence of head structures, while the trunk is

normal. This demonstrates the importance of this molecule in head formation (Niehrs, 1999). In zebrafish, *dkk1* is initially expressed in the extraembryonic YSL. During gastrulation, *dkk1* is expressed in the embryonic shield and later in the prospective prechordal plate (Hashimoto et al., 2000). Over-expression of *dkk1* directly promotes forebrain and axial mesendoderm development (Hashimoto et al., 2000; Shinya et al., 2000). Co-expression of *dkk1* RNA and *Wnt8b* DNA suppressed the phenotype caused by *wnt8b* plasmid alone, indicating that zebrafish Dkk1 antagonises Wnt signalling. Frzb1 is a secreted protein that contains a domain similar to the putative Wnt-binding region of the Frizzled family of transmembrane receptors. In *Xenopus*, *frzb1* is expressed in the organizer and later in the prechordal plate. Injection of *frzb1* RNA leads to embryos with enlarged heads and shortened trunks. It was shown that Frzb1 can bind directly Wnt proteins (Wang et al., 1997). Co-injection of *frzb1* and *tBR* leads to strong expression of *cerberus* in the ventral endoderm (Piccolo et al., 1999). Genetic evidence that supports the idea that Wnt signalling has to be repressed for head formation comes from the zebrafish mutant *headless* (*hdl*). The *hdl* mutant embryos show a complete lack of eyes, forebrain and part of the midbrain. These head defects are due to a mutation that eliminate the repressor function of Tcf3, which is a regulator of the Wnt signalling pathway (Kim et al., 2000).

Analysis of chimeric mice has shown that Nodal activity in the AVE is required for head formation (Varlet et al., 1997). However, biochemical studies of Cerberus activity suggest that it may be necessary to inhibit Nodal signalling in order to induce head structures in *Xenopus* embryos (Piccolo et al., 1999). One possibility is that early and late nodal signalling have different effects. In fact, it seems that *cerberus* expression requires an early Nodal signal since it can be induced by *Xnr1* mRNA, but not DNA. Therefore, it was proposed that an early Nodal signal would be required to pattern the anterior endoderm and the organizer, and perhaps to induce *cerberus* which then would feedback negatively on Nodal signalling in order to inhibit trunk fate and initiate head fate (Piccolo et al., 1999). In zebrafish, differential Nodal signalling is required before gastrulation to establish anterior and posterior fates within the organizer (Gritsman et al.,

2000). If it is necessary to antagonise Nodal signalling at later stages for the head to form is not known at present.

A two-inhibitor model was recently proposed which tries to incorporates the concepts of Nieuwkoop's activator-transformer and Spemann's head and trunk organizers (Niehrs, 1999). According to this model, BMP and Wnt signals in the ectoderm prevent neuralisation. Inhibitors released from the anterior organizer and its derivatives antagonise BMP and Wnt signals in the ectoderm, leading to anterior neural induction (head organizer; activator signal). Posteriorly, Wnt inhibitors are progressively less expressed, allowing Wnt signals to posteriorise neural fates induced by BMP inhibition alone (trunk organizer; transformer signal).

1.6. New insights into head induction

The cell movements that occur during gastrulation bring several tissues in contact with the forming neuroectoderm (Fig. 1.6). This raises the possibility that other tissues, in addition to the organizer and its derivatives, could be involved in induction and patterning of the neural plate. Special attention has been given to the anterior visceral endoderm (AVE) of the mouse embryo, the anterior endoderm of the *Xenopus* embryo, the anterior hypoblast of the chick embryo and the dorsal YSL of the zebrafish embryo, since these embryonic regions underlie tissues fated to became neuroectoderm.

1.6.1. The mouse AVE

Like other vertebrate organizers, the mouse node can induce a secondary neural axis when transplanted to a host embryo. In contrast to other vertebrates organizers, the node from either a full-length or an early-streak mouse embryo can not induce the forebrain and midbrain regions (Beddington, 1994; Tam and Steiner, 1999). These results
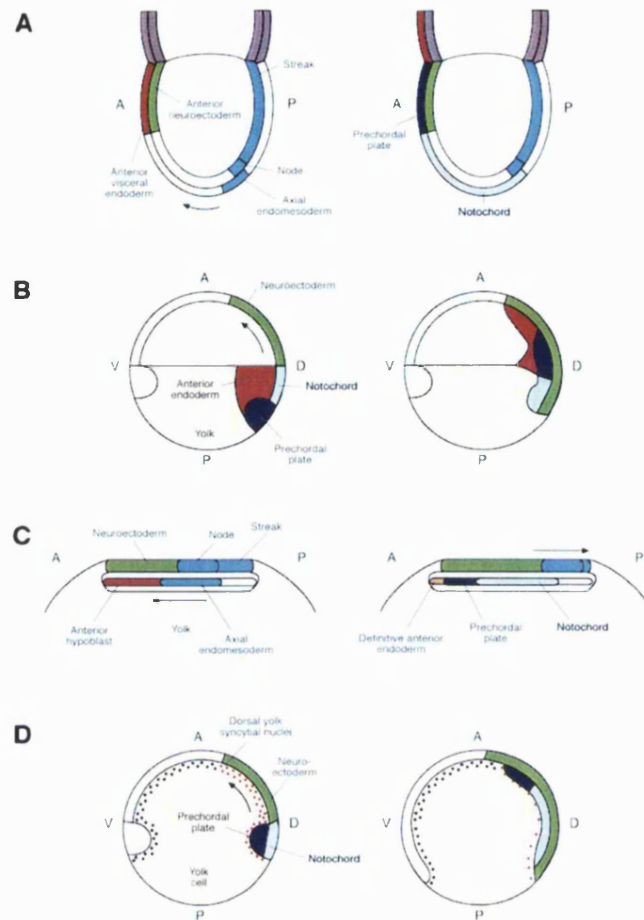
Fig. 1.6. Comparative scheme of the relative position of several tissues in vertebrate gastrulae. (A) Left: Sagittal representation of a mouse gastrula. In the anterior side, the AVE contacts the future anterior neural plate. In the posterior-distal side, definitive axial endomesoderm (anterior definitive endoderm, prechordal plate and notochord) leaves the node. Right: As gastrulation proceeds, axial endomesoderm migrates anteriorly and displaces visceral endoderm coming into contact with the anterior neuroectoderm. (B) Left: Sagittal representation of a *Xenopus* at the beginning of gastrulation. The organizer consists of prospective prechordal plate and notochord. The anterior endoderm cells are adjacent to the organizer and are the first cells to migrate towards the animal pole. Right: As gastrulation proceeds, the anterior endoderm, prospective prechordal plate and notochord migrate towards the animal pole (arrow) and contact the neural plate. (C) Left: Sagittal representation of a chick embryo at the onset of gastrulation. The anterior region of the extraembryonic endoderm (the hypoblast) contacts the future neuroectoderm. Right: Axial endomesoderm derived from the Hensen's node migrates towards the anterior side and displaces the hypoblast. (D) Left: Sagittal representation of a zebrafish gastrula embryo. The extraembryonic YSL contacts the embryonic shield and prospective neural ectoderm. Right: As gastrulation proceeds the shield derivatives (prechordal plate and notochord) migrate towards the animal pole and will be in contact with the neural ectoderm. A, anterior; P, posterior; V, ventral; D, dorsal. Adapted from de Souza and Niehrs, 2000.

suggested that in the mouse, the induction of anterior aspects of the neural tube requires developmental information not contained in the node. Evidence from embryological, genetic and molecular studies support a model in which the AVE is necessary for anterior development in the mouse, by providing additional signals that are not contained in the node (reviewed in Beddington and Robertson, 1999). In a mouse embryo, cells that will give rise to the AVE are located at the distal tip of the egg cylinder. Before formation of the primitive streak these cells move anteriorly to underlie the prospective forebrain and hindbrain regions (Thomas et al., 1998).

Genetic evidence supporting the role of the AVE in anterior neural induction and patterning comes from the analysis of mouse mutants, including *hnf3β*, *otx2* and *lim1*. Homozygous mutant embryos for these genes have brain deletions rostral to the otic vesicle. The absence of brain tissue in these mutants is due to a failure to induce the anterior neural plate (Acampora et al., 1995; Ang and Rossant, 1994; Shawlot and Behringer, 1995). Recent studies have shown that AVE markers like *cerl*, *lim1* and *hesx1* are reduced and mislocalised in these mutants, demonstrating that additionally these mutants have defects in the patterning and localisation of the AVE.

Analysis of chimeric embryos, containing different combinations of normal and mutant cells in extraembryonic regions, have provided the most convincing evidence that the AVE is important for anterior patterning in the mouse embryo. It was shown previously that ES cells injected into a blastocyst colonise all epiblast derivatives, but almost never the visceral endoderm (Beddington and Robertson, 1989). This developmental bias allowed the generation of chimeras where the embryo proper was of one genotype and the visceral endoderm of another. This technique was used to study the function of several genes, like *otx2*, *nodal*, *hnf3β* and *lim1*, in the visceral endoderm. For example, chimeric embryos where the epiblast is wild-type and the visceral endoderm is *otx2* mutant have the same brain defects as seen in the *otx2* mutants. Conversely, chimeric embryos with wild-type visceral endoderm and an *otx2* mutant epiblast rescue the early anterior neural defects, providing strong evidence that *otx2* is required in the visceral endoderm for normal brain development (Acampora et al., 1998; Rhinn et al., 1998).

Using the same technique, the function of *nodal*, *hnf3β* and *lim1* in the visceral endoderm was proven to be essential for normal forebrain and midbrain development (Dufort et al., 1998; Shawlot et al., 1999; Varlet et al., 1997).

Embryological evidence for the role of AVE in anterior neural patterning comes from ablation experiments. Removing the anterior region of the visceral endoderm during early stages of gastrulation prevents or severely compromises the expression of the forebrain marker *hesx1* in anterior neural ectoderm but does not affect the expression of the hindbrain marker *gbx2* (Thomas and Beddington, 1996). Taken together these results indicate that the AVE is necessary to establish anterior identity in the neural plate.

Although required for normal induction of the forebrain and midbrain regions of the neural tube, the AVE is not sufficient for this inductive process. Grafts of mouse AVE fail to induce neural epiblast in non-neural ectoderm and the same is true for a combination of AVE and the overlying epiblast tissue. Only a combination of AVE, anterior epiblast and early gastrula organizer (EGO) can induce anterior neural characteristics in an induced secondary axis (Tam and Steiner, 1999; Tam et al., 1997). EGO is a term used to define a group of cells located at the distal tip of the primitive streak of the early-streak mouse that display cell fates, gene expression and patterning activity characteristic of the morphological recognisable node of a full-length-streak stage mouse. These results suggest that the formation of the anterior neural plate requires co-operation between signals derived form the EGO and anterior germ layers tissues (Tam and Steiner, 1999). It is still possible that anterior neural characteristics might originate from non-anterior visceral endoderm, since these authors never reported the results of EGO plus non-anterior visceral endoderm control grafts.

Genetic evidence that EGO is required for anterior neural patterning has been provided by the analysis of the *wnt3*, *β-catenin*, *fgf8* and *cripto* mutant mice. In both *wnt3* and *β-catenin* mutants, EGO is not formed properly, as revealed by the lack of *T* and *gsc* expression, leading to no primitive streak or mesoderm formation. The AVE in these

36

mutants is correctly patterned as it expresses *cerl* and *lim1*. The AVE in the *wnt3* mutant is mislocalised. The epiblast of these mutants does not acquire however neural character, neither anterior nor posterior (Liu et al., 1999). In contrast, *fgf8 and cripto* mutants have a properly formed EGO, which expresses genes like *T, lim1* and *gsc*, and a properly specified AVE. However, in *fgf8* and *cripto* mutants the AVE has failed to move anteriorly. These mutants shown an expansion of forebrain and midbrain markers and the embryos resemble a head without a trunk (Ding et al., 1998; Sun et al., 1999). Taken together, the results from all these experiments show that in the absence of the early node, the AVE by itself is not sufficient to induce anterior neural character to the overlying epiblast. A recent report has shown that rabbit and mouse nodes can induce a complete neural axis when transplanted to chick ectoderm (Knoetgen et al., 2000). These authors proposed that the different results obtained between the mouse-to-mouse and the rabbit-to-chick or mouse-to-chick grafts are due to a difference in competence of the responding host tissue and not in the inducing capacity of node tissue.

1.6.2. Do other vertebrates have an AVE equivalent?

Unlike the mouse, the *Xenopus* embryo does not have any extraembryonic tissues. Nevertheless, a region adjacent to the organizer, called the anterior endoderm is thought to be the equivalent of the mouse AVE. These yolky cells are fated to became foregut, liver and the heart primordium. The anterior endoderm expresses genes that are also present in the mouse AVE, like *cerberus* and *hex* (Bouwmeester et al., 1996; Jones et al., 1999). It was shown that *hex*-expressing cells in *Xenopus* are first localised in the central part of the blastocoel floor and then move and populate the anterior endoderm adjacent to the organizer (Jones et al., 1999). The dorsal endoderm does not induce neural markers like *N-CAM* or *otx2* when recombined with dorsal ectoderm from an early gastrula embryo (Bouwmeester et al., 1996; Jones et al., 1999). This inability to generate anterior markers is also shared with the mouse AVE (Tam and Steiner, 1999). At this point, the results suggested that the anterior endoderm, could be involved in head induction in *Xenopus*. In contrast with the mouse AVE, however, embryological

experiments revealed that removal of the anterior endoderm in *Xenopus* does not affect head induction, in particular the expression of *otx2* and *en2* in the neural ectoderm remains normal. It does however, compromise the formation of the heart (Schneider and Mercola, 1999). It seems therefore, that *Xenopus* anterior endoderm cells are essential for heart development, but are not necessary for head induction (Schneider and Mercola, 1999). The anterior endoderm could, however, provide planar signals that could pattern the neuroectoderm before the onset of gastrulation. Another possibility is that anterior endoderm could induce head-organising properties in the organizer, since these two regions are adjacent before gastrulation begins. In fact, *cerberus* and *hex* are already expressed in the anterior endoderm by blastula stages (Jones et al., 1999; Zorn et al., 1999) and it has been suggested that these molecules prevent the trunk organizer to form in anterior regions of the organizer (Brickman et al., 2000; Piccolo et al., 1999).

In the chick, the equivalent tissue of the mouse AVE could be the anterior region of the hypoblast. This region is extraembryonic and expresses *hex* and a *cerberus* homologue, *caronte* (Rodriguez-Esteban et al., 1999; Viebahn, 1999; Yatskievych et al., 1999). It has been proposed that the migration of the hypoblast towards the anterior might be equivalent to the migration of *Xenopus* anterior endodermal cells towards the animal pole (Arendt and Nubler-Jung, 1999). Anterior hypoblast from pre-streak and mid-streak stage chick embryos does not have the ability to induce the forebrain marker *Ganf*, the homologue of mouse *hesx1* in transplantation experiments (Knoetgen et al., 1999). This shows that, as discussed for mouse AVE and *Xenopus* anterior endoderm, the chick anterior hypoblast is not able to induce neural tissue. In contrast with the mouse AVE, removal of the chick anterior hypoblast does not prevent the normal expression of *Ganf* in the ectoderm (Knoetgen et al., 1999). This results suggest that chick hypoblast is not required for anterior development. A recent study confirmed that the hypoblast is not able to induce neural tissue but it can, however, induce transient expression the early neural markers, *sox3* and *otx2* (Foley et al., 2000). These authors also propose that the role of the chick hypoblast is to direct the adjacent prospective forebrain cells away from the posteriorising influence of the organizer. A heterotopic experiment showed that rabbit AVE is able to induce the anterior molecular marker *Ganf*

in chick host embryos, suggesting that induction of anterior character by extraembryonic tissue might be a specific mammalian characteristic (Knoetgen et al., 1999).

In zebrafish, the region regarded as the AVE equivalent is the dorsal YSL. This a based on the fact that this particular region of the fish embryo is extraembryonic and expresses the gene *hex* (Ho et al., 1999). In contrast with the situation in *Xenopus*, over-expression of zebrafish *hex* downregulates *wnt8* and *bmp2* expression. This suggests that the YSL might be involved in inhibiting Wnt and BMP signalling, which as been shown to be a requisite for head induction (Ho et al., 1999). To date there is no evidence that signals from the YSL are required for head formation in zebrafish.

1.7. Aims and outline of this thesis

The aim of my project was to investigate several aspects of the dorsal organizer, using the zebrafish as a model system. The results are divided into four chapters representing the different aspects of the dorsal organizer studied.

The inducing abilities of the zebrafish dorsal organizer and the existence of separable head and trunk activities within the organizer are investigated in Chapter 3: Axis-Inducing Activities of the Embryonic Shield. I have used a new surgical method for shield removal and transplantation. Shields were transplanted to host embryos and the induced secondary axes were analysed. In addition, two distinct shield domains, defined by the molecular markers *gsc* and *flh*, were studied with regard to head and trunk inducing abilities.

The phenotype of zebrafish dorsal organizer removed embryos is analysed in Chapter 4: Developmental Consequences of Embryonic Shield Removal. Using a set of molecular markers, I have characterised the effect of partial and complete shield removal on mesoderm and neural patterning.

In Chapter 5: Insights into the Mechanism of Shield Derivative Regeneration after Morphological Shield Removal, I describe investigations into the processes that could be involved in shield tissue regeneration after morphological shield removal, namely cell proliferation and cell fate change.

In Chapter 6: Contribution of the New Surgical Method to Study Gene Function in Axial Midline Mutants, I describe the use of the new shield removal and transplantation technique to study autonomy and cell movement in *sneezy* and *siberblick/wnt11* mutants.

Each Chapter of results has a short introduction specific to the aspect of dorsal organizer analysed and a discussion of the results obtained. The last Chapter is a general discussion of the contribution of this work to our understanding of the role of the dorsal organizer.

Chapter 2

Materials and Methods

2.1. Abbreviations

BCIP	X-phosphate/5-Bromo-4-chloro-3-indolyl-phosphate
BSA	Bovine serum albumin
DAB	Diaminobenzidine
DEPC	Diethylpirocarbonate
DIG	Dioxigenin
DTT	Dithiothreitol
EDTA	Ethylene-diamine-tetra-acetate
HEPES	N-2-hydroxyethylpiperazine-N'-2-ethanesulfonic acid
HRP	Horseraddish peroxidase
IPTG	Isopropylthio-β-D-galactosidase
NBT	4-Nitro blue tetrazolium chloride
OD	Optical density
PEG	Polyethylene glycol
SDS	Sodium lauryl sulfate
X-Gal	5-bromo-4-chloro-3-indolyl-β-D-galactosidase
ATP	Adenosine 5'-triphosphate
CTP	Cytidine 5'-triphosphate
UTP	Uridine 5'-triphosphate
GTP	Guanidine 5'-triphosphate
TTP	Thymidine 5'-triphosphate

2.2. Molecular Biology Techniques

2.2.1. Preparation and storage of competent bacteria

TOP10 One Shot Chemical Competent (Invitrogen) bacterial cells were used in this work.

2.2.1.1. Chemical competent cells

A single colony was inoculated in 10 ml of LB medium and shaken at 37°C overnight. An appropriate amount of this culture was used to inoculate LB medium so that the initial culture would have an OD_{600} of 0.075. The culture was then incubated at 37°C with agitation. At the beginning of the exponential phase (OD_{600} of 0.3 to 0.5) the culture of 50 ml was put in ice for a period of 10 minutes. After washing in ice-cold 25 ml of 0.1 M $MgCl_2$, cells were repelled. Cells were resuspended in ice-cold 25 ml of 0.1 M $CaCl_2$ and incubated on ice for 20 minutes. Finally, the cells were pelleted and resuspended in 3.3 ml of ice-cold 0.1 M $CaCl_2$ and 15% (v/v) glycerol, aliquoted and quickly frozen in dry ice before being stored at -80°C.

2.2.1.2. Electrocompetent cells

A single colony was inoculated in 10 ml of SOB-Mg medium shaken at 37°C overnight. 500 ml of pre-warmed SOB-MG medium was inoculated with 5 ml of the overnight culture and shaken at 37°C until the OD_{600} reached 0.75. The cells were decanted into a chilled 450 ml bottle and spun. The pellet was resuspended in 400 ml ice-cold 10% glycerol by swirling or pipetting. This spin and the resuspension in 10% glycerol were repeated again. The pellet was resuspended in the last few drops of liquid and transferred to a disposable plastic tube and the volume was measured. A small aliquot was diluted 300X to 1000X and the OD_{600} was measured. The concentration of cells

was adjusted to a final concentration OD_{600} of 250 units/ml (meaning that a 1000X dilution would have an OD_{600} of 0.25). The cells were aliquoted and quickly frozen in dry ice before stored at -80°C.

2.2.2. Plasmid transformation of competent bacteria

2.2.2.1. Transformation of chemical competent bacteria

Up to 100 ng of DNA was added to 100 μl of cells thawed on ice. The bacterial cells were kept on ice for 5 to 30 minutes and then heat shocked at 42°C for 30 seconds followed by cooling on ice for a few minutes. After this period, 250 μl of SOC medium was added and the mixture was incubated at 37°C for 1 hour with agitation. An aliquot of 10 to 200 μl from each transformation were spread in a selective agar plate (100 mg/ml of ampicillin) and incubated overnight at 37°C. To select recombinants 40 μl of X-Gal (20 mg/ml in dimethylformimide) and 40 μl of IPTG (200 mg/ml) were used per plate.

2.2.2.2. Transformation of electrocompetent bacteria

Up to 100 ng of DNA were added to 20 μl of cells thawed on ice and immediately transferred to a pre-cooled 0.1 cm electroporation chamber. Cells were electroshocked under 1.8 kV, 25 μF and 200 Ω. 1 ml of SOC medium was immediately added, the mixture was transferred to a plastic tube and incubated with shaking at 37 °C for 1 hour. Each transformation was platted as described in section 2.2.2.1.

2.2.3. Preparation of plasmid DNA

2.2.3.1. Small scale preparation of DNA

From a 3.5 ml overnight culture of transformed TOP10 One Shot bacteria in LB medium with 100 mg/ml of ampicillin, 1.5 ml was transferred to a 1.5 ml microcentrifuge tube and spun for 20 seconds. The supernatant was removed completely and the pellet resuspended in 300 μl of Resuspension Buffer (Qiagen; 10 mM EDTA, 50 mM Tris.HCl pH 8.0, 100μg/ml RNase). 300 μl of Lysis Buffer (Qiagen; 0.2 M NaOH, 1% SDS) was added, mixed and left for 2 minutes at room temperature to allow alkaline lysis of the cells. Lysis solution was then neutralised by adding 300 μl of ice-cold Neutralisation Buffer (Qiagen; 3 M KOAc pH 5.5) and mixed carefully by inverting the tube a few times followed by 10 minutes incubation on ice. The tube was spun for 15 minutes at room temperature. 700 μl of the supernatant was transferred into a fresh microcentrifuge tube and phenol/chloroform extraction was performed (see section 2.2.5.). DNA was precipitated from the aqueous upper layer by adding 650 μl of isopropanol, leaving 15 minutes and then spinning for 15 minutes, all at room temperature. After centrifugation the pellet was washed in 70% ethanol, dried and resuspended in distilled water with 0.1 mg/ml RNase A (Sigma).

2.2.3.2. Medium scale preparation of DNA

0.1 to 1 ml of plasmid bacterial culture was placed in 100 ml of LB medium containing 100 mg/ml ampicillin, and shaken at 37°C overnight. The Qiagen midi kit was then used to isolate the DNA, according to the QIAfilter Midi protocol as suggested by the manufacturers.

2.2.4. DNA quantification and manipulation

DNA and RNA were quantified by spectrophotometry at 260 nm (an OD of 1 equates to 50 µg/ml double stranded DNA, 35 µg/ml single stranded DNA and 40 µg/ml RNA). The ratio between the readings at 260 nm and 280 nm provided an estimate of the purity of the nucleic acid preparation (pure preparations of DNA and RNA should have OD_{260}/OD_{280} values of 1.8 and 2.0, respectively).

2.2.5. Phenol/Chloroform extraction

To remove proteins from nucleic acid solutions, a mixture of phenol:chloroform:isoamyl-alcohol (25:24:1 volume ration) was added in a 1:1 volume ratio to the DNA solution and vortexed for 1 minute. After a 3 minutes centrifugation, the upper (aqueous) layer was transferred into a new microcentrifuge tube and extracted with an equal volume of chloroform.

2.2.6. Precipitation

2.2.6.1. Ethanol Precipitation

Ethanol precipitation was carried out by adding 3 M NaOAc pH 5.5 (to a final concentration of 0.3 M) and 2.5 volumes of 100% ethanol to the DNA solution that was then left on dry ice for approximately 20 minutes. 1 µl of 10 mg/ml glycogen was often used as a carrier if the DNA amount to be purified was too small to be visualised as a pellet at the bottom of the tube. Centrifugation at 20 000 g for 5 to 20 minutes was performed and the DNA pellet was then washed in 70% ethanol, dried and resuspended in TE or distilled water.

2.2.6.2. PEG precipitation

PEG precipitation was performed before sequencing to ensure removal of contaminant RNA. PEG precipitation was carried out by adding 30 μl of 20% PEG/2.5 M NaCl to 50 μl of DNA solution, followed by incubation on ice for 30 minutes and centrifugation for 10 minutes at 4°C. The pellet was washed in 70% ethanol, dried and then resuspended in a suitable volume of distilled water or TE.

2.2.7. Restriction digestions

Restriction enzyme digests were performed at the recommended temperature for approximately 1 hour using commercially supplied restriction enzymes and buffers (Boehringer Mannheim, Promega, New England Biolabs). The enzyme component of the reaction never comprised more than 10% of the reaction volume. For enzyme digests using more than one restriction enzyme, the buffer suggested by the manufacturer was used.

2.2.8. Agarose gel electrophoresis of DNA and RNA

DNA separation and size estimation were performed by agarose gel electrophoresis. Gels were prepared by dissolving agarose in 0.5X TAE to a final concentration of 0.8% to 2% depending on the expected size of the DNA fragment. To visualise the DNA, 0.5 mg/ml ethidium bromide was added to the gel. DNA samples were mixed with 6X gel loading buffer and electrophoresis was performed at 5 to 20 V/cm of gel length, until the appropriate resolution was achieved. The resolved DNA was visualised using ultraviolet light at 302 nm, and the size was estimated by comparison with known size markers such as the 1 kb size marker (Gibco BRL).

2.2.9. Purification of specific DNA fragments from gels

In order to purify DNA fragments of interest, DNA was subjected to agarose gel electrophoresis and the region of the gel containing the appropriate band was excised under ultraviolet light (302 nm). DNA was purified using the QAIquick Gel Extraction Kit protocol using a microcentrifuge, according to the instructions of the manufacturer (Qiagen).

2.2.10. *In vitro* transcription

2.2.10.1. RNA for *in situ* hybridisation

The RNA probes were prepared in a 20 μl reaction mixture containing: 1 μg of linearized template DNA, 1x transcription buffer, 1x DIG-RNA labelling mix (Boehringer Mannheim), 20 units of RNase inhibitor (Promega), 40 units of the appropriate T7 (Promega), T3 (Boehringer Mannheim) or SP6 (Boehringer Mannheim) RNA polymerase. The reaction mixture was incubated for 2 hours at 37°C. To remove the plasmid DNA, the reaction mixture was incubated for 30 minutes at 37°C with 2 units of RNase-free DNase I (Promega). The mixture was then subjected to size exclusion chromatography using Chroma Spin-30+DEPC-H2O columns (Clontech) to remove free nucleotides.

Table 2.1. Templates for antisense RNA probes used in this thesis

Gene	Linearization site	RNA polymerase	Reference
dlx3	EcoRI	T7	(Akimenko et al., 1994)
emx1	BamHI	T3	(Morita et al., 1995)
en1	XbaI	T3	(Ekker et al., 1992)
EphA4	EcoRI	T3	(Xu et al., 1994)
flh	EcoRI	T7	(Talbot et al., 1995)
gsc	EcoRI	T7	(Stachel et al., 1993)
hgg1	XhoI	T3	(Thisse et al., 1994)
hlx-1	XbaI	T7	(Fjose et al., 1994)
isl-1	XbaI	T3	(Inoue et al., 1994)
ntl	XhoI	T7	(Schulte-Merker et al., 1994)
shh	HindIII	T7	(Krauss et al., 1993)
twh	PstI	T7	(Ekker et al., 1995)
zADMP	EcoRI	SP6	This thesis
zanf	XhoI	T7	(Kazanskaya et al., 1997)

2.3. Embryo Manipulations

2.3.1. Embryo collection

Zebrafish (Danio rerio) embryos were raised at 28°C in embryo water (red sea salt 0.03 g/l, methylene blue 2 mg/l) or in 0.3X Danieau solution (full strength (1X) Danieau solution is 58 mM NaCl, 0.7 mM KCl, 0.4 mM $MgSO_4$, 0.6 mM $Ca(NO_3)_2$, 5 mM HEPES, pH 7.6) (Shih and Fraser, 1996). Approximate stages are given in hours-post-fertilisation (hpf) at 28°C according to the morphological criteria provided in (Kimmel et al., 1995).

2.3.2. Embryo labelling

Donor embryo chorions were removed by 4 minutes incubation in 0.5 mg/ml pronase (Sigma, P-8811) in 0.3X Danieau solution followed by several washes in 0.3X Danieau solution. Donor embryos were then transferred into ramps made of 2% agarose in 0.3X Danieau solution covered with 0.3X Danieau solution. Donor embryos were labelled at the 1-4 cell stage by micro-injection into the yolk cell with 5% lysine-fixable fluorescein or lysine-fixable rhodamine dextran (Molecular Probes) and 5% lysine-fixable biotin dextran (Molecular Probes) in 0.2 M KCl.. Caged biotinylated lysine-fixable fluorescein dextran dye (Molecular Probes) was dissolved at 2.5% in 5 mg/ml Phenol red in 0.2 M KCl and centrifuged for 5 minutes. The supernatant was microinjected into embryos at the 1-4 cell stage. The caged fluorescein-dextran injected embryos were handled in the dark as much as possible. Injected embryos were cultured at 28°C in 2% agarose-coated dishes.

2.3.3. Embryo microsurgery

Transplantation pipettes were pulled from 1 mm borosilicate glass capillaries (World Precision Instruments, 1B100-4) and cut with a diamond pencil to an inner diameter of approximately 200 μm. A sharp inner edge is optimal and the plane of the cut was orthogonal to the long axis of the pipette. The pipettes were initially filled with medium and then loaded into a pipette holder filled with mineral oil. The pipette holder (World Precision Instruments, 5430-10), carried by a 3-axis micro-manipulator (Narishige, MN-153), was connected, via a continuous column of mineral oil, to a 50 μl Hamilton syringe driven by micrometer controlled syringe pump (Stoelting, 51218).

Microsurgery was performed at 19-21°C in 1X Danieau solution containing 5% penicillin/streptomycin (Gibco-BRL, 15140-114). Chorions of host embryos were removed with watchmaker's forceps shortly before transplantation. Donor and host embryos were loaded into transplantation wells that had been pre-formed with an acrylic

mould in 2% agarose 1X Danieau solution. Transplantation wells were 1.0 mm deep by 1.0 mm wide, with the bottom surface of the well sloping from the back wall of the well approximately 1.3 mm to the surface of the agarose.

To remove shield tissue, donor embryos were oriented such that the shield faced the pipette tip and the transplantation pipette was placed over the shield. Shield tissue was gently drawn in and out of the pipette generally 3 or 4 times until the yolk cell and shield tissue became separated. Two tissue removals were necessary for complete shield region ablation.

To transplant the shield tissue, hosts were oriented so that the site of transplantation was 180° from the host shield. With the donor shield in the pipette, the tip of the pipette was placed onto the host embryo, at the margin, and a piece of ventral tissue was removed and discarded. The donor shield was pushed to the tip of the pipette, which was placed over the hole in the host embryo. The donor shield was very gently expelled into the host embryo. Typically, the enveloping layer (EVL) of the host inflated a little, making space for the donor tissue. For acceptable transplants, the donor shield tissue became trapped under the EVL either directly beneath or immediately adjacent to the hole. Transplanted embryos were left in the transplantation well for about 10 minutes to recover then transferred to 0.3X Danieau 5% penicillin/streptomycin on 2% agarose 0.3X Danieau for overnight culture.

In some experiments explanted shields were further manipulated before transplantation in order to separate deep and superficial shield tissue. Explanted shields were laid on a flat agarose surface, held with a hair loop, while several cuts were made with an eyebrow hair knife. Two vertical cuts were made to divide the shield into 3 equal pieces. The central piece was discarded. The shield fragment originally adjacent to the yolk syncytial layer (i.e. the deep fragment) was further trimmed by two lateral cuts to minimise contamination with superficial cells. Fragments were then transplanted as described for whole shields above.

2.3.4. Whole-mount *in situ* hybridisation

Whole-mount *in situ* hybridisations were performed essentially as described by Thisse and Thisse (Thisse and Thisse, 1998). Embryos fixed with 4% paraformaldehyde/PBS at 4°C were dehydrated with methanol at -20°C and rehydrated by soaking for 5 minutes each in 75% methanol/PBT; 50% methanol/PBT; 25% methanol/PBT and then 4 times 5 minutes in 100% PBT. All the 24 hpf embryos were digested with proteinase K (10 µg/ml) for 15 minutes. Embryos were refixed in 4% paraformaldehyde for 20 minutes at room temperature and then washed in PBT 5 times 5 minutes. They were then transferred to hybridisation buffer (50% formamide, 5X SSC (pH7.0), 500 µg/ml type VI torula yeast RNA, 50 µg /ml heparin, 0.1% Tween 20, 9 mM citric acid to pH 6.0-6.5) for 2-5 hours at 70°C. The hybridisation buffer (Hyb) were then replaced with the mixture containing 150 ng of DIG-labelled RNA probe in 200 µl of preheated hybridisation solution and the embryos were incubated at 70°C overnight. Washes were done at the hybridisation temperature with preheated solutions for 15 minutes each with 75% Hyb/2X SSC; 50% Hyb/2X SSC; 25% Hyb/2X SSC; 100% SSC and finally 2 times 30 minutes in 0.2X SSC. A series of washes were performed at room temperature for 10 minutes each in 75% 0.2X SSC/PBT; 50% 0.2X SSC/PBT; 25% 0.2X SSC/PBT and 100% PBT. The embryos were blocked in 2 mg/ml BSA, 2% goat serum in PBT for several hours. The embryos were incubated with alkaline-phosphatase (AP)- conjugated anti-DIG Fab fragments diluted 1:5000 in 2 mg/ml BSA, 2% goat serum in PBT at 4°C overnight with agitation. After washing at least 8 times for 15 minutes with PBT, the embryos were rinsed 3 times 5 minutes in NTMT reaction buffer (0.1 M Tris-HCl pH9.5; 50 mM $MgCl_2$; 0.1 M NaCl; 0.1% Tween 20). Detection was performed using NBT/BCIP (112.5 µl of 100 mg/ml NBT in 70% dimethylformamide and 175 µl of 100 mg/ml BCIP in 70% of dimethylformamide added to 50 ml of NTMT). After stopping the reaction with 100% PBS, the embryos were refixed in 4% paraformaldehyde/PBS. Embryos were cleared with 20% glycerol/80% PBS, 50% glycerol/50% PBS and stored at 4°C in 80% glycerol/20%PBS.

2.3.5. Immunolocalisation of the lineage tracers

The fate of transplanted embryonic tissues labelled with rhodamine dextran and biotin dextran was recorded by direct fluorescence observation or by staining with avidin-HRP (Vector Labs). Embryos were fixed in paraformaldehyde, dehydrated in series of methanol and treated with proteinase K as described in section 2.3.4. For staining, embryos were incubated for 1 hour at room temperature with avidin-HRP complex in PBT, then washed 5X with PBT and incubated in 0.4 mg/ml DAB in PBT for 1 hour at room temperature. The staining reaction was initiated by the addition of a fresh solution of 0.4 mg/ml DAB/PBT containing 0.003% of H_2O_2. After stopping the reaction with several washes of PBT, embryos were re-fixed in 4% paraformaldehyde/PBS. Embryos were cleared with 20% glycerol/80% PBS, 50% glycerol/50% PBS and stored at 4°C in 80% glycerol/20% PBS.

The fate of transplanted embryonic tissues labelled with fluorescein dextran was recorded by direct fluorescence or staining with NBT/BCIP. Embryos were fixed in paraformaldehyde, dehydrated in series of methanol and treated with proteinase K as described in section 2.3.4. The endogenous alkaline phosphatase was inactivated by placing the embryos for 30 minutes at 65°C. The embryos were blocked in 2 mg/ml BSA, 2% goat serum in PBT for several hours. The embryos were incubated with alkaline-phosphatase (AP)- conjugated anti-Fluorescein Fab fragments diluted 1:2000 in 2 mg/ml BSA, 2% goat serum in PBT at 4°C overnight with agitation. After washing at least 8 times for 15 minutes with PBT, the embryos were rinsed 3 times 5 minutes in NTMT reaction buffer (0.1 M Tris-HCl pH9.5; 50 mM MgCl2; 0.1 M NaCl; 0.1% Tween 20). Detection was performed using NBT/BCIP (11.25 μl of 100 mg/ml NBT in 70% dimethylformamide and 17.5 μl of 100 mg/ml BCIP in 70% of dimethylformamide added to 50 ml of NTMT). After stopping the reaction with 100% PBS, the embryos were refixed in 4% paraformaldehyde/PBS. Embryos were cleared with 20% glycerol/80% PBS, 50% glycerol/50% PBS and stored at 4°C in 80% glycerol/20%PBS.

2.3.6. Whole-mount antibody staining

The embryos were fixed in 4% paraformaldehyde, rehydrated in series of methanol and then digested with proteinase K as described in section 2.3.4. The endogenous alkaline phosphatase was inactivated by placing the embryos for 30 minutes at 65°C. The embryos were blocked in 2 mg/ml BSA, 2% goat serum in PBT for several hours. The embryos were incubated with the primary antibody diluted in 2 mg/ml BSA, 2% goat serum in PBT at 4°C overnight with agitation. After washing at least 8 times for 15 minutes with PBT, the embryos were blocked again and incubated at 4°C overnight with the secondary antibody. The secondary antibody was washed at least 8 times 15 minutes. Detection was performed using the avidin-HRP (Vector Labs) as described in section 2.3.5.

Immunolocalisation of cells in mitosis was carried out using the Anti-phospho-Histone H3 (Upstate Biotechnology, 1ug/ml), a polyclonal antibody specific for phosphorylated histone H3 (Hendzel et al., 1997). Secondary antibody was HRP-conjugated goat anti-rabbit IgG (BioRad, 1:1000). Immunolocalisation of primary neurons and their ventral root axonal projections was carried out using the znp1 monoclonal antibody (Trevarrow et al., 1990). Secondary antibody was HRP-conjugated goat anti-mouse IgG (BioRad, 1:100).

2.3.7. Fate mapping

A siliconised glass ring was placed on the top of glass slide. A drop of 3% methylcellulose (1.500 centipoises, Sigma) was placed in the middle of the ring and then an early shield stage embryo was placed inside the methylcellulose. The glass ring was filled with 1X Danieau solution. Uncaging was performed with a 10 second pulse of a 365 nm pulsed nitrogen laser (Micropoint) focused through a 40X water-immersion objective of a Leica compound microscope onto a single cell at a time.

2.3.8. Sectioning

Embryos were first processed by whole mount *in situ* hybridisation, as described in section 2.3.4. Stained embryos were dehydrated in a graded series of ethanol and then embedded in Agar 100 Resin Kit, Agar Scientific, Ltd. overnight at room temperature. The next day the embryos were transferred into trapezoid molds (Pelco, Inc.) filled with freshly prepared resin. After 1 hour at 65°C, the embryos were oriented by hand and then baked for an additional 24 hours. 3 μm sagittal sections were cut on a Reschert-Jung Ultracut E microtome.

2.3.9. Electron microscopy

Embryos for scanning electron microscopy were fixed overnight in half-strength Karnovsky fixative (Karnovsky, 1965), rinsed in 0.1 M cacodylate buffer, and post-fixed in ice-cold 1% osmium tetroxide in 0.1 M cacodylate buffer. Samples were then dehydrated through graded concentrations of ethanol, rinsed twice in acetone, and critical-point dried in CO_2, before being sputter coated with gold and viewed with a Philips 515 scanning electron microscope.

2.3.10. Photomicrography

Nomarski and live fluorescence images were obtained using a Leica compound microscope fitted with a Princeton Instruments, MicroMax cooled-CCD camera. MetaMorph image processing software was used to acquire images and overlay fluorescence and Nomarski images. Whole-mount *in situ* hybridisation images were obtained using a Zeiss Axiophot microscope fitted with a Kodak DCS420 digital camera.

2.4. Formulation of Frequently Used Solutions

1X PBS	137 mM NaCl, 2.7 mM KCl, 4.3 mM Na2HPO4.7H2O, 1.4 mM KH2PO4
1X PBT	1X PBS, 0.1% Tween 20
1X TAE	40 mM Tris.acetate, 2 mM Na2EDTA.2H2O (pH 8.5)
1X TE	1 mM EDTA, 10 mM Tris.HCl pH 8.0
20X SSC	3 M NaCl, 0.3 M Na3citrate.2H2O, adjust pH to 7.0 with 1 M HCl
6X gel loading buffer	6X TAE, 50% v/v glycerol, 0.25% w/v bromophenol blue

2.5. Formulation of Frequently Used Bacterial Growth Media

LB (L-Broth)	1% w/v bacto-tryptone, 0.5% w/v bacto-yeast extract, 1% w/v NaCl
SOC	2% Tryptone, 0.5% Yeast Extract, 10 mM NaCl, 2.5 mM KCl, 10 mM MgCl$_2$, 10 mM MgSO$_4$, 20 mM glucose

Chapter 3

Axis-Inducing Activities of the Embryonic Shield

3.1. Introduction

Characterisation of the teleost fish organizer by various researchers has led to similar but distinct conclusions. In her pioneering work, Oppenheimer showed that transplanted pieces of embryonic shield from *Perca* were able to induce a complete secondary axis in host embryos (Oppenheimer, 1936; Oppenheimer, 1953). Shih and Fraser (1996) found that pieces of embryonic shield from zebrafish grafted to host embryos were able to induce secondary axes but were never able to induce the most anterior structures, such as eyes or telencephalon. These data suggested the possibility that anterior specification in zebrafish, similar to mouse, requires spatially distinct activities. The fact that the embryonic shield of another teleost fish, *Perca,* is capable of inducing the formation of a complete secondary axis suggests that part of the organizer activities were lost in previous zebrafish shield transplantation experiments (Shih and Fraser, 1996).

The notion of separable head and trunk organizer activities arises from experiments in *Xenopus* and chick, which have shown that progressively older organizers induce neural tissue of increasingly posterior character (reviewed in Hamburger, 1988; Storey et al., 1995). It was known that the *Xenopus* organizer is subdivided into anterior and posterior domains defined by the expression of *gsc* and *Xnot*, respectively (Cho et al., 1991; von Dassow et al., 1993). Zoltewicz and Gerhart (1997) found that these domains are not only distinct in terms of gene expression but also in their developmental fate and neural inducing ability. The anterior domain, which will give rise to prechordal mesoderm of the head, is able to induce a secondary axis possessing only anterior structures. By contrast, the posterior domain, which will became notochord and somites, can induce secondary axes uniquely possessing posterior structures (Zoltewicz and Gerhart, 1997).

When the zebrafish embryonic shield becomes morphologically apparent, it consists of superficial epiblast and deep hypoblast layers resting on the yolk cell and covered by a tight epithelium called the enveloping layer (EVL). The structure of the shield is also manifest in differential gene expression. For example, epiblast cells of the shield

express the homeobox gene *floating head* (*flh*) (Talbot et al., 1995), whereas the deeper hypoblast cells express the homeobox gene *goosecoid* (*gsc*) (Stachel et al., 1993). A recent study has shown that *gsc*-expressing cells are fated to give rise to prechordal plate, whereas *flh*-expressing cells give rise to notochord (Gritsman et al., 2000). The same study also showed that the activity of the Nodal signalling pathway has a role in AP patterning of the embryonic shield. High levels of Nodal signalling are necessary for *gsc* expression and prechordal plate formation, while lower levels of Nodal signalling are required for *flh* expression and formation of the notochord. In *one-eyed pinhead* mutants in which the Nodal signalling is impaired, *gsc* expression is down regulated and *flh* expression is expanded and in consequence the prechordal plate domain is transformed into notochord (Gritsman et al., 2000). A study in the chick showed that the specification of axial mesoderm into prechordal plate and notochord domains is only established at later stages through BMP and Activin signals derived from the anterior endoderm (Vesque et al., 2000).

As in *Xenopus*, the zebrafish organizer seems to be subdivided into distinct domains of gene expression and developmental fate. Whether or not these domains correspond to functionally distinct regions was a question that required investigation. We have developed a new method for shield removal and transplantation suitable for zebrafish embryos. Using this method, I have reinvestigated the question of whether the fish organizer can induce a complete secondary axis. I have also investigated the structure of the zebrafish organizer by testing whether the *gsc*-expressing domain and the *flh*-expressing domain have distinct organizer activities.

3.2. Results

3.2.1. A new method for shield removal and transplantation

The tools traditionally used for surgery of amphibian embryos (i.e. the hair-loop and the eyebrow-hair knife) are inadequate for the zebrafish because of structural differences between these embryos. The large yolk cell of the zebrafish embryo is fragile and can be easily punctured, when attempting to cut through the overlying blastoderm. In order to consistently remove and transplant embryonic shields from zebrafish embryos a new method was developed. This method (Fig. 3.1; see also Chapter 2, section 2.3.3.), employs a glass pipette with an inner diameter approximately the size of the morphological shield, connected by a column of oil to a microsyringe pump. Shield removal and transplantation were performed on 6 hours-post-fertilisation (hpf) zebrafish embryos when the embryonic shield first becomes visible. As the shield was drawn into the pipette a protuberance of yolk was also pulled in. Once the shield was withdrawn it was possible to see that the protruding yolk was free of blastoderm cells. Using this technique, I was able to completely remove both the superficial epiblast and the deep hypoblast cells (i.e. the full thickness of the embryonic shield) without damaging the yolk cell. After removal, the shield was kept within the pipette while a piece of host ventral germ-ring was removed. The piece of ventral tissue was immediately discarded and the space created in the ventral side was used to graft the donor shield into the host embryo.

3.2.2. The shield can induce a complete secondary axis

To test the inducing abilities of the zebrafish organizer, the morphologically defined shield was removed from lineage tracer labelled 6 hpf embryos and transplanted into the ventral germ-ring of 6 hpf host embryos. Experimental embryos were cultured until 24 hpf and analysed. The inductive potential of the grafted shield was compared with that of ventral germ-ring grafts of similar size. Shield-to-ventral margin grafts could induce
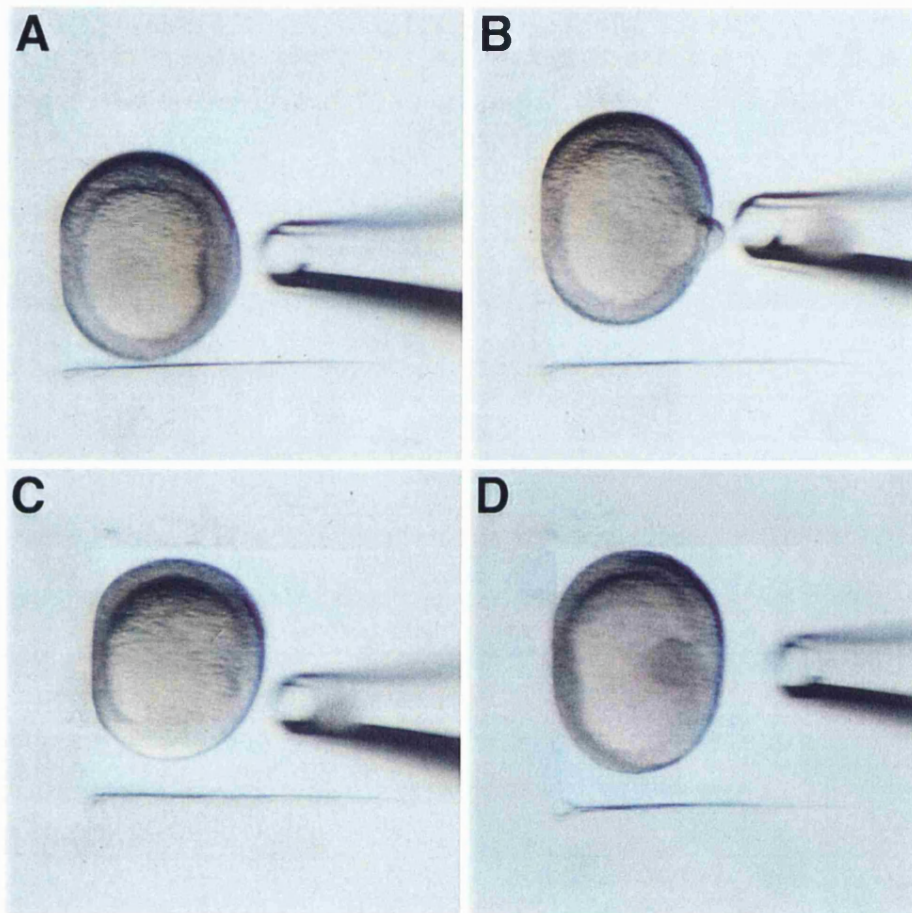
Fig. 3.1. Experimental method for shield removal and transplantation. Shield removal is accomplished by aspiration from a 6 hpf embryo previously labelled with a lineage tracer dye. (**A**) The donor embryo is positioned with the shield facing the pipette. (**B**) The shield is removed from the embryo by gentle trituration and kept within the pipette. (**C**) Prior to transplantation, an equivalent size piece of host ventral tissue is removed and discarded. (**D**) The donor shield is then inserted under the EVL in the ventral side of a host embryo.

a complete secondary axis, with eyes, a beating heart, notochord and somites in 51% (n=151) of the transplantation experiments (Table 3.1; Fig. 3.2). Incomplete secondary axes were seen in 41% of shield-to-ventral margin grafts. These incomplete axes included embryos with a range of anterior truncations and embryos possessing only trunk (Table 3.1). No induction was observed in 8% of the shield grafting experiments (Table 3.1). In all of the ventral germ-ring grafts no induction was observed (n=14). In all the complete and incomplete secondary axes the anterior end was facing the animal pole. The anterior-most part of the secondary axis, however, could be at some distance from the anterior-most part of the primary axis (Fig. 3.2A, B) or could be touching the anterior-most part of the primary axis (Fig. 3.3A). In addition, secondary axes were found at all angles from the primary axis ranging from 180° (Fig. 3.3A) to adjacent or even overlapping (data not shown).

The anterior patterning of induced complete secondary axes was examined by whole-mount *in situ* hybridisation using antisense riboprobes complementary to the receptor tyrosine kinase *EphA4* (Xu et al., 1995; Xu et al., 1994) and the homeobox gene *emx1* (Morita et al., 1995). In all complete secondary axes analysed (n=18), *EphA4* expression was detected in the presumptive dorsal thalamus and the region adjacent to the otic vesicle. This expression pattern indicates the proper induction and patterning of the diencephalon (posterior part of the forebrain) (Fig. 3.2D, E). *EphA4* was also expressed in rhombomeres 1,3 and 5 demonstrating that the hindbrain was also normally patterned (Fig. 3.2D, E). *emx1* was expressed in all complete secondary axes (n=8), indicating that the telencephalon (anterior part of the forebrain) was present in the induced axes (Fig. 3.2F, G). These results show that the induced complete secondary axes had a fully patterned forebrain and hindbrain. The extent of anterior patterning in the induced complete secondary axes, was independent of its position relative to the primary axis (compare Fig. 3.2D, F with Fig. 3.2E, G).

Table 3.1. Transplantation of the embryonic shield to the ventral side of a 6 hpf embryo

	number induced / number grafted											%
complete	15/32	1/8	4/4	13/21	8/9	18/20	4/11	5/14	2/9	3/8	5/15	**51±9**
incomplete												
telenceph.	3	0	0	0	0	0	7	4	3	5	5	**21±8**
inc. heart	8	6	0	6	1	2	0	0	0	0	0	**14±7**
inc. o.v.	0	1	0	1	0	0	0	1	0	0	3	**4±2**
trunk only	2	0	0	1	0	0	0	0	0	0	1	**2±1**
no induction	4	0	0	0	0	0	0	4	4	0	1	**8±4**

% = average of the percentage of each experiment ± standard error of the mean (s.e.m.)

telenceph. = an embryo with telencephalon, as defined by the presence of *emx1*, but no eyes

inc. heart = an embryo with no forebrain, but with a beating heart

inc. o.v. = an embryo induced anterior only to the level of the otic vesicle
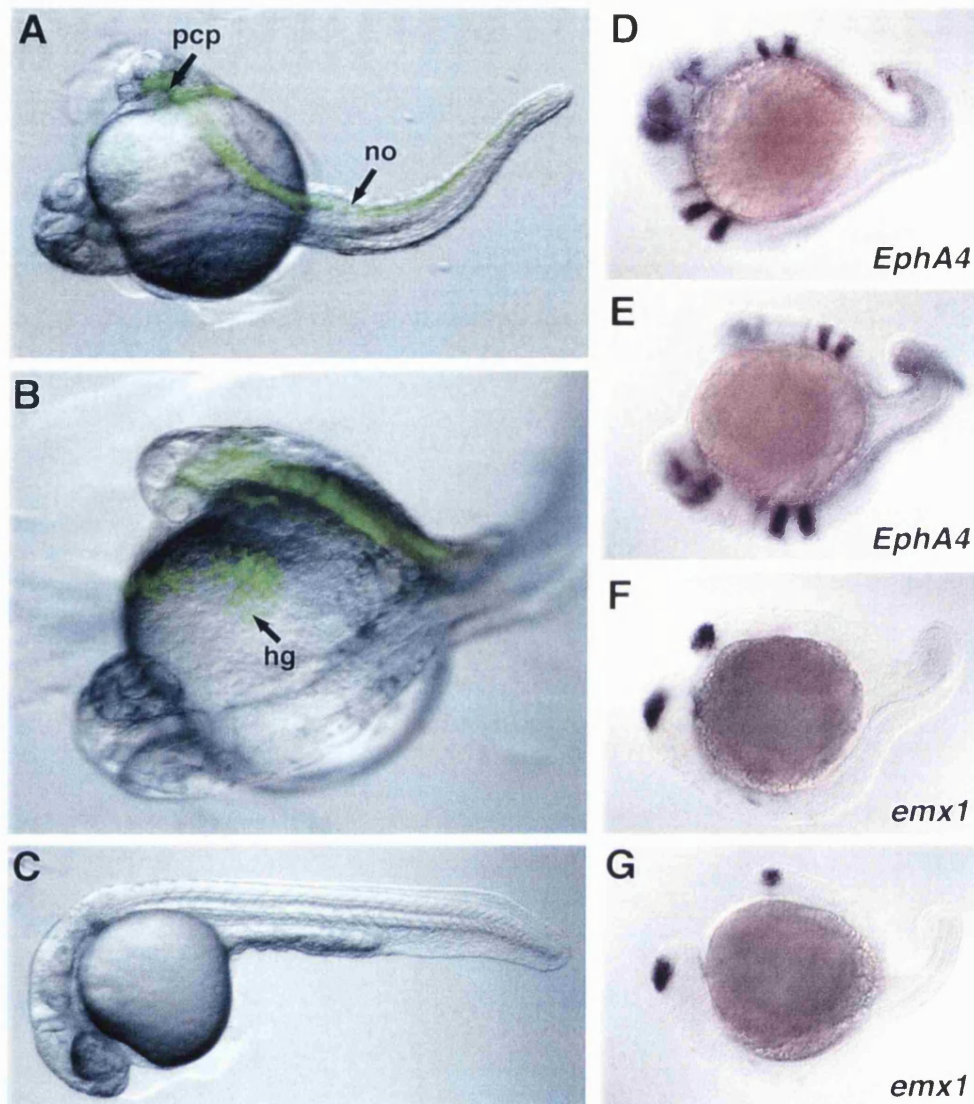
Fig. 3.2. Transplantation of the embryonic shield to the ventral side of a host embryo. (A, B) A morphologically defined shield, derived from a 6 hpf embryo, is able to induce a complete secondary axis when transplanted to the ventral side, within the germ-ring. The induced secondary axes possess the most anterior structures including a normal head with two eyes. **(C)** A differential interference contrast (DIC) image showing that the shield donor embryo developed completely normal. **(D, E)** In a complete secondary axis, the diencephalon is normally patterned as revealed by *EphA4* expression in the presumptive dorsal thalamus and the region adjacent to the otic vesicle. The rhombencephalon is also normally patterned as revealed by the expression of *EphA4* in rhombomeres 1, 3, and 5. **(F, G)** The telencephalon of a complete secondary axis is normally patterned as revealed by *emx1* expression. **(D, E, F, G)** Lateral views of 24 hpf embryos with anterior to the left and induced secondary axis up. hg, hatching gland; pcp, prechordal plate; no, notochord

3.2.3. Cell fates of the grafted shield

The fates of shield-derived cells, determined either by homotopic transplantation or by fate mapping are hatching gland, prechordal plate, notochord, floor plate and hypochord (Melby et al., 1996; Shih and Fraser, 1996); see also Chapter 5, section 5.2.3.). To ensure that grafted tissue was exclusively shield type, I followed the fate of transplanted shields by using donor tissue from embryos that had been injected with a lineage tracer dye. Analysis of the cell fate in living embryos revealed that the transplanted shield contributed predominantly to the hatching gland, prechordal plate, notochord, floor plate and hypochord of secondary axes (Fig. 3.2A, B and Fig. 3.3A, B). These tissues appeared to be entirely derived from the transplanted shield. Histological sections of secondary axis revealed that in addition to the axial structures, a few donor shield-derived cells were found scattered throughout the ventral nervous system and throughout the overlying ectoderm (Fig. 3.3D). The vast majority of tissues in the secondary axis, including the brain, dorsal spinal cord and somites, however, were not labelled and therefore derived from host blastoderm. These results show that the fates of shield-derived cells in the induced secondary axes are identical to the fates of shield derived cells in an intact embryo.

3.2.4. Shield fragments enriched for deep *gsc*-expressing cells can induce secondary axes possessing only anterior structures

As mentioned earlier, the morphological shield is able to induce a complete secondary axis in 51% of the shield grafts. Incomplete secondary axes were also obtained and these induced axes varied from some that possessed a head lacking eyes (21%) to some possessing only a trunk and tail (2%) (see Table 3.1). In order to understand the causes of this variation, I performed a series of *in situ* hybridisation studies using embryos that were fixed 20 minutes after shield transplantation. These studies revealed that cells expressing *flh* were efficiently transplanted in every case (n=8) (Fig. 3.4D, E), whereas cells expressing *gsc* were transplanted 78% (n=9) of the time (Fig. 3.4A, B). This is
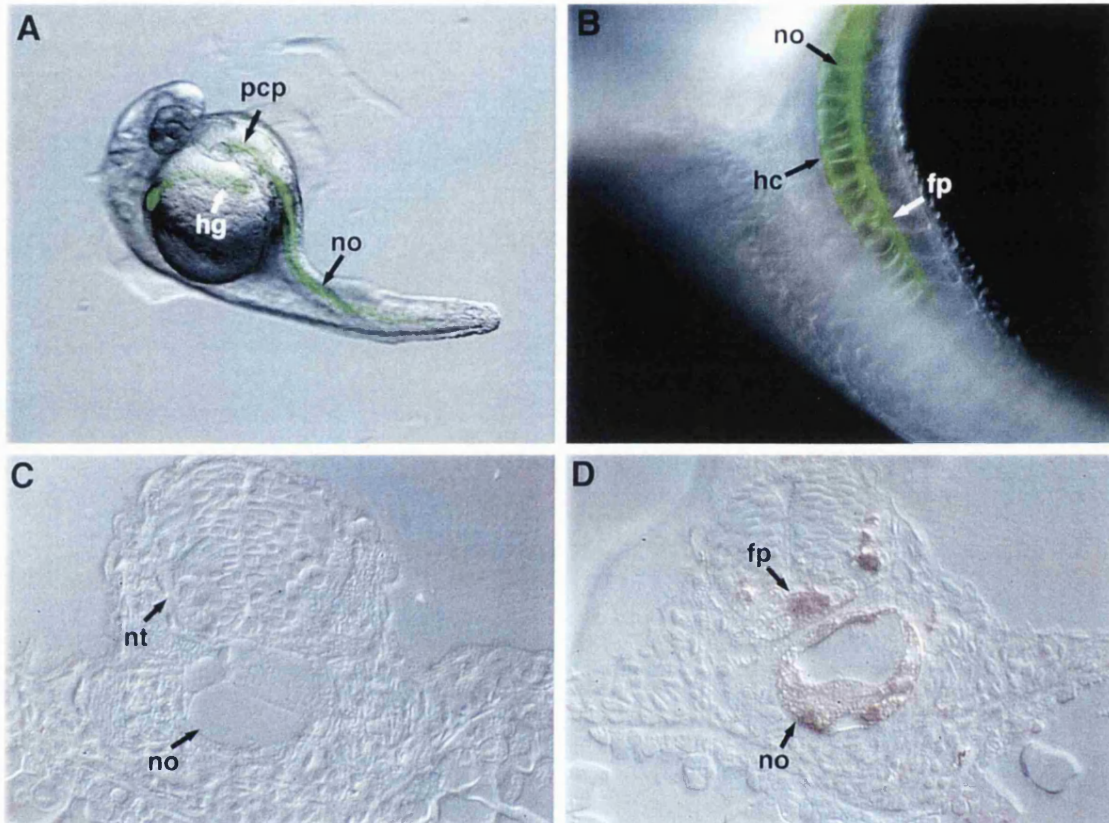
Fig. 3.3. Fate of transplanted shield tissue. (**A**) Using epifluorescence it was possible to determine the contribution of the transplanted fluorescein-dextran labelled shield to notochord, prechordal plate and hatching gland (green). (**B**) A higher magnification of the tail shows fluorescein-dextran labelled cells in the notochord, hypochord and floor plate. (**C**) A histological section through the primary axis showing the notochord and the neural tube completely devoid of labelled tissue. (**D**) A histological section through the secondary axis shows that the biotin-dextran labelled shield cells (brown) become notochord and floor plate. The majority of the neuroectoderm, however, is free of labelled cells. hg, hatching gland; pcp, prechordal plate; no, notochord; fp, floor plate; hc, hypochord; nt, neural tube
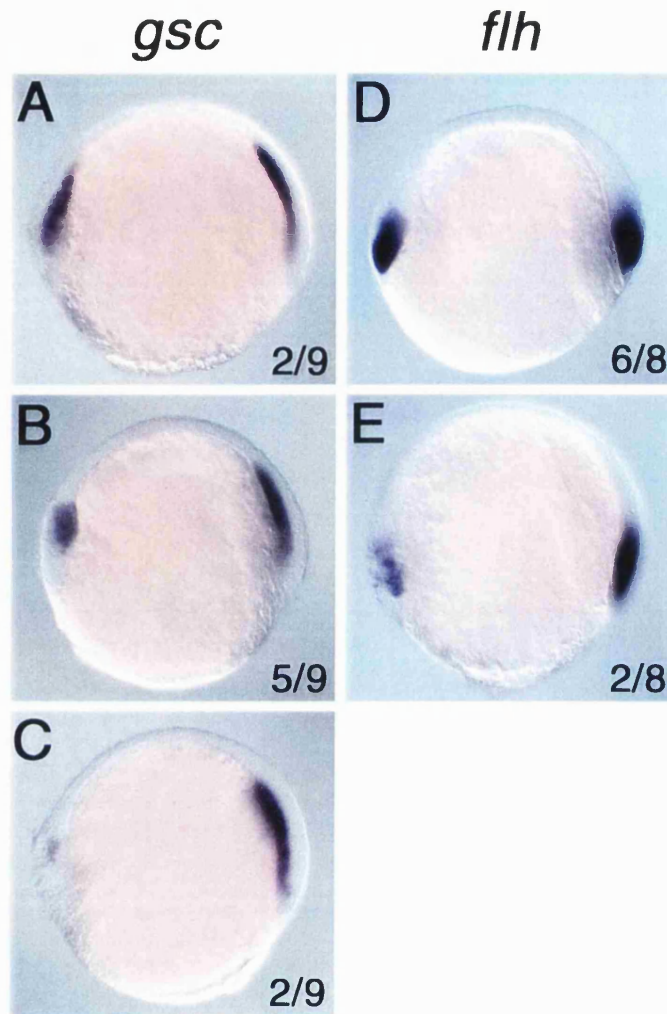
Fig. 3.4. Expression of *gsc* and *flh* in embryos that received a shield graft. (A-C) *gsc* expression in the primary and secondary induced axes. (A) The amount of *gsc*-expressing tissue in the transplant is roughly equal to that of the endogenous shield in 22% (n=9) of the cases. (B) In 56% (n=9) of the cases the amount of *gsc*-expressing tissue in the transplant correspond to approximately half of the endogenous shield. (C) A few or no *gsc*-expressing cells were found in the transplanted tissue in 22% (n=9) of the cases. (D, E) *flh* expression in the endogenous and transplanted shields. (D) The amount of *flh*-expressing tissue in the transplanted shield is equal to the endogenous shield in 75% (n=8) of cases. (E) In 25% (n=8) of the cases, the amount of *flh*-expressing tissue in the transplant is approximately half of the endogenous shield. All panels show endogenous shield to the right and transplanted shield to the left.

consistent with the hypothesis that a combination of deep *gsc*-expressing cells and superficial *flh*-expressing cells is required to obtain complete secondary axes.

To test directly whether deep and superficial regions of the shield have distinct organizer properties, I separated deep and superficial shield tissue and then transplanted these fragments into the ventral side of host embryos (Fig. 3.5B). Both superficial (schematic grey piece in Fig. 3.5B) and deep (schematic red piece in Fig. 3.5B) fragments induced secondary axes. I observed, however, a qualitative difference between secondary axes induced by deep versus superficial shield fragments. When deep fragments were grafted, the resulting secondary axes often possessed a head (11/21 embryos) (Fig. 3.5D-G; Table 3.2). By contrast, a high proportion of secondary axes induced by superficial shield fragments comprised posterior structures (14/26 embryos) (Fig. 3.5C; Table 3.2). These data suggest that anterior and posterior organizer activities are separable within the zebrafish embryonic shield. In an attempt to correlate these distinct inducing activities with differential expression of *gsc* and *flh*, *in situ* hybridisation studies were performed 20 minutes after deep or superficial shield fragment transplantation. These experiments showed that nearly all deep shield fragment transplants contained a high proportion of *gsc*-expressing cells (5/5 embryos) and in some cases had few or no *flh*-expressing cells (2/5 embryos). On the other hand, most superficial fragment transplants had a high proportion of *flh*-expressing cells (6/10 embryos) and in some cases had few or no *gsc*-expressing cells (4/8 embryos) (Table 3.3).

The detection of contaminating *gsc*-expressing cells in superficial grafts and *flh*-expressing cells in deep grafts most likely reflects a technical limitation, in that the tissue fragments are surgically separated without the aid of a vital expression marker. The contamination of deep and superficial fragments could explain the fact that both types of fragment can sometimes induce complete secondary axes (Table 3.2). I was able to overcome the contamination of superficial grafts with *gsc*-expressing cells by transplanting cells from the region adjacent to the morphological shield. All transplants of adjacent marginal fragments contained no *gsc*-expressing cells (11/11 embryos)

68
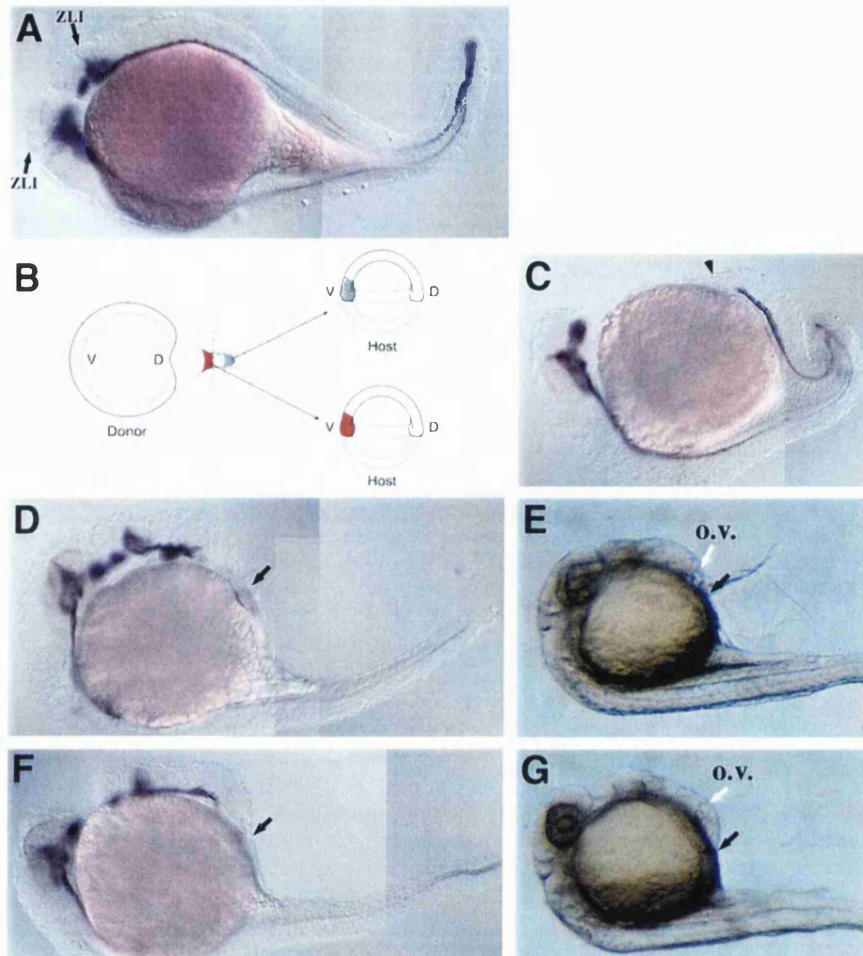
Fig. 3.5. Transplantation of deep versus superficial fragments of the embryonic shield. (A) The morphologically defined shield is able to induce a complete secondary axis. The expression of *shh* can be detected in the ventral midline of the brain, in the zona limitans intrathalamica (ZLI) and in the floor plate of the trunk and tail. **(B)** Schematic diagram of the dissection of the shield to obtain separate deep and superficial shield fragments for transplantation. The dotted lines represent cuts made with an eyebrow-hair knife into a removed shield. The grey area corresponds to the superficial cells and the red area to the deep cells. **(C)** An example of a secondary axis lacking head structures (arrowhead) induced by one superficial shield fragment. In these anterior truncated secondary axes the expression of *shh* is restricted to the floor plate of the trunk and tail. No *shh* expression characteristic of the head is seen. **(D-G)** Example of secondary axes lacking trunk and tail induced by two deep shield fragments. **(D, F)** The presence of a normally patterned head is revealed by the expression of *shh* in the ventral brain and the ZLI. The absence of trunk (arrow) is revealed by the interruption of *shh* expression in the floor plate at the level of the otic vesicle. **(E, G)** Live DIC images of the embryos stained in D and F showing that the induced heads are complete with eyes and otic vesicles.

Table 3.2. Transplantation of deep, superficial and lateral shield fragments to the ventral side of a 6 hpf embryo
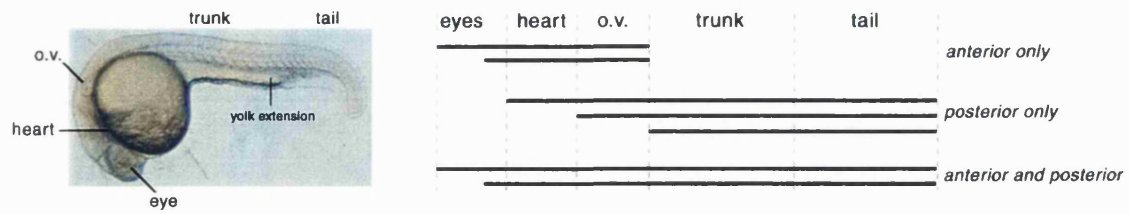
		Anterior only	Posterior only	Anterior and Posterior
1 piece	Deep	11/21	6/21	4/21
	Superficial	1/26	14/26	11/26
	Adjacent	0/67	64/67	3/67
2 pieces	Deep	6/16	2/16	8/16
	Superficial	0/9	7/9	2/9
	Adjacent	0/16	13/16	3/16

o.v. = otic vesicle

anterior only = telencephalon through o.v.

posterior only = heart (or o.v.) through tail

anterior and posterior = complete axis

The telencephalon did not always include eyes.

The tail begins posterior to the yolk extension.

Table 3.3. Expression of *gsc* and *flh* in embryos that have received shield fragment grafts
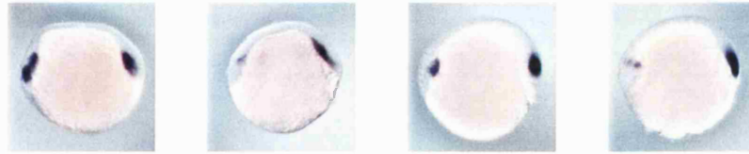
		High *gsc*	Low or Absent *gsc*	High *flh*	Low or Absent *flh*
	Deep	5/5	0/5	3/5	2/5
1 piece	Superficial	4/8	4/8	6/10	4/10
	Adjacent	0/11	11/11*	6/15	9/15
	Deep	3/5	2/5	4/5	1/5
2 pieces	Superficial	2/4	2/4	4/6	2/6
	Adjacent	1/9	8/9	5/8	3/8

Pictures are oriented with endogenous shield to the right and transplanted fragments to the left.

gsc expression was absent in all embryos.

(Table 3.3) and the vast majority of axes they induced consisted of posterior structures only (64/67 embryos) (Table 3.2).

Since the dissected fragments represent only a fraction of the embryonic shield, I wanted to ensure that the observed differences in induced axes were not a simple consequence of the quantity of transplanted tissue. I found that grafting two pieces of each fragment-type showed the same axis inducing activity and the same profile of *gsc* and *flh* expression as grafting one piece (Table 3.2; Table 3.3). I did, however, find that the size of axes induced by two pieces was generally larger than axes induced by one piece. I conclude, therefore, that it is the quality rather than the quantity of fragment that determines whether anterior or posterior structures are induced.

3.3. Discussion

The data presented in this chapter shows that the embryonic shield is able to induce a secondary body axis possessing head and trunk structures. These results are in contrast to another study, which suggested that the embryonic shield was only capable of inducing anterior-truncated secondary axes (Shih and Fraser, 1996). I believe that this discrepancy is due to differences in the transplantation method employed. In order to obtain proper induction of the head, I find it is essential to transplant the deeper *gsc*-expressing cells of the shield. For zebrafish, the use of an eyebrow hair knife to remove shield tissue may prevent the removal of the deep cells. These cells reside immediately adjacent to the yolk cell and aggressive manipulations result in the puncture of the yolk cell and collapse of the embryo. The method I have described here allows complete removal of the deep *gsc*-expressing cells by suction, leaving the yolk cell intact. Using this method, it was also possible to test directly the inductive properties of deep *gsc*-expressing cells versus superficial *flh*-expressing shield tissue. When the shield is divided into fragments and the deep cells are transplanted into the ventral side of a host embryo it is possible to obtain secondary axes with complete heads that lack

posterior structures. With superficial fragment transplants it is possible to obtain secondary axes possessing posterior structures but lacking heads. These results show that in the embryonic shield the domains of gene expression and developmental fate correspond also to functionally distinct regions. This is consistent with earlier studies of the organizer activities of teleost embryonic shield, in which transplanted anterior and posterior fragments of the *Fundulus* shield showed a tendency to induce the formation of typical head and trunk structures, respectively (Brummett, 1969; Brummett, 1972; Oppenheimer, 1953). Taken together these results suggest that the quality of signalling imparted by the deep shield tissue is required for normal head formation. The mechanical approach used to obtain deep versus superficial shield grafts, however, does not allow consistent separation of *gsc*-expressing and *flh*-expressing tissue. Deep grafts were often contaminated with *flh*-expressing cells. Similarly, superficial grafts were often contaminated with *gsc*-expressing cells. In the future, through the use of transgenic embryos expressing green fluorescent protein (GFP) under the control of *gsc* or *flh* promoters (Henry Roehl, Miranda Gompertz and Steve Wilson, personal communication), a more precise separation of the deep and superficial shield fragments should be possible.

It has been suggested that it is not the quality of organizer tissue that governs whether head will form but the position of the transplant (Koshida et al., 1998). These investigators found that transplantation of shield, Hensen's node, or COS7 cells expressing Noggin/Chordin could induce neuroectoderm formation but the anterior-posterior identity of the induced neural tissue was dependent upon the position of the graft relatively to the epiblast. They have proposed that in order to obtain a complete secondary axis in zebrafish it is necessary to transplant the embryonic shield near the animal pole. In contrast to this interpretation, I found that transplantation of shield to the margin of a host embryo is sufficient to obtain a complete secondary axis. In agreement with my results, it was shown that the embryonic shield is crucial for forebrain patterning since embryos from which the entire shield region was ablated, at late-blastula to early-gastrula stages, do not express the *odd paired-like* (*opl*) gene in the telencephalon (Grinblat et al., 1998). Therefore, while the animal cap shows a tendency

to take on anterior neural fates it is clearly not committed to such fates nor can these fates be manifest without a dorsal/marginal signal such as that emanating from the shield.

Chapter 4

Developmental Consequences of Embryonic Shield Removal

4.1. Introduction

Functional equivalents of Spemann's organizer have been discovered in many vertebrate systems. The importance of the organizer, as a signalling centre capable of inducing a body axis which includes neural tissue, has been demonstrated by transplantation experiments (reviewed in Harland and Gerhart, 1997). Subsequent work has shown that organizer derivatives are a source of signals that confer axial polarity to the overlying neural tissue. Transplantation experiments in the chick showed that the prechordal plate possess neural anteriorising ability (Foley et al., 1997; Pera and Kessel, 1997). The prechordal plate is also involved in the dorsal-ventral (DV) patterning of anterior neural tissue in *Xenopus* (Ruiz i Albata, 1992), zebrafish (Schier et al., 1997), chick (Dale et al., 1997; Foley et al., 1997) and mouse (Shimamura and Rubenstein, 1997). The notochord has a strong ventralising influence on the developing neural tube (reviewed in Placzek, 1995).

Whether there is an actual requirement for the organizer and its derivatives in vertebrates is a question raised by the phenotype of organizer-ablated embryos. Surgical ablation experiments, at gastrula stages, in *Xenopus*, zebrafish, chick and mouse showed that a correct anterior-posterior (AP) patterned body axis, including a neural tube, can still form following organizer removal. In the chick there have been several reports of extensive regeneration of Hensen's node and it derivatives after surgical removal of Hensen's node and the rostral part of the primitive streak (Joubin and Stern, 1999; Psychoyos and Stern, 1996; Yuan and Schoenwolf, 1998). A recent study of the chick organizer describes the continuous renewal of organizer tissue as development proceeds (Joubin and Stern, 1999). Specifically, a region of the embryo is described that induces organizer fate to otherwise unspecified tissue as it passes through the node. The capacity for the avian organizer to regenerate could account for the fact that normal chick embryos are obtained after Hensen's node ablation. In contrast to the situation in avian embryos, there is no evidence that regeneration of organizer derivatives occurs in *Xenopus* or mouse embryos after organizer ablation (Cooke, 1985; Davidson et al.,

1999; Klingensmith et al., 1999). In zebrafish, the analysis of shield-ablated embryos revealed that 36% were cyclopean and 73% developed with at least a few hatching gland and notochord cells (Shih and Fraser, 1996). The presence of shield-derived cells in these shield-ablated embryos suggests that either the embryonic shield was not completely removed or that the loss of the embryonic shield and the axial mesoderm progenitors within was restored by tissue regeneration.

The shield ablation studies performed in zebrafish did not use tissue specific markers to assess the extent of shield removal and patterning defects. Using a new method for shield removal and a range of molecular markers, I have characterised the effects of complete shield ablation at early gastrula stage on the formation of axial mesoderm and patterning of the central nervous system (CNS).

4.2. Results

4.2.1. Complete shield removal leads to axial defects

Mechanical removal of the morphological shield was achieved by aspiration with a pipette of inner diameter approximately the size of the shield (see Chapter 2, section 2.3.3. and Chapter 3, section 3.2.1.). Removal of the morphological shield does not eliminate all tissue expressing the organizer-specific genes *goosecoid* (*gsc*) (Stachel et al., 1993) and *floating-head* (*flh*) (Talbot et al., 1995) as shown by *in situ* hybridisation (Fig. 4.1B). These results show that the extirpation of the morphological shield only partially removes axial mesoderm progenitors. However, complete shield ablation, that is complete removal of tissue expressing *gsc* and *flh*, was achieved by extirpating two adjacent pieces from the dorsal margin (Fig. 4.1C). These results show that the morphological shield, although sufficient to induce a complete secondary axis in transplantation experiments (see Chapter 3, section 3.2.2.), does not correspond to the entire shield region in zebrafish gastrula embryos.
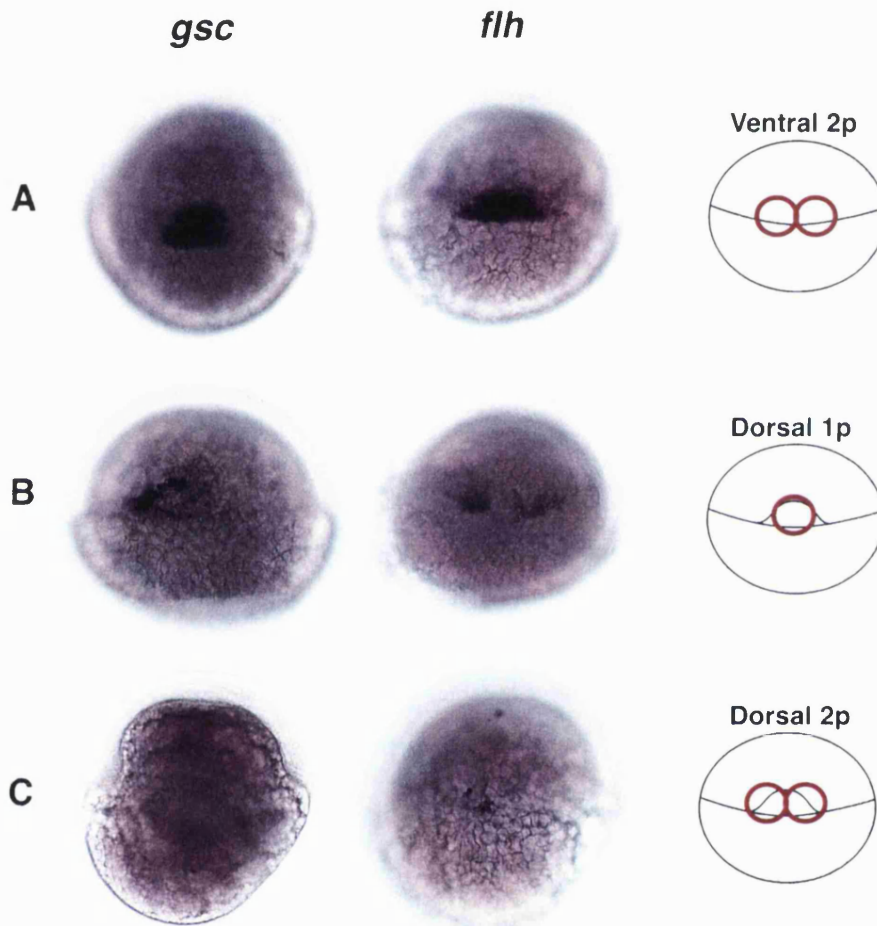
Fig. 4.1. Expression of *gsc* and *flh* in shield-ablated embryos. (**A**) As a control, two pieces of ventral germ-ring were removed. The control embryos show normal *gsc* and *flh* expression. (**B**) The morphologically defined shield was removed using a glass pipette, roughly the diameter of an embryonic shield. This is insufficient to remove all the *gsc-* and *flh-*expressing cells, as confirmed by *in situ* hybridisation. (**C**) When two pieces of dorsal margin are ablated the *gsc-* and *flh-*expressing cells are completely removed. All panels show dorsal views of 6 hpf embryos with anterior up.

To assess the developmental consequences of partial (morphological shield only) and complete (morphological shield and adjacent marginal tissues) shield removal, experimental embryos were cultured until 24 hours-post-fertilisation (hpf) and analysed. Embryos that had undergone morphological shield removal developed normally in 71% (n=75) of the cases (Fig. 4.2E-H). By contrast, only 6% (n=70) of embryos subjected to complete shield removal developed normally (Fig.4.2I-M). In all cases of ventral margin removal embryos developed normally (n=52) (Fig. 4.2A-D).

Complete shield removal produced embryos that were generally shorter than control embryos (Fig. 4.2I). By morphological criteria, these embryos completely lacked the axial tissues: notochord, floor plate and hatching gland (Fig. 4.2I). Expression of *sonic hedgehog* (*shh*) and *no tail* (*ntl*) in the midline were significantly reduced in complete shield-ablated embryos, consistent with the morphological deficiencies in notochord and floor plate (Fig. 4.2J, M) (Krauss et al., 1993; Schulte-Merker et al., 1994). By the two-somite stage, complete shield-ablated embryos, displayed a total loss of prechordal plate as detected by whole mount *in situ* hybridisation with an antisense probe to *hlx-1*, a marker of the anterior axial mesoderm (Fig. 4.4J) (Fjose et al., 1994). Consistent with a role for the notochord in somite patterning, the somites formed compressed rectangles instead of characteristic chevrons (Fig. 4.2I). Normally, muscle pioneer cells develop from a subset of adaxial cells that remain adjacent to the notochord. The muscle pioneers are induced by Hedgehog proteins and express *engrailed-1* (*en1*) (Du et al., 1997; Ekker et al., 1992). Except for regions where a few notochord cells remained, *en1* expression was abolished in complete shield-ablated embryos (Fig. 4.2L). By contrast, *en1* expression at the midbrain-hindbrain boundary was unaffected (data not shown). These results show that complete removal of the shield early in development leads to a complete loss of shield-derived tissues at later stages and subsequently notochord-dependent patterning does not occur. Despite complete removal of shield tissue, the body axis still forms and has clear AP neural structures.
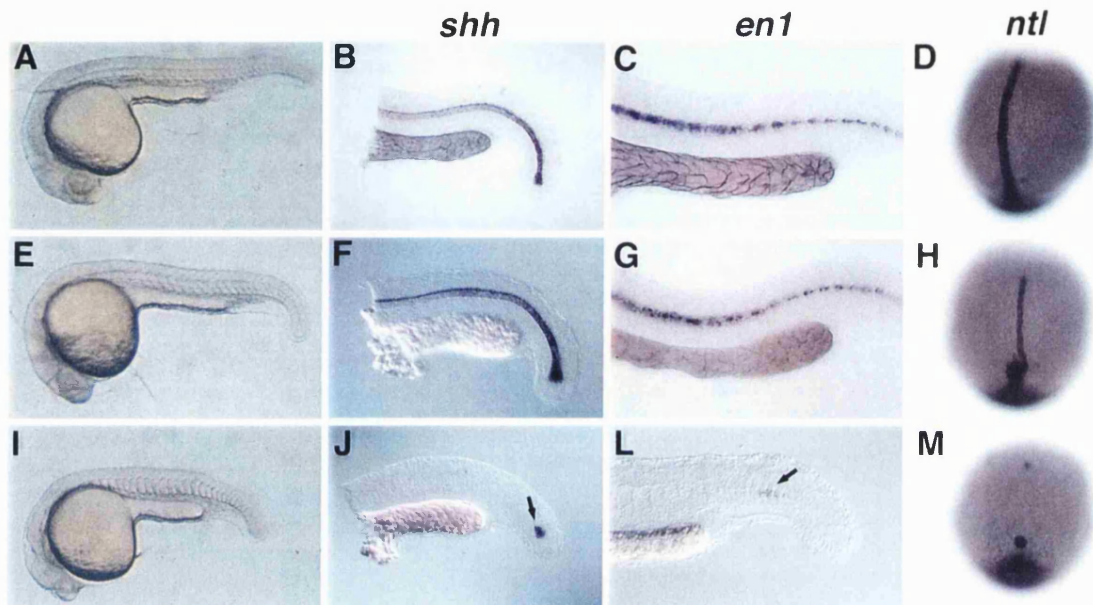
Fig. 4.2. Complete shield removal leads to axial defects. (**A-D**) Control embryos, where two pieces of ventral germ-ring were removed. (**E-H**) Removal of the morphological shield leads to normal development of axial structures, as revealed by *in situ* hybridisation with the molecular markers *shh*, *en1* and *ntl*. (**I**) Complete shield removal leads to lack of notochord and chevron shaped somites. (**J, M**) The absence of differentiated notochord cells in complete shield-ablated embryos is confirmed by the reduction in *shh* and *ntl* expression. The arrow identifies residual *shh*-expressing cells in the tail bud. (**L**) Expression of *en1* is not detected in muscle pioneer cells of notochordless embryos, as revealed by *in situ* hybridisation. The arrow identifies some *en1*-expressing cells adjacent to residual notochord cells. (**A, C, E, G, I, L**) Lateral views of 24 hpf embryos with anterior to the left. (**B, F, J**) Lateral views of 18 hpf embryo with anterior to the left. (**D, H, M**) Dorsal view of 2 somite stage embryos with anterior up.

4.2.2. Complete shield removal leads to CNS defects

Given the known roles for axial mesendoderm in patterning the neuroectoderm, I examined the DV organisation of the CNS in complete shield-ablated embryos (van Straaten et al., 1988; Yamada et al., 1991). I found that 56% (n=70) of these embryos were cyclopean (Fig. 4.3F). This defect correlates with a loss of ventral neuroectoderm throughout the body axis as seen by the reduction in *tiggy winkle hedgehog* (*twh*) and *shh* expression, both of which mark medial floor plate cells and the ventral brain (Fig. 4.3G, H) (Ekker et al., 1995). I also investigated the effect of axial tissue loss on motorneuron specification in complete shield-ablated embryos. The monoclonal antibody Znp1 marks primary neurons and their ventral root axonal projections (Trevarrow et al., 1990). Complete shield-ablated embryos lacked motorneuron ventral root projections (Fig. 4.3I). At the neural plate stage, *islet-1* (*isl-1*) marks all primary neurons of the forming spinal cord (Inoue et al., 1994). Laterally, *isl-1* marks Rohon-Beard sensory neurons and medially, it marks motorneurons. I found Rohon-Beard sensory neurons to be present in complete shield-ablated embryos while motorneurons were either absent or severely reduced in number, forming at most a single sparse column at the midline (Fig. 4.3J). The results show that ventral patterning of the CNS is disrupted in complete shield-ablated embryos.

The AP patterning of complete shield-ablated embryos was examined using *EphA4* (Xu et al., 1995; Xu et al., 1994), *emx1* (Morita et al., 1995) and *zanf*. The latter is a marker of the zebrafish telencephalon homologous to the mouse *hesx1* gene (Kazanskaya et al., 1997; Thomas and Beddington, 1996). In complete shield-ablated embryos *EphA4* expression at 24 hpf revealed an AP expansion of rhombomeres 1, 3 and 5 (Fig. 4.4F). Although head morphology was clearly abnormal, I detected *emx1* expression in complete shield-ablated embryos at 24 hpf (Fig. 4.4H). At the two-somite stage of development, the *emx1* expression domain was compressed toward the midline of complete shield-ablated embryos, but occupying an area of similar size to that of controls (Fig. 4.4I). Finally, I found that *zanf* was expressed in complete shield-ablated embryos, adding further evidence that the telencephalon is specified (Fig. 4.4G).
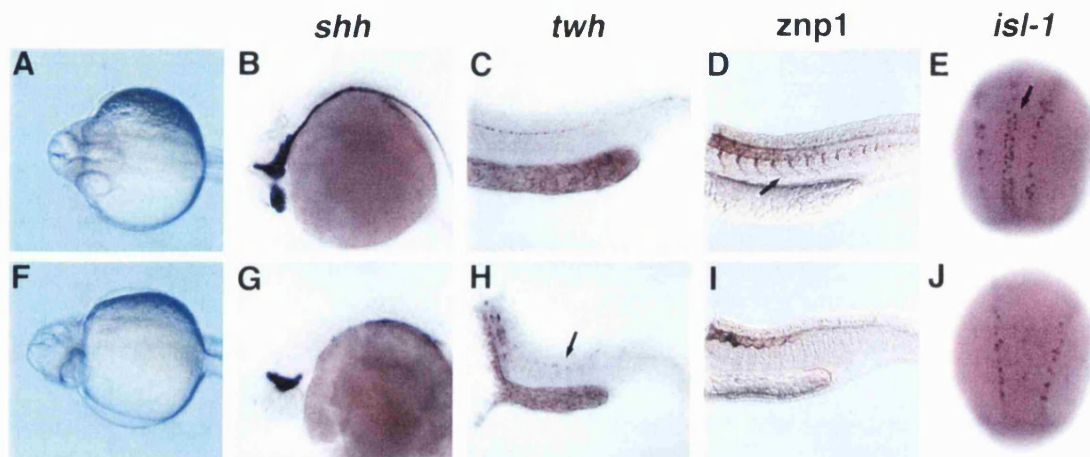
Fig. 4.3. Ventral patterning of the CNS is disrupted in complete shield-ablated embryos. (A-E) Control embryos. **(F)** Complete shield-ablated embryos become cyclopean. **(G, H)** The reduction of ventral neuroectoderm in complete shield-ablated embryos is reflected by the reduction in *twh* and *shh* expression, which mark the midline floor plate cells and the ventral brain. The arrow shows remaining floor plate cells. **(I)** znp1 reveals the absence of motorneuron ventral root projections (arrow) in complete shield-ablated embryos. **(J)** In complete shield-ablated embryos, *isl-1* expression is severely reduced in medial motorneurons (arrow) and normal in the lateral Rohon-Beard sensory neurons. **(A, C, D, F, H, I)** Lateral views of 24 hpf embryos with anterior to the left. **(B, G)** Lateral views of 18 hpf embryos with anterior to the left. **(E, J)** Dorsal views of 5 somite stage embryos with anterior up.
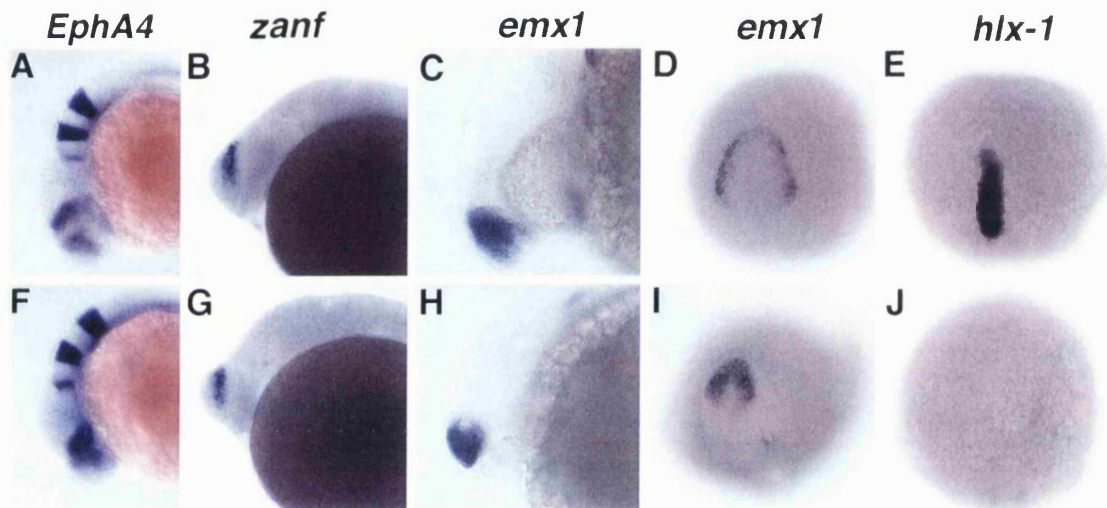
Fig. 4.4. In complete shield-ablated embryos AP patterning is not severely affected. (**A-E**) Control embryos. (**F**) After complete shield removal, *EphA4* expression in rhombomeres 1, 3 and 5 is slightly expanded. (**G-I**) In complete shield-ablated embryos, the telencephalon is patterned as revealed by *zanf* and *emx1* expression. (**J**) *hlx-1* expression is absent in complete shield-ablated embryos confirming the loss of prechordal plate tissue in the head. (**A, B, C, F, G, H**) Lateral views of 24 hpf embryos with anterior to the left. (**D, E, I, J**) Dorsal views of 2 somite stage embryos with anterior up.

Complete shield ablation at shield stages does not prevent the formation of the most anterior neuroectodermal tissues. Together, these results show that complete shield removal at early gastrula stage leads to hindbrain expansion, however it does not lead to loss of forebrain tissue.

4.3. Discussion

A new method suitable for zebrafish embryos was used to remove shield tissue at the onset of gastrulation (see Chapter 2, section 2.3.3. and Chapter 3, section 3.2.1.). Ablation of the morphological shield did not remove all *gsc-* and *flh*-expressing cells and as a consequence of this, embryos recovered and were completely normal by 24 hpf. Removal of the morphological shield plus the adjacent marginal tissue, however, led to loss of *gsc-* and *flh*-expressing cells and in this case the embryos developed without prechordal plate and notochord. In addition these embryos were cyclopean, showed a significant loss of floor plate and primary motorneurons and displayed disrupted somite patterning. These results show, first, that the morphological shield does not constitute the entire zebrafish shield region and second that the formation of shield derivatives occurs only when some lateral *gsc-* and *flh*-expressing cells are left in the embryo. This demonstrates that *de novo* regeneration of the organizer does not occur in zebrafish embryos. This observation, taken together with the results obtained in mouse and *Xenopus,* suggest that continuous organizer renewal is unique to the avian embryo.

In complete shield-ablated embryos the shield derivatives fail to form and there are patterning defects in the CNS. In these embryos, however, the embryonic axis forms and has clear AP patterning. This suggests that by the time the embryonic shield tissue is removed, the dorsal organizer has already acted both to specify and to impart AP pattern to the neuroectoderm. Alternatively, the presence of neural structures in shield-ablated embryos may suggest that neural inducing activities could be present outside the embryonic shield region. Since we rely on shield morphology to guide the

removal of tissue, I was unable to ablate the shield earlier than gastrula stages. This stage corresponds to nearly one hour after organizer-specific genes like *gsc* (Stachel et al., 1993), *flh* (Talbot et al., 1995), *axial* (Strahle et al., 1993) and *lim-1* (Toyama et al., 1995) are first expressed. Therefore, neural inducing and patterning events may have already occurred. The results presented here also show that neural induction and AP patterning can still occur without the presence of an embryonic shield and without the prolonged expression of shield-specific genes. The role of the embryonic shield and its derivatives, could perhaps be to maintain and refine the pattern initiated earlier in development. Accordingly, the results presented in this chapter indicate that the axial mesoderm derived from the shield is critical for some aspects of axial patterning since complete shield-ablated embryos show AP and DV patterning problems in the neural tube and in the somites.

If the development of neural tissues with a clear AP patterning in surgically-shield-ablated embryos can be explained by a timing issue the same is not true for genetically shield-ablated embryos. Mutations in the zebrafish *bozozok* (*boz*) locus affect both shield morphology and the development of shield-derived tissues very early in development. The most severely affected *boz* mutants do not form a morphological embryonic shield, but similar to our complete shield-ablated embryos, the *boz* mutants have an embryonic axis with clear AP patterning (Fekany et al., 1999). Later in development, severely affected *boz* mutant embryos display loss of the shield derivatives (hatching gland, prechordal plate, notochord, floor plate and hypochord) and exhibit cyclopia. The *boz* mutant embryos show deficiencies in the CNS, namely, reduction or absence of the forebrain marker *emx1* and expansion of *krox20* expression domains in rhombomeres 3 and 5 of the hindbrain (Fekany et al., 1999). Hence, all the defects seen in the *boz* mutant embryos are phenocopied by shield-ablated embryos with the exception that severely affected *boz* mutants do not specify properly the forebrain region. It has been proposed that *boz* may play a role in anterior neural induction. It is possible that the loss of anterior neuroectoderm results from the failure to specify prechordal mesendoderm prior to shield stage, as seen from the down-regulation of *gsc* in *boz* mutant embryos (Fekany et al., 1999). It is tempting to predict that removal of

zebrafish organizer prior to morphological shield formation would also lead to anterior defects similar to those seen in severe *boz* mutant embryos. In agreement, it was shown that removal of dorsal marginal tissue at 40% epiboly leads to the loss of the anterior part of the forebrain as revealed by the absence of *odd-paired like* (*opl*) expression during the neural plate stage (Grinblat et al., 1998). Taken together these results suggest that the defects seen in *boz* mutant embryos seem to be a direct consequence of the failure to form axial tissues and not a direct involvement in anterior neural induction. The comparison of the complete shield-ablated embryos and the *boz* mutation highlights the separable nature of formation of axial mesendoderm and induction of embryonic axis at early stages of the organizer specification.

Chapter 5

Insights into the Mechanism of Shield Derivative Regeneration after Morphological Shield Removal

5.1. Introduction

In Chapter 3, I have shown that marginal tissue adjacent to the morphological shield possesses organizer activity, as it can induce secondary axes in transplantation experiments. In addition, the expression domains of the organizer-specific genes, *goosecoid* (*gsc*) and *floating head* (*flh*), include marginal cells beyond the limits of the morphological shield (see Chapter 4). When the morphological shield plus the adjacent marginal tissue are removed, shield derivatives, such as the notochord, are eliminated. If only the morphological shield is ablated, about 80% of the *gsc*- and *flh*-expressing cells are removed, yet classical shield derivatives form and the embryos appear completely normal by 24 hours-post-fertilisation (hpf) (see Chapter 4). Based on these results, we define the shield region as the morphological shield plus adjacent marginal tissue.

The fact that morphological shield-ablated embryos can form all the normal shield derivatives suggests that regeneration mechanisms occur after surgical removal. Initially, I examined the wound healing process to see how it would effect shield regeneration. Then, I tested two mechanisms that could contribute to the regeneration of shield derivatives: cell proliferation and alterations of cell fates. Either the residual shield cells are sufficient to complete gastrulation and to form all shield derivatives or there is an increase in their rate of proliferation in other to compensate for the loss. To test this hypothesis, I have compared the number of mitotic cells between control and morphological shield ablated embryos at gastrulation stages. As another possibility, non-shield cells surrounding the shield region could be recruited to a shield fate. The cell fate switch could be triggered by the residual shield cells, through homeogenetic signals. The cell fate switch could also be achieved by signals coming from residual Nieuwkoop centre activity. To test these possibilities, I have tested the potential of ventral cells to switch from a blood and somite fate to a shield fate in the presence of adjacent marginal shield cells near and away from the Nieuwkoop centre. I have also attempted to do a comparative fate map of the cells surrounding the shield region in the presence and in the absence of the morphological shield. Due to time restrictions, the

question about the signals involved in the shield regeneration process has been addressed partially to date.

5.2. Results

5.2.1. Factors affecting formation of shield derivatives following morphological shield removal

I examined whether wound healing has any role in the restoration of shield derivatives by allowing wound healing to occur in several different concentrations. In initial shield removal experiments, which were done in 0.3X Danieau solution, I noticed a high proportion of embryos that failed to regenerate the shield. When I started doing the transplants in 1X Danieau solution, I noticed that nearly all of the embryos regenerated their shield. Removal of the morphological shield in 1X Danieau solution, which has a salt concentration similar to interstitial fluid, allowed the recovery of a high percentage of embryos (71%; 53/75 embryos). By contrast, morphological shield removal in 0.3X or 0.1X Danieau solution yielded a much reduced percentage of normal embryos 37% (18/48 embryos) and 44% (16/36 embryos), respectively (Fig. 5.1, Dorsal 1 piece). When both the morphological shield and adjacent marginal tissue were removed there was only a small difference in the percentage of normal embryos 6% (4/70 embryos), 6% (2/34 embryos) and 8% (1/13 embryos) obtained after operating in 1X, 0.3X and 0.1X Danieau solution, respectively (Fig. 5.1, Dorsal 2 pieces). I wanted to test whether the sensitivity to salt concentrations was due to altered cellular re-association dynamics after surgery. In collaboration with Katie Woolley (Paul Martin's laboratory, UCL), we examined embryos by scanning electron microscopy after morphological shield removal in 0.3X or 1X Danieau solution. In 0.3X Danieau solution, cells had completely covered the exposed yolk cell membrane by 10 minutes after extirpation, while those operated in 1X Danieau solution took more than 10 minutes to heal (Fig. 5.2). These results show
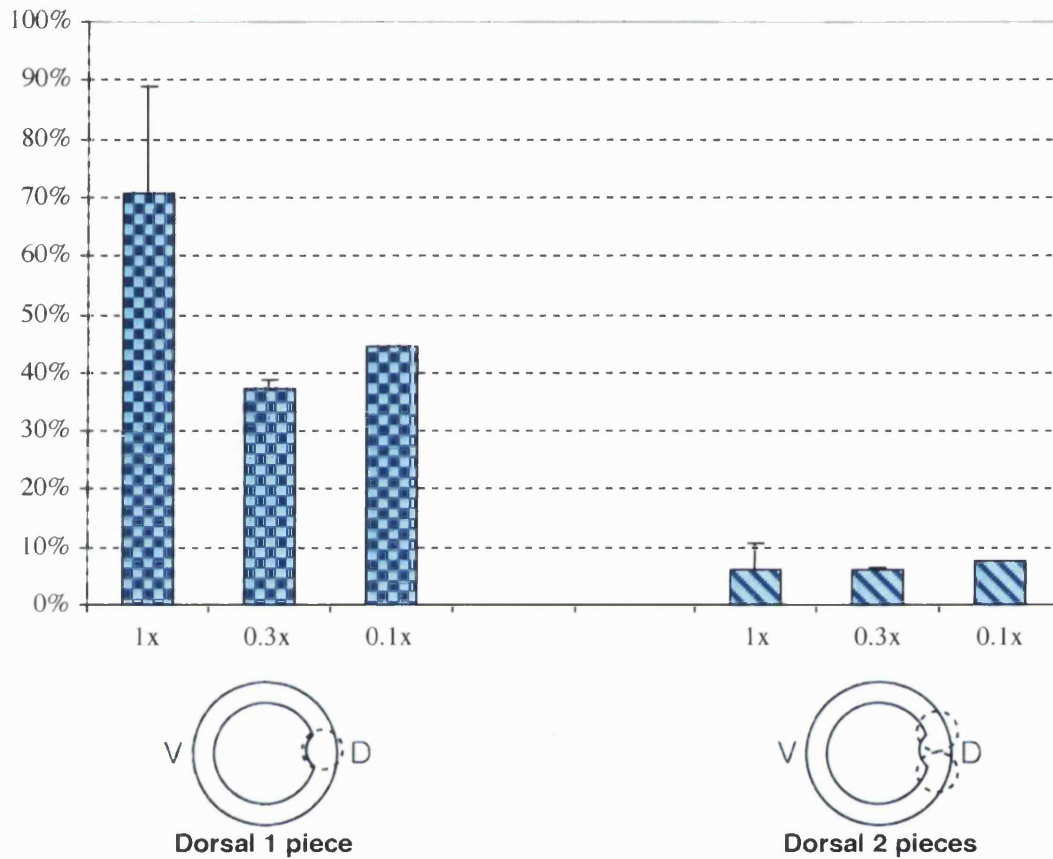
Fig. 5.1. Percentage of normal embryos obtained after morphological shield (Dorsal 1 piece) and complete shield region (Dorsal 2 pieces) removal as a function of Danieau solution concentration. Removal of the morphological shield in 1X Danieau solution allows the development of 71% of normal embryos. The percentage of normal embryos drops to 37% and 44% when the removals are done in 0.3X and 0.1X, respectively. Removal of complete shield region yield a low percentage of normal embryos, 6%, 6% and 8% when the removals were done in 1X, 0.3X and 0.1X, respectively.
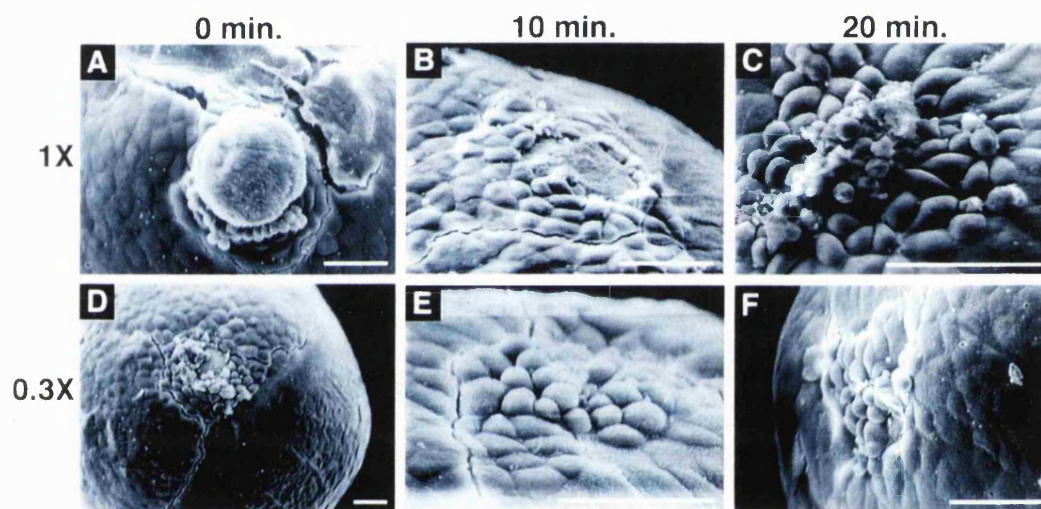
Fig. 5.2. Scanning electron micrographs of 6 hpf embryos after morphological shield removal. (**A, D**) A wound immediately after shield removal performed in 1X and 0.3X Danieau solution. (**B, E**) Shown are the wounds of shield-ablated embryos 10 minutes post-surgery in 1X or 0.3X Danieau solution. Healing seems to occur more rapidly in 0.3X Danieau solution. (**C, F**) The wounds of shield-ablated embryos are healed after 20 minutes in either 1X or 0.3X Danieau solution. Scale bars=50 μm.

that restoration of shield derivatives is not only dependent upon the presence of adjacent marginal tissue, but also upon the proper healing of the extirpated domain after morphological shield removal. It is possible that the rapid re-association of the EVL with the yolk cell prevents proper contact among deep cells.

5.2.2. Cell proliferation after morphological shield removal

Reconstitution of shield derivatives after morphological shield removal could be due to compensatory proliferation and differentiation of residual shield cells. I investigated cell proliferation by comparing the number of mitotic cells in intact and morphological shield-ablated embryos. Morphological shields were removed from embryos at shield stage as described before (Chapter 2, section 2.3.3. and Chapter 3, section 3.2.1). One group of shield-ablated embryos was immediately fixed, another group was incubated for 40 minutes at 28°C prior to fixation and a third group was left at 28°C for 90 minutes and then fixed. The number of mitotic cells in experimental and control embryos was then revealed by imunohistochemistry using an anti-phospho-histone H3 antibody conjugated with horseradish peroxidase (Hendzel et al., 1997). This analysis showed that in control embryos, mitotic cells are equally dispersed throughout the blastoderm at all time points studied (Fig. 5.3A-C). In morphological shield-ablated embryos, the mitotic cells were also equally dispersed in the blastoderm and no apparent increase in the number of mitotic cells was observed at any of the time points investigated (Fig. 5.3D-F). These results demonstrate that there is no dramatic increase in cell proliferation during the first 90 minutes after shield removal. It is possible that a compensatory increase in cell proliferation occurs later in development. The fact that reduced numbers of notochord progenitors are detected as late as the tailbud stage in morphological shield-ablated embryos (see Chapter 4, Fig. 4.2H), however, argues that such proliferation does not occur until the end of gastrulation.
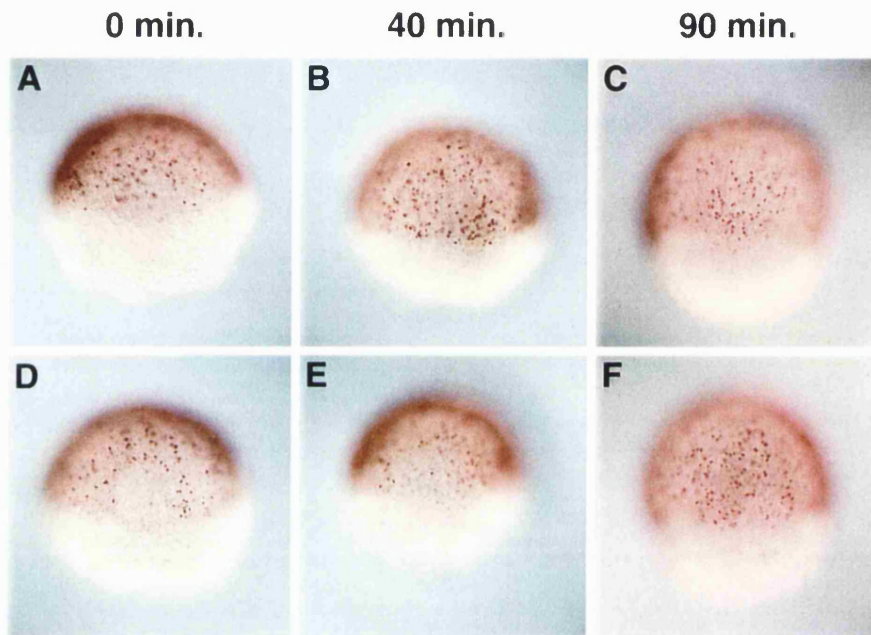
Fig. 5.3. Cell proliferation after morphological shield removal. (A-C) Control embryos that were not subjected to surgical manipulation. Mitotic nuclei are distributed equally in the blastoderm. (D-F) Experimental embryos in which the morphological shield was removed. The amount of mitotic nuclei around the wound is not increased. (A, D) Embryos at shield stage. (B, E) Embryos kept at 28°C for 40 minutes after shield stage. (C, F) Embryos kept at 28°C for 90 minutes after shield stage. (A-F) Cell proliferation was visualised using an antibody specific for phosphorylated histone H3 to reveal mitotic nuclei (brown).

5.2.3. Cell fate switch

Since early cell proliferation does not explain the restoration of shield derivatives, I performed experiments to test another possibility. It may be that shield cells recruit non-shield cells to a shield fate. To test this idea, I compared the fate of biotin-labelled ventral cells transplanted into the dorsal side of a shield stage embryo in the presence or in the absence of adjacent marginal tissue. As a control, the normal fate of shield and ventral cells was established by replacing the morphological shield with a labelled morphological shield (Fig. 5.4A), or a piece of ventral tissue with a labelled one (Fig. 5.4C). The shield cells contributed to hatching gland, prechordal plate, notochord, floor plate and hypochord along the entire anterior-posterior body axis (Fig.5.4B). The ventral cells gave rise to posterior somites and blood (Fig. 5.4D). In these control experiments, the fate of both shield and ventral cells was in agreement with published zebrafish gastrula fate maps (Kimmel et al., 1990; Melby et al., 1996; Shih and Fraser, 1996). When the morphological shield and adjacent marginal tissue were replaced by labelled ventral tissue, the ventral cells became primarily neural tissue and somites (Table 5.1). By contrast, when the morphological shield was replaced by labelled ventral tissue, the ventral cells, now in contact with the adjacent marginal tissue, contributed not only to neural tissue and somites (Table 5.1; Fig. 5.4F-O), but also to floor plate, hypochord and posterior notochord (Table 5.1; Fig. 5.4F-M), which are typical fates of shield cells. Together, these results show that ventral tissue, in the presence of adjacent marginal tissue, can be induced to form notochord, floor plate and hypochord. This suggests that, after morphological shield removal, residual shield cells might also convert non-shield cells into shield fates.

The shield region lies on the top of a signalling centre, the dorsal yolk syncytial layer (YSL). This signalling centre is considered to be the zebrafish equivalent of the Nieuwkoop centre and has been implicated in the induction of the shield (Erter et al., 1998; Fekany et al., 1999; Feldman et al., 1998; Koos and Ho, 1998; Rebagliati et al., 1998; Yamanaka et al., 1998). It is possible that combined signals from the dorsal YSL and the adjacent marginal tissue are necessary for the recruitment of ventral cells to the
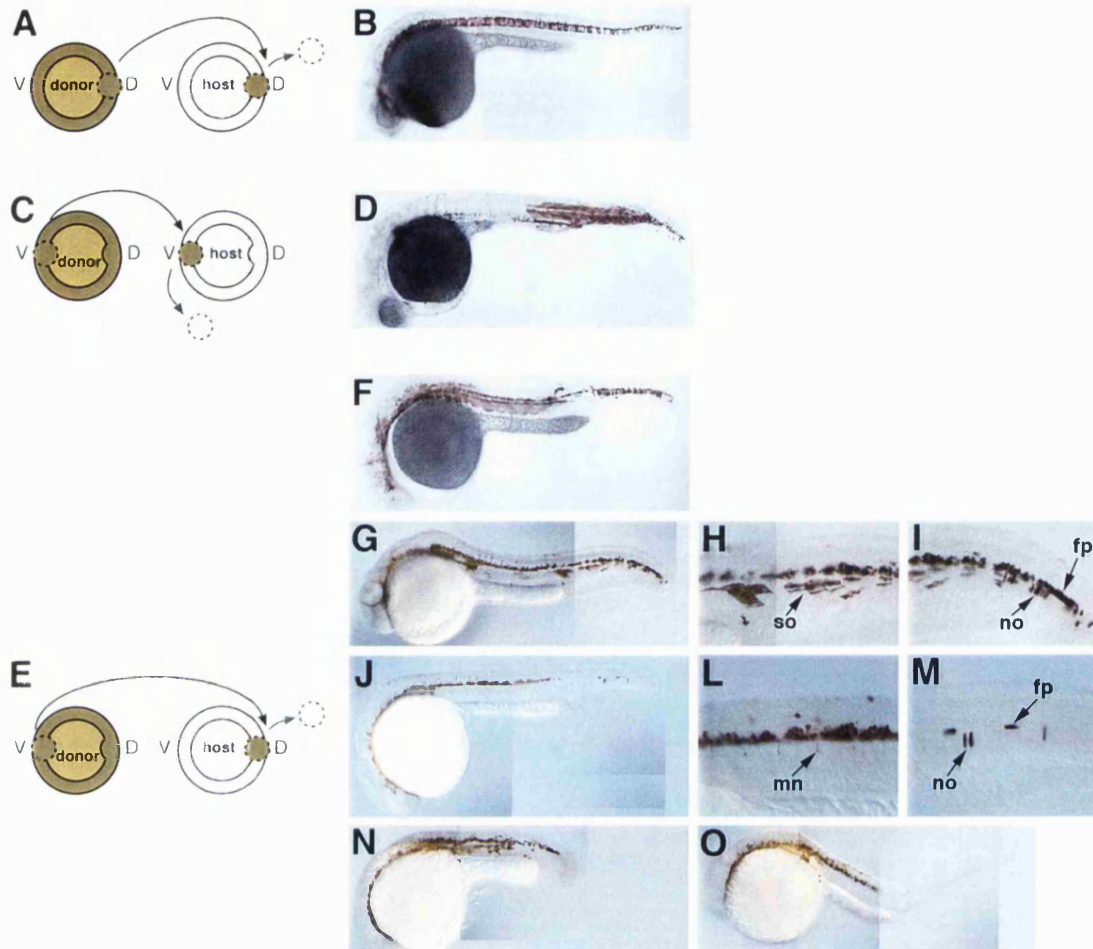
Fig. 5.4. Ventral cells can be recruited to a shield fate in the presence of the adjacent marginal tissue. (A, B) The morphological shield was replaced by a biotin-labelled morphological shield. The labelled morphological shield contributed to the hatching gland, prechordal plate, notochord, floor plate and hypochord along the entire A-P axis. **(C, D)** The ventral cells were replaced by biotin-labelled ventral cells. The labelled ventral cells contributed to posterior somites and blood islands. **(E)** The morphological shield was replaced by biotin-labelled ventral cells. **(F, G)** The labelled ventral cells gave rise to neural tissue, somites, posterior notochord, floor plate and hypochord. **(H, I)** Closer up of the tail region of the embryo in (G) showing ventral cells in neural tissue, somites and notochord. **(J)** The labelled ventral cells ended up in the neural tissue, floor plate and notochord. **(L, M)** Closer up of the trunk and tail region of the embryo in (J) showing ventral cells in neural tissue, motorneurons and notochord. **(N)** The labelled ventral cells gave rise to neural tissue and somites. **(O)** The labelled ventral cells ended up in neural tissue. no, notochord; fp, floor plate; so, somites; mn, motorneurons

Table 5.1. Cell fate of ventral tissue in shield replacement experiments

	Ventral into Dorsal 1 piece	Ventral into Dorsal 2 pieces
Neural	58 (54%)	7 (37%)
Neural + somites	23 (21%)	10 (53%)
Neural + notochord	4 (4%)	2 (10%)
Neural + somites + notochord	22 (21%)	0 (0%)
No. of experimental embryos	107	19

shield fate observed. To rule out this possibility, biotin-labelled ventral cells together with fluorescein-labelled adjacent marginal tissue were transplanted into the ventral side of an unlabelled host embryo at 6 hpf (Fig. 5.5D). In the presence of adjacent marginal tissue, the transplanted ventral cells gave rise not only to neural tissue and somites but also to notochord cells in the tail of the induced axis in 16% (n=63) of the cases (Fig. 5.5E, F). I also transplanted biotin-labelled ventral cells together with a fluorescein-labelled morphological shield into the ventral side of an unlabelled host embryo (Fig. 5.5A). In this context, the labelled ventral cells gave rise to neural tissue and somites in 98% (n=45) of the cases and did not contribute to the notochord of the induced axis (Fig. 5.5B, C). These experiments show that adjacent marginal tissue can convert ventral cells to a shield fate, away from the dorsal YSL.

5.2.4. The *zADMP* gene, a candidate inhibitor present in the shield

The preceding experiments demonstrate that adjacent marginal tissue has the ability to induce shield fates in non-shield cells. Only a limited region of the dorsal marginal blastoderm is fated to become shield in intact embryos, suggesting the existence of a counteracting signal. Such an inhibitor of shield fates could be secreted by the embryonic shield to prevent the formation of ectopic shield tissue in adjacent regions. A good candidate, for such an inhibitor, has been identified in *Xenopus*. The BMP family member, anti-dorsalising morphogenetic protein (xADMP; Moos et al., 1995) has the paradoxical properties of suppressing dorsal fates, while being expressed in the Spemann's organizer itself. It has been proposed that xADMP may moderate organizer-associated dorsalising influences. The chick ADMP (cADMP) was also cloned and it was shown that the avian organizer, the Hensen's node, produces it. cADMP represses the induction of ectopic organizer markers by the node inducing centre (Joubin and Stern, 1999). I decided to undertake the cloning of the zebrafish homologue in collaboration with Pedro Coutinho (Derek Stemple's laboratory).
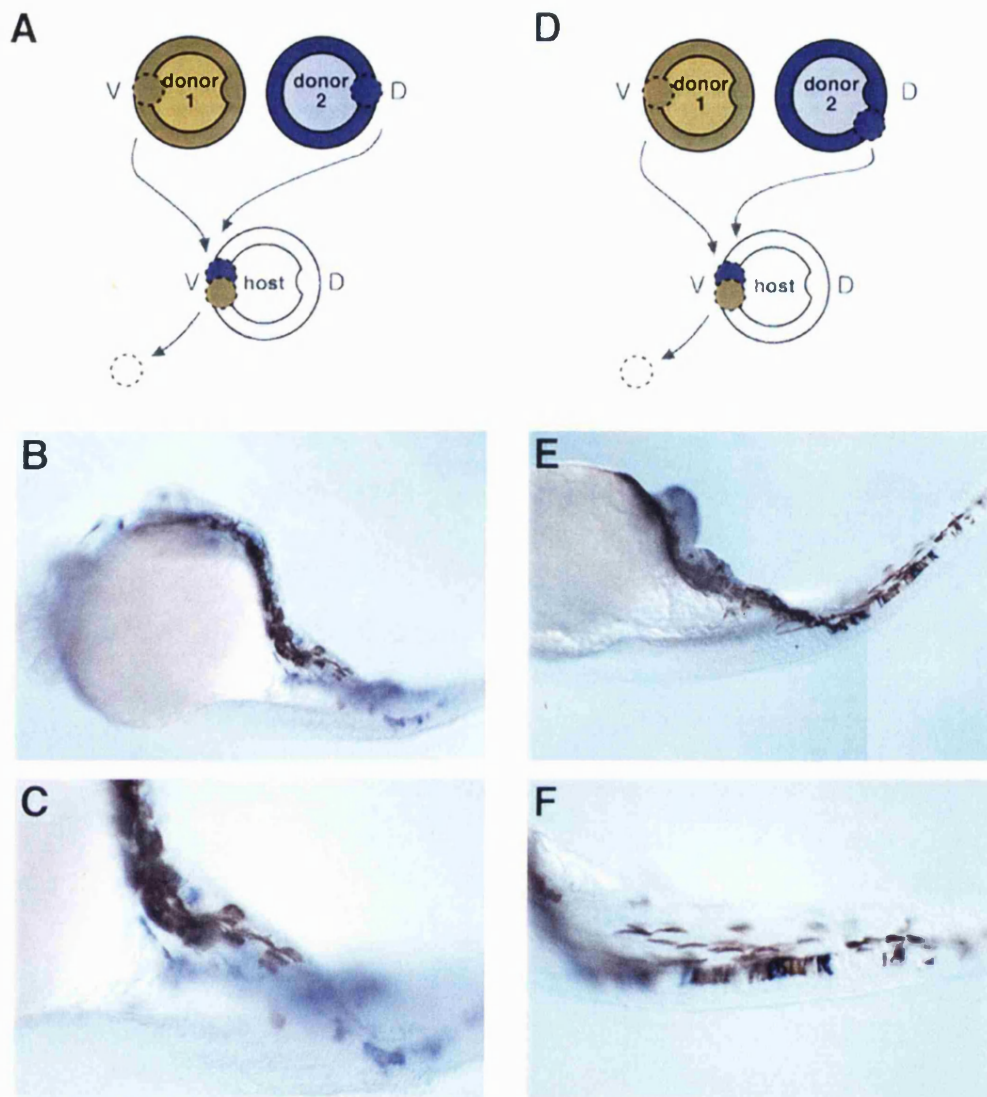
Fig. 5.5. Adjacent marginal tissue can convert ventral cells into a shield fate away from the dorsal YSL. (A) Biotin-labelled ventral cells and a fluorescein-labelled morphological shield were transplanted to the ventral side of an host embryo. **(B)** The morphological shield induced a secondary axis in which the ventral cells contributed to neural tissue and somites. **(C)** Closer up of the trunk region of the induced axis. **(D)** Biotin-labelled ventral cells and fluorescein-labelled adjacent marginal tissue were transplanted to the ventral side of an host embryo. **(E)** The adjacent marginal tissue induced a secondary axis in which the ventral cells contributed to neural tissue, somites and notochord. **(F)** Closer-up of the trunk region of the induced axis, where it is possible to see labelled ventral cells intermingled with host ventral cells and shield cells in the notochord.

One expressed Sequence Tag (EST), similar to ADMP 1 precursor, was found in the nucleotide database of GenBank (accession number AW165171). This EST corresponds to the RZPD clone MPMGp609I0870. The 1.405 kb EST fragment was sequenced and contained the entire 1.176 kb open reading frame for the putative zebrafish ADMP (zADMP). The predicted protein is a member of the TGF-ß superfamily and is related most closely to BMP2. The sequence landmarks of the BMP family, such as six conserved cysteine residues in the carboxy-terminal domain (Kingsley, 1994; Reddi, 1992) are present in the deduced amino acid sequence of zADMP (Fig. 5.6). The BMP family members are synthesised as proproteins and subsequently cleaved at a RXXR site (Barr, 1991). A putative cleavage site in the zADMP sequence is a RSPR motif positioned at amino acids 273-276 (Fig. 5.6). In the mature domain following the first conserved cysteine, the deduced amino acid sequence of zADMP is 87% identical to xADMP and 83% identical to cADMP. In the prodomain region, the deduced amino acid sequence of zADMP is 69% identical to xADMP and 59% identical to cADMP.

In order to produce a zADMP antisense riboprobe, the plasmid was digested with EcoRI and transcribed with SP6 RNA polymerase. The *in situ* hybridisation analysis revealed that the expression of zADMP is zygotic and transient. zADMP is expressed from shield stage (6 hpf) to 8 hpf. No expression was detected at later stages tested up to 16 hpf. At shield stage, zADMP is expressed in the embryonic shield in both the superficial epiblast and the deep hypoblast (Fig.5.7A-C). From a dorsal view, the borders of zADMP appear more similar to the borders of the organizer-specific gene *gsc* than to the borders of the organizer-specific gene *flh* (compare Fig. 5.7C with Fig 4.1A in Chapter 4). At 8 hpf, zADMP is expressed in the nascent axial mesoderm (prechordal plate and notochord) (Fig. 5.7D, E). Therefore, zADMP expression is at the right time and place to be an inhibitory signal secreted by the embryonic shield. However, several functional experiments need to be done in order to test this hypothesis.

```
1   M - - - - - L G T V L L L L L A L - - - A R P A A - - - - - - - - - - - - - P E S   cADMP
1   M D L R K M L G F I F L F F I I Q E C T S R P T D M V D - S T D L E L E D P E L   xADMP
1   M - L S A M F - F A M L S T M M G L S F A R P G F F N E L E E H L A V E S E P K   zADMP


21  R R A E A L K K L L E V F G M E D P P P P A H V K Q P P Q Y M V D L F N A V A   cADMP
40  V R A E A L K R L L E V F G I E P P Q P L Q H V K Q P P Q Y M V D L Y N T V A   xADMP
39  V R S E A I R R L L E V F G M E D P P A A L G H - K Q P P Q Y M L D L Y N T I A   zADMP


61  N A D G V T K N P D V L E G N T V R S F L D R T H G E K M R F L F V L S S V A R   cADMP
80  D E D G V T K D P D L L E G N T V R S F F D K I H S D H M H F L F N L W T V A R   xADMP
78  D V D G V T K D P T L L E G N T V R S F F D K L H S E R I E Y L F N M S T V A K   zADMP


101 N E K I L T A E L H L F R L W P R A A E G P - - R R H H F C Q V S V Y Q I I D E   cADMP
120 N E K I L T A E L H L F K L K P R P S E Q A Y F K R H H F C Q I S V Y M V D K   xADMP
118 S E K I L T A E L H L F K L R P K T S I V - - L N R H H F C Q V S V Y Q V L D S   zADMP


139 S E P D S P E G Q K L L A T R L L S L Q G S G W E V F A I T Q A V R D W T Q D E   cADMP
160 N K I Q L P Q G R K L L S S K L V P I H S S G W E V F S I T Q A V R A W - N D E   xADMP
156 G K K N V S Q G K K L L S S R L V P I H S T G W E V F T I T Q A V R S W M S D E   zADMP


179 S S N R G L L V T V H G L G G S A L E A P A V Q F A S S G D H H E S K K P M L V   cADMP
199 S A N H G I L V T V R N L G G A Q V D P N I I R F A S G R D H H E S K Q P M L V   xADMP
196 G S N L G L L V S V R T L A G S Q M D L K M V R F A S G R D H H H S K Q P M L V   zADMP

                                                                     • • •
219 L F T D D G R R G A S L P M A G V P A S Q P R D F P A K L S G P - - - - - R S A   cADMP
239 L F T D D G R R G I - V S V N N Q P D D Q L M P L P N V P M A P T S N R T R L G   xADMP
236 L F T D D G R R A A S L E A T S K G S D V S P G S P S Q P L P S V P A S R R S P   zADMP

    •                           *
254 R S L D R - - - - - L Q P C Q R H P L S V D F E E I G W S G W I I S P R G Y N A   cADMP
278 R S V - - - E E D G Q L P C Q R H P L Y V D F E E I G W S G W I I S P R G Y N A   xADMP
276 R S V D Y D E R G E K M A C Q R Q P L Y V D F E E I G W S G W I V S P K G Y N A   zADMP

            *       *                                                        *
289 Y H C R G S C P F P L G E N M R P T N H A T V Q S I I N A L K L S E G V S S P C   cADMP
315 Y H C K G S C P F P L G Q N M R P T N H A T V Q S I I N A L K L T K G V S S P C   xADMP
316 Y H C K G S C I F P L S Q N M R P T N H A I V Q S I I N T L K L N K G I Q T P C   zADMP

    *                                                         *   *
329 C V P D K L H S I N L L Y F D D D E N V V L K Q Y D D M V A G S C G C H   cADMP
355 C V P D K L F S I N L L Y F D D D E N V V L K Q Y D D M V A G S C G C H   xADMP
356 C V P D K L Y S I S L L Y F D D D E N V V L K Q Y D D M V A G S C G C R   zADMP
```

Fig. 5.6. Zebrafish ADMP. Alignment of the amino acid sequence of zebrafish ADMP (zADMP) and its *Xenopus* (xADMP) and chick (cADMP) homologues. The putative cleavage site is signed with black dots. The asterisk indicates the seven conserved cysteine residues. The mature domain of the ADMP lies to the right of the cleavage site.
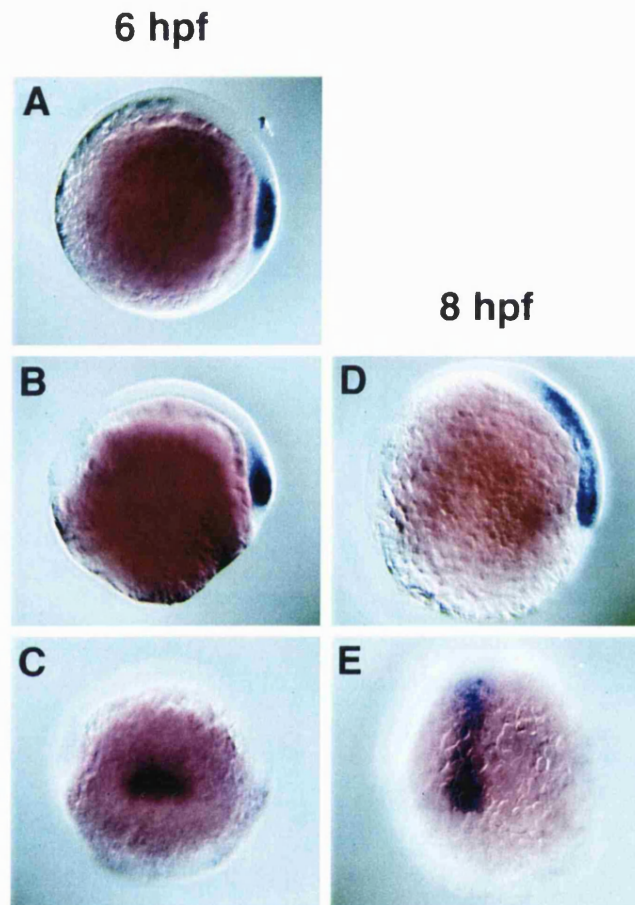
6 hpf

8 hpf

Fig. 5.7. *zADMP* **expression in the embryonic shield.** (**A-C**) At shield stage (6 hpf), *zADMP* is expressed in the embryonic shield. (**D, E**) At 8 hpf, *zADMP* is expressed in the nascent axial mesoderm that derives from the shield. (**A**) Animal view. (**B, D**) Lateral views. (**C, E**) Dorsal views.

5.2.5. Fate map of the areas surrounding the shield region

The transplantation experiments described above showed that the adjacent marginal tissue of the shield region could induce shield fates. This observation and the lack of compensatory proliferation following morphological shield removal, suggest that shield derivatives restoration occurs via a recruitment of cells that surround the shield region to a shield fate. To directly test this idea, the following experiment was planned. Embryos at 1- to 4-cell stage would be injected with caged-fluorescein-dextran dye and left to develop until shield stage. The shield region (morphological shield and adjacent marginal tissue) is about 20 cells in width along the margin (Melby et al., 1996; Shih and Fraser, 1996). To establish the fate of cells proximal to the shield region in intact embryos, small clusters of cells located about 15 cells diameters from the centre of the morphological shield would be labelled by laser-assisted uncaging of caged fluorescein-dextran. The position of the labelled cells would then be documented by overlying fluorescent and differential interference contrast (DIC) images. The embryos would then be incubated until beyond 24 hpf and the fate of labelled cells would be detected by imunohistochemistry using an alkaline phosphatase-conjugated antibody against fluorescein. To determine whether the fate of cells proximal to the shield region is altered by removal of the morphological shield, the morphological shield would be removed immediately after monitoring the position of the labelled cells. The fates of the labelled cells could then be compared to those seen in control embryos. In collaboration with Toby Rogers (Summer student in Derek Stemple's laboratory), I mastered several of the techniques required for this experiment. Although we were unable to precisely target cells outside the shield region, our preliminary data, as described below, demonstrate the feasibility of this approach.

When labelled cells were close to the borders of the morphological shield of intact embryos (Fig. 5.8A, C, G, I, L), they contributed to notochord, floor plate and hypochord, which are normal shield derivatives (Fig. 5.8B, D, H, J, M). Since the shield region is broader than the morphological shield, it is not surprising that these fates were observed. In one experiment, where labelled cells were further away from the

102
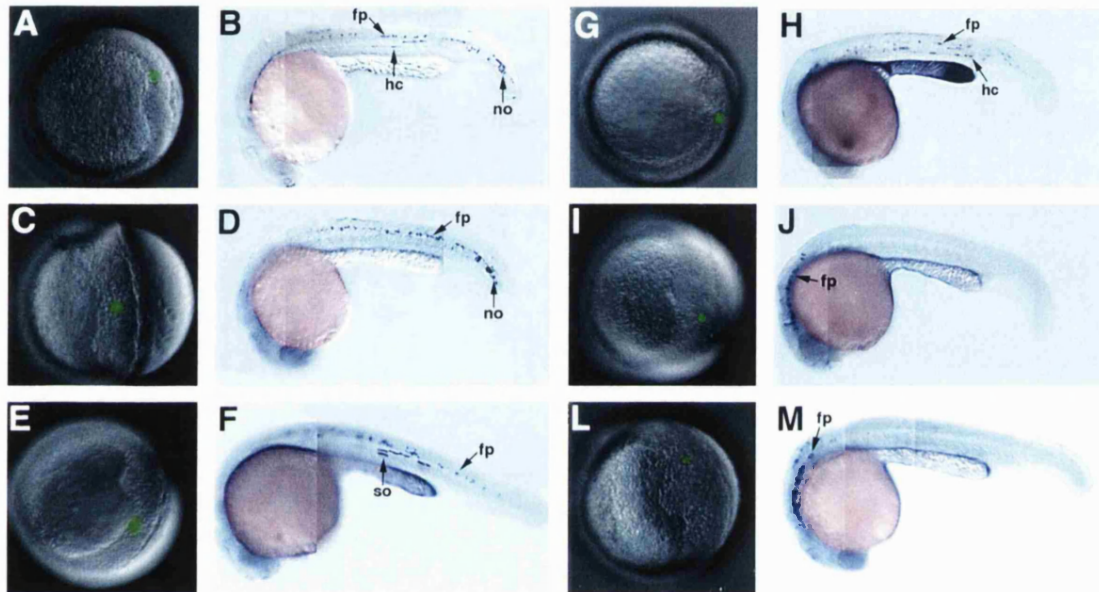
Fig. 5.8. Fate map of cells located in the dorsal blastoderm margin in intact embryos. (**A, C, E, G, I, L**) DIC images of shield stage embryos overlayed with fluorescence image of the uncaged cells in green. (**B, D, F, H, J, M**) Lateral views of the embryos shown in (A, C, E, G, I, L) at 24 to 32 hpf stained with anti-fluorescein antibody, anterior to the left. (**A, C, G, I, L**) The cells labelled were localised near the borders of the morphological shield and (**B, D, H, J, M**) ended up in shield derivatives. (**E**) The labelled cells were localised away from the morphological shield and (**F**) gave rise to floor plate plus somites. no, notochord; fp, floor plate; hc, hypochord; so, somites

morphological shield (Fig. 5.8E), they contributed to floor plate and to medial somites (Fig. 5.8F). Medial somites are not normal shield derivatives. In fate map experiments performed in morphological shield-ablated embryos, only one embryo showed labelled cells in the notochord (Fig. 5.9B), while the others had labelled cells contributing to floor plate (Fig.5.9E, G, I). However, as in control embryos, these labelled cells were rather close to the morphological shield and it seems likely that these cells were already fated to become shield derivatives. Thus, fate mapping experiments in intact and morphological shield-ablated embryos show that cells beyond the morphological shield but within the shield region are progenitors for notochord, floor plate and hypochord. These experiments also showed that somite precursors can be found lateral to the shield region in intact embryos. These results are in agreement with previous fate maps (Melby et al., 1996).

The difficulty in identifying the position of cells to be labelled lies from the inability to visualise the borders of the shield region at the magnification required for uncaging cells. In the future, this experiment will be modified. Fate mapping will be performed on transgenic embryos expressing green fluorescent protein (GFP) under the control of *gsc* or *flh* promoters (Henry Roehl, Miranda Gompertz and Steve Wilson, personal communication), which should help to visualise the borders of the shield region at either high or low magnification.

5.3. Discussion

Formation of shield derivatives after morphological shield removal is dependent upon appropriate wound healing, which itself depends on the ionic balance of the experimental medium. Initially, I performed the shield removal experiments in 0.3X Danieau solution and found that the majority of embryos did not properly generate axial mesoderm. I propose that the enveloping layer (EVL) cells, which are rapidly moving to seal the embryo from the low-salt extraembryonic condition, form a scar that prevents
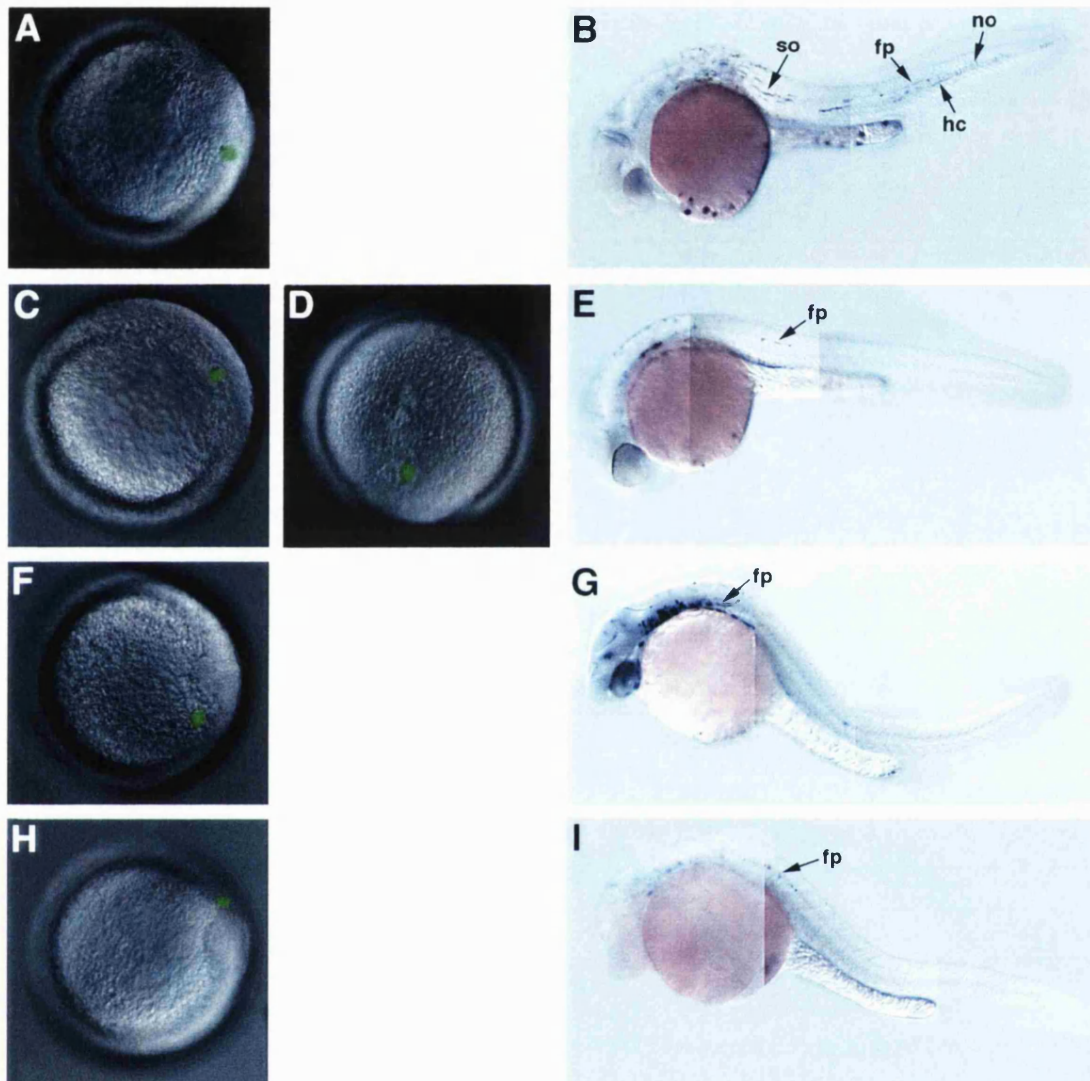
Fig. 5.9. Fate map of cells located in the dorsal blastoderm margin in morphological shield-ablated embryos. (A, C, F, H) DIC images of shield stage embryos overlayed with fluorescence image of the uncaged cells in green. **(D)** DIC image of the embryo shown in (C) at 90 % epiboly overlayed with fluorescence image of the uncaged cells in green. **(B, E, G, I)** Lateral views the embryos shown in (A, C, D, F, H) at 24 to 32 hpf stained with anti-fluorescein antibody, anterior to the left. **(A, C, D, F, H)** The cells labelled were localised near the morphological shield and **(E, G, I)** ended up in shield derivatives and **(B)** somites. no, notochord; fp, floor plate; hc, hypochord; so, somites

the coalescence of deep cells. In the high salt condition (1X Danieau solution), according to this model, EVL cells fail to rapidly close the wound and deep cells are able to re-associate and go on to form normal shield derivatives. The formation of shield derivatives requires not only the presence of adjacent marginal tissue relative to the morphological shield, but also that this tissue heals properly.

A zebrafish embryo at gastrula stage consists of around 2^{14}=16,384 cells (Solnica-Krezel et al., 1995) and the amount of cells removed in the morphological shield removal experiments was around 400 cells (estimated by counting nuclei stained with Hoechst, a DNA fluorochrome). Since this corresponds to a loss of only 2%, it is perhaps not surprising that morphological shield-ablated embryos have a normal size by 24 hpf. However, removal of the morphological shield represents a loss of 80% of axial mesoderm, floor plate and hypochord precursors. I have investigated whether compensatory mechanisms, such as cell proliferation and cell fate change, could account for the recovery of shield derivatives.

Proliferation analysis revealed that there is no increase in proliferation in regions surrounding the site of ablation in the 90 minutes following morphological shield removal. However, considering that only a few extra cell divisions would be sufficient to replace the number of cells removed, an increase in proliferation could be very difficult to detect. It is also possible that there is a decrease of cell death in morphological shield-ablated embryos.

Evidence for a cell fate change, as a compensatory mechanism after morphological shield removal, came from replacement and transplantation experiments. Ventral cells in intact embryos gave rise to somites and blood cells. When the entire shield region (i.e. morphological shield plus the adjacent marginal tissue) was replaced by ventral tissue, the ventral tissue was dorsalised and gave rise to anterior somites and neural tissue. When the morphological shield was replaced by ventral cells, they were put in contact with the adjacent marginal tissue. In this situation, the ventral cells still gave rise to somites and neural tissue but also acquired new fates. Some ventral cells became

notochord, floor plate and hypochord, which are structures normally derived from the shield. These results are in agreement with previous findings that ventral tissue at gastrula stage is not committed to a ventral fate and that the shield can dorsalise ventral tissue (Ho and Kimmel, 1993; Shih and Fraser, 1996); see also Chapter 3). In addition, these experiments suggest that upon morphological shield removal, adjacent marginal tissue have the ability to recruit non-shield cells to a shield fate. It seems that notochord, floor plate and hypochord precursors can induce more notochord, floor plate and hypochord precursors. This type of induction in which "like induces like" is called homeogenetic induction. The concept of homeogenetic induction originates from experiments done by Mangold in 1933. He found that strips of neural plate could induce similar types of neural tissue in an Einsteck experiment (reviewed in Doniach, 1993). Homeogenetic neural induction has been proposed to play a role in normal formation of the neural plate in amphibians (Albers, 1987; Nieuwkoop, 1952; Nieuwkoop, 1985; Servetnick and Grainger, 1991). The analysis of the zebrafish *cyclops* mutation also suggests the existence of homeogenetic induction between floor plate precursors (Hatta et al., 1991). In the chick, it was shown that homeogenetic signals derived from the medial floor plate cells could recruit more lateral cells to a floor plate fate. The extent of floor plate induction was proposed to be limited by the loss of competence of neural plate cells to respond to the inductive signals (Placzek et al., 1993). Another type of homeogenetic induction was reported to occur in the mesoderm. Recombinant experiments in *Xenopus* showed that animal pole ectoderm forms somites when juxtaposed to ectoderm that has been previously induced to become mesoderm (Cooke et al., 1987; Slack et al., 1988). The results presented in this chapter suggest, for the first time, that notochord cells may also be induced by homeogenetic signals in zebrafish embryos.

Unrestricted homeogenetic induction by the shield would result in the expansion of the shield region. Since this does not normally happens, a counteracting signal must exist in the shield region. A model for inductive and inhibitory interactions in the shield region is presented in Fig. 5.10. Transplantation experiments support the existence of such an inhibitory signal. When adjacent marginal tissue is transplanted to the ventral side of a

host embryo, it can induce an incomplete secondary body axis. In the induced axis, the notochord is chimeric, made of adjacent marginal tissue and ventral cells. In contrast, when the morphological shield is transplanted to the ventral side of a host embryo, it can induce a complete second body axis in which the notochord derives exclusively from the transplanted shield. The activity of an inhibitor of shield fates in the morphological shield could explain the fact that in an induced secondary axis, shield derivatives do not have any contribution from host ventral cells (Shih and Fraser, 1996; see also Chapter 3). In *Xenopus*, it was shown that ventral tissue inserted into the middle of the dorsal blastopore lip changed its fate and became somite tissue, splitting the notochord into two (Smith and Slack, 1983). According to the model presented here (Fig. 5.10), the *Xenopus* ventral cells were not converted into notochord, because the source of inhibitory signals (the dorsal blastopore lip) was not removed.

The expression of *zADMP* in the shield region at gastrulation stages makes it a good candidate for an inhibitory signal secreted by the embryonic shield. However, over-expression experiments and loss of function studies need to be done in order to understand its function in zebrafish embryos. *antivin* , a member of the Lefty subfamily of TGF-β molecules, is also expressed in the shield region and negatively regulates mesoderm induction by antagonising Nodal signalling though a feedback loop (Meno et al., 1999; Thisse and Thisse, 1999). Whether Nodal signalling is involved in homeogenetic induction of the notochord and whether ADMP and Antivin are inhibitors of this process is not known at present.
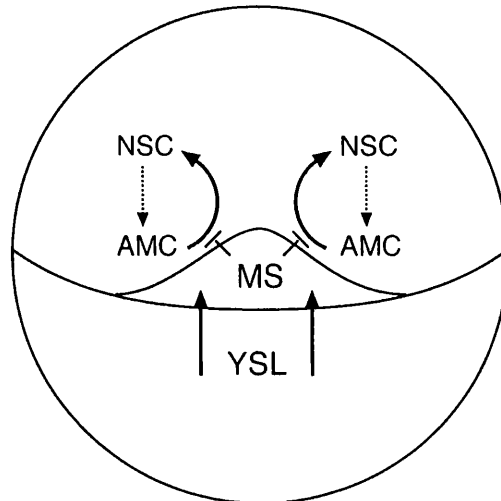
YSL - Yolk syncytial layer
MS - Morphological shield
AMC - Adjacent marginal cells
NSC - Non-shield cells

Fig. 5.10. Model of the interactions that confines the physical domain of the embryonic shield region. The figure represents a dorsal view of a shield stage zebrafish embryo. On the dorsal side the YSL induces the embryonic shield. The embryonic shield comprises the MS and the AMC. The AMC have the ability to recruit NSC into a shield fate. However, this recruitment is prevented by the presence of inhibitors in the MS. The balance between inducers and inhibitors defines the embryonic shield region.

Chapter 6

Contribution of the New Surgical Method to Study Gene Function in Axial Midline Mutants

6.1. Introduction

Classical forward genetics has been a hugely informative approach in developmental biology. Analysis of mutant phenotypes often improves understanding the function of gene products. The zebrafish is one of the most suitable vertebrate models for genetic studies. The small size, high fecundity, external fertilisation and optical clarity of zebrafish made possible large-scale mutagenesis screens. Following the genetic screens, positional cloning and candidate gene approaches have led to the identification of several mutations that affect early development (reviewed in Kodjabachian et al., 1999). Due to the pleiotropic nature of many genes, it is often difficult to observe the distinct roles that a gene product has during development. For example, an early lethal mutation prevents studying gene function at later stages.

Genetic mosaic analysis has proven to be a powerful technique to reveal mechanisms of gene function that could not be recognised by simple analysis of the mutant phenotype. In a broad definition, genetic mosaics are embryos that contain both wild-type and mutant cells. Making embryonic mosaics helps to define the primary site of action of a mutation and allows determining whether a gene product acts cell-autonomously or cell-non-autonomously. When cells carrying a cell-autonomous mutation are used to generate mosaic embryos, the mutant phenotype occurs only in the cells that are genotypically mutant. If the gene product is essential to specify a distinct cellular fate, then in the mosaic embryo the genotypically mutant cells will be absent in specific tissues. This means that studying the fate of mutant cells in mosaic embryos can give information about where a gene product is required. In mosaics, non-autonomous action of a mutation in a given tissue is revealed by the presence of genotypically wild-type cells that exhibit the mutant phenotype, or genotypically mutant cells that are phenotypically wild-type (reviewed in Moens and Fritz, 1999; Rossant et al., 1998).

When the gene responsible for a particular mutation is not known, mosaic analysis can give an indication about the nature of the gene product. For example, transcription

factors, signal-transducing molecules and receptors are molecules that act within a cell and therefore are likely to act in a cell-autonomous manner. Conversely, secreted molecules are likely to act in a cell-non-autonomous way. Therefore, testing autonomy of gene action can be used as a strategy to narrow the number of candidate genes for a particular mutation (reviewed in Moens and Fritz, 1999; Rossant et al., 1998).

In zebrafish, genetic mosaics have been made by transplanting cells from a donor embryo labelled with a lineage tracer to an unlabeled host embryo at blastula stages and determining later the cell fate of the donor-derived cells (Ho and Kane, 1990). Wild-type cells that are transplanted near the margin of the host blastoderm contribute to the mesoderm, while cells transplanted to the animal pole will contribute to the neuroectoderm (Kimmel and Warga, 1987; Wilson et al., 1995). Since at blastula stages there is no morphological indication of dorsal-ventral polarity it can be difficult to target specific structures within the embryo. However, by performing transplantations at early gastrula stages and using the fate maps as guides, it has been possible to target specific embryonic structures like the midbrain, hindbrain and spinal cord (Moens et al., 1998; Moens et al., 1996).

We used the new method for shield removal and transplantation to generate genetic mosaic embryos in which consistently and specifically the entire axial midline tissues derived from the donor embryo of a particular genotype. Using this strategy we investigated gene function in two mutations that affect the axial midline: *sneezy* (*sny*) that disrupts differentiation of the notochord (Stemple et al., 1996) and *silberblick* (*slb*) that perturbs convergent extension movements (Heisenberg et al., 1996).

6.2. Results

6.2.1. Analysis of the *sny* mutant

The notochord is the major skeletal element of fish embryos and it is also an important signalling source that patterns the neuroectoderm and paraxial mesoderm (Holley and Nusslein-Volhard, 2000; Placzek, 1995). The zebrafish axial mesoderm is derived from the embryonic shield and as a consequence of gastrulation movements migrates anteriorly and lays down the prechordal plate and the notochord rudiment, named the chordamesoderm (Kimmel et al., 1995). The chordamesoderm can be distinguished from the paraxial mesoderm because it expresses several genes including *no tail (ntl)*, *sonic hedgehog (shh)* and *α1-collagen Type II (col2a1)* (Schulte-Merker et al., 1992; Yan et al., 1995). The notochord cells differentiate during the segmentation period and vacuolate. When this differentiation occurs the expression of *ntl*, *shh* and *col2a1* is down regulated in the notochord (Schulte-Merker et al., 1992). In *sny* mutant embryos, the chordamesoderm cells do not vacuolate and the expression of early notochord markers, like *ntl*, *shh* and *col2a1* persist well after they are down regulated in wild-type siblings. The number of muscle pioneer and pigment cells is reduced in *sny* mutants relative to wild-type siblings. Later in development, *sny* mutant embryos degenerate (Stemple et al., 1996).

We do not know what is the gene mutated in *sny* mutant embryos. To gain some insight into how the *sny* gene product functions, we generated genetic mosaic embryos in which the axial midline tissues were genotypically different from the rest of the embryo. Experimental embryos were obtained by crossing heterozygotes for *sny*, yielding both wild-type and *sny* embryos (3:1 ratio). As the mutant phenotype is not visible at shield stage, the choice of donors and hosts for the transplantation experiments was done blindly. Using the new surgical method (Chapter 2, section 2.3.3. and Chapter 3, section 3.2.1.), morphological shields from 6 hours-post-fertilisation (hpf) embryos were transplanted into the ventral germ-ring of 6 hpf host embryos. The fact that the embryo from which the morphological shield is removed develops normally (see Chapter 4,

113
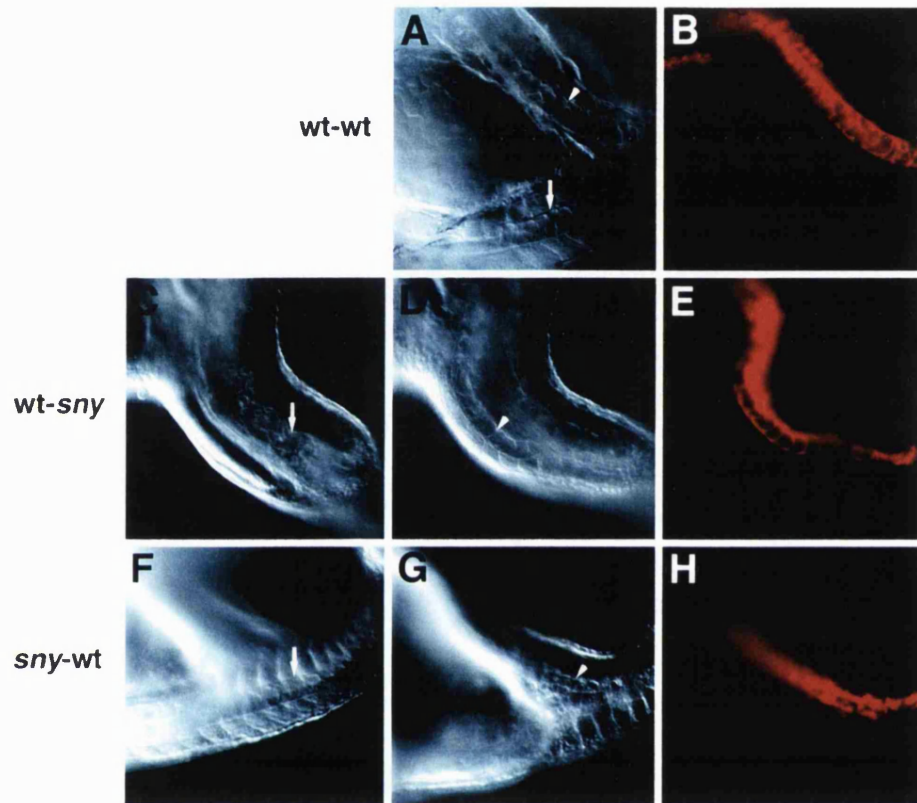
Fig. 6.1. *sny* **acts autonomously within the shield derivatives. (A-H)** A rhodamine-dextran labelled shield from a donor embryo was grafted into the ventral germ ring of a 6 hpf host embryo. Embryos were examined at 30 hpf for the presence or absence of vacuoles within the notochord cells. **(A, B)** As a control, a wild-type (wt) shield gave rise to a vacuolated notochord when transplanted into a wt host. **(C-E)** A wt shield when transplanted into a *sny* mutant host gave rise to a vacuolated notochord. **(F-H)** A *sny* mutant shield was transplanted into a wt host and gave rise to a non-vacuolated notochord. **(A, C, D, F, G)** Differential interference contrast (DIC) images of the trunk-tail region of the experimental embryos. **(B, E, H)** Epifluorescence image of the same embryo shown in (A, C, D, F, G). All panels are lateral views with the induced secondary axis up. The arrows indicate the notochord of the primary axis. The arrowhead indicates the notochord of the induced secondary axis.

section 4.2.1.) constitutes a clear advantage of the new surgical method. In fact, the donor embryo has to be kept in perfect conditions so that its genotype can be identified at later stages by observing its phenotype. Each pair of donor and host experimental embryos was kept together and cultured until 30 hpf. The donor embryo was classified as wild-type or mutant depending on the presence or absence of vacuolated cells in the notochord, respectively. The host was classified as wild-type or mutant by the presence or absence of vacuolated cells in the notochord of the primary axis. Shields from wild-type embryos transplanted into the ventral side of *sny* mutant embryos induced secondary axes with wild-type notochords (Fig. 6.1C-E). Shields from *sny* mutant embryos transplanted into the ventral side of wild-type host embryos induced secondary axes with mutant notochords (Fig. 6.1F-H). In these transplantation experiments, the notochord in the induced secondary axis always developed according to the genotype of the donor embryo. This indicates that the *sny* gene product is required within the shield derivatives for correct notochord differentiation in an autonomous way. This work was done in collaboration with Pedro Coutinho (Derek Stemple's laboratory, NIMR).

6.2.2. Analysis of the *slb* mutant

In gastrulating embryos, during the process of convergent extension, cells converge towards the dorsal midline accompanied by medial-lateral cell intercalation, which subsequently leads to anterior-posterior extension of the embryonic body axis (Keller et al., 1992; Warga and Kimmel, 1990). In *slb* mutant embryos, the extension of the axial mesoderm and overlying ventral central nervous system is disrupted, followed by a slight fusion of the eyes at later developmental stages (Heisenberg and Nusslein-Volhard, 1997). *In situ* hybridisation studies at tailbud stages revealed that in *slb* mutant embryos, the prechordal plate is elongated and posteriorly displaced relatively to the neural plate and the notochord is short (Heisenberg et al., 2000). It was shown by candidate gene approach that the *slb* phenotype is due to a mutation in the *wnt11* gene. By late gastrulation, *wnt11* is expressed within the anterior paraxial head mesoderm and the anterior lateral neuroectoderm. The paraxial head mesoderm domain lies directly

anterior to the presumptive paraxial somitic mesoderm and the lateral neuroectoderm domain is posterior to the presumptive forebrain. Since in wild-type embryos, *wnt11* is expressed in non-axial tissues, it seemed possible that the Wnt11 activity is required in paraxial cells to mediate the normal axial movement of axial tissues (Heisenberg et al., 2000).

Using the new surgical method, morphological shields from host embryos were replaced at 6 hpf by shields derived from biotin-dextran labelled donor embryos. In this way we generated mosaic embryos in which the axial mesoderm was genetically different from the paraxial tissue. There was no need to keep the donor embryo, since homozygous *slb* mutant fish are viable and fertile and therefore could be used to generate offspring consisting exclusively of *slb* homozygous embryos. We then determined if the movement pattern of the axial mesoderm at tailbud stage was phenotypically similar to the one seen in wild-type or *slb* mutant embryos. In order to do this, we examined the extension of the axial mesoderm relative to the overlying anterior edge of the neural plate by *in situ* hybridisation with *dlx3* (marks the edge of the neural plate) (Akimenko et al., 1994), *hgg1* (marks the anterior end of the hypoblast, the polster) (Thisse et al., 1994) and *ntl* (marks the notochord) (Schulte-Merker et al., 1994). The behaviour of *slb* mutant shield derivatives in an otherwise wild-type embryo was indistinguishable from that of wild-type shield derivatives (compare Fig. 6.2B with Fig. 6.2A; Table 6.1). Conversely, wild-type shield derivatives in otherwise *slb* mutant embryos behaved like *slb* mutant shields derivatives in a *slb* mutant embryo (Fig. 6.2C; Table 6.1). These results suggest that *wnt11* in paraxial cells is required for normal convergent extension of midline tissues in a non-autonomous manner.

We also investigated if Wnt11 secreted from lateral cells acts directly upon midline cells to mediate cell movement. To test this possibility, we replaced the shield of *slb* mutant embryos with a shield from *slb* mutant embryos that had been injected at one cell stage with RNA encoding *wnt11* or a truncated form of *dishevelled (dsh-ΔN)*. It was shown that this particular form of Dsh can transduce Wnt signals that regulate morphogenetic
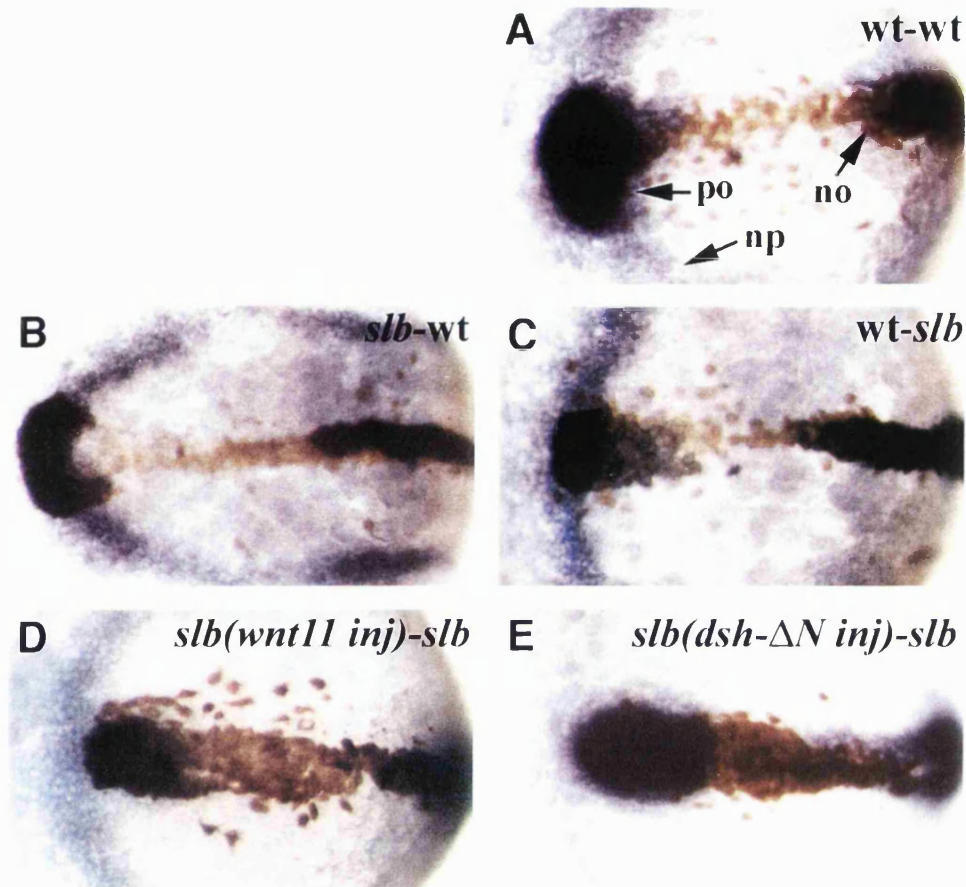
Fig. 6.2. Wnt11 is required in lateral cells for convergent extension movements during gastrulation. (A-E) The host shield was replaced by a biotin-dextran labelled shield from a donor embryo. The extension of the axial mesoderm relative to the overlying anterior edge of the neural plate was examined at tailbud stage. (A) As a control, a wild-type (wt) shield was replaced by a wt shield. The wt shield derived polster was localised anterior to the neural plate. (B) A wt shield was replaced by a *slb* mutant shield. The *slb* mutant shield derived polster was localised anterior relative to the edge of the neural plate. (C) A *slb* mutant shield replaced by a wt shield. The polster derived from the wt shield was displaced posterior relative to the neural plate. (D) *slb* mutant shield replaced by a *slb* mutant shield over-expressing *wnt11* RNA. The *slb(wnt11 inj)* shield derived polster was displaced posterior relative to the neural plate. (E) *slb* mutant shield replaced by a *slb* mutant shield over-expressing *dsh-ΔN* RNA. The *slb(dsh-ΔN inj)* derived polster was displaced posterior relative to the neural plate. Embryos were stained in blue for the expression of *dlx3* (edge of the neural plate, np), *hgg1* (polster, po) and *ntl* (notochord, no). Transplanted cells were stained for biotin (brown). All panels show dorsal views of tailbud stage embryos.

Table 6.1. *slb/wnt11* is required in lateral cells to regulate convergent extension

donor	host	wild-type (%)	*slb* (%)	total (n)
wt	wt	100	0	9
wt	*slb*	4	96	18
slb	wt	93	7	30
slb (*wnt11*)	*slb*	2	98	41
slb(*dsh-ΔN*)	*slb*	0	100	20

Normal convergent extension movements were classified as either "wild-type" or "*slb*" by the shape and position of the prechordal plate in relation to the anterior edge of the neural plate.

movements, but not those involved in the canonical Wnt pathway (Tada and Smith, 2000). Ectopic expression of *wnt11* or *dsh-ΔN* in *slb* mutant shield derivatives did not restore wild-type convergent extension movements of axial tissue (Fig. 6.2D, E; Table 6.1). These results indicate that Wnt11 activity in the midline cells is not sufficient for normal convergent extension movements of axial tissue. This work was done in collaboration with Carl-Philipp Heisenberg (Derek Stemple's laboratory, NIMR and Steve Wilson's laboratory, UCL) and Masazumi Tada (Jim Smith's laboratory, NIMR).

6.3. Discussion

6.3.1. *sny* function in notochord differentiation

We used the new surgical method to perform a genetic mosaic analysis. The mosaic embryos, containing wild-type or *sny* mutant cells within the axial midline tissues, gave us an indication of where and how *sny* might act within the embryo. The genetic mosaic analysis showed that a *sny* mutant shield always gave rise to a mutant notochord in both wild-type and *sny* mutant host embryos. These results indicate that *sny* acts autonomously within the shield derivatives suggesting that it is expressed within axial midline tissues. In order to determine in which of the shield derivatives *sny* is required, transplanted cells should be targeted more specifically in sub-structures of the shield such as the notochord or the floor plate and the phenotype of the transplanted cells subsequently analysed.

6.3.2. *wnt11* function in convergent extension during gastrulation

Using the new surgical method to generate genetic mosaic embryos, we showed that Wnt11 is required in paraxial cells for normal convergent extension of midline tissues in a non-autonomous manner. We also showed that Wnt11 activity in the midline cells is

not sufficient for normal convergent extension movements of axial tissue. Additional data have indicated that Wnt11 functions in a cell non-autonomous manner throughout the non-axial mesoderm by regulating medial-lateral cell intercalation leading to anterior-posterior extension of the body axis (Heisenberg et al., 2000).

These results provide genetic evidence that Wnt genes regulate convergent extension movements in the non-axial mesoderm during gastrulation. So it seems that the signals for convergent extension movements originate in lateral tissues of the embryo rather than at the dorsal midline where convergent extension is most pronounced. The expression of *wnt11* in non-axial ectoderm, in addition with the observations that extension movements occur in the neural plate (Elul et al., 1997; Kimmel et al., 1994), indicates a possible role for Wnt mediated regulation of cell behaviour in ectodermal tissues. The finding that Dsh acts downstream of Wnt11 via a non-canonical Wnt pathway (Heisenberg et al., 2000; Tada and Smith, 2000) also reveals similarities between the intracellular pathways regulating convergent extension movements in vertebrates and planar polarity in *Drosophila* (Axelrod et al., 1998; Boutros et al., 1998). It raises the possibility that Wnt-mediated establishment of cell polarity might contribute to the morphogenetic movements seen at gastrulation. Accordingly, it was shown that inhibition of the morphogenetic function of Dsh compromises the formation of stable mediolateral protrusions and was correlated with lack of convergent extension along the anterior-posterior axis (Wallingford et al., 2000).

Chapter 7

General Discussion and Future Work

7.1. The dorsal organizer and head induction

Genetic and embryological experiments support the idea that head induction in the mouse embryo requires the co-operation between the organizer and the anterior visceral endoderm (AVE). This suggests the possibility that signals coming from embryonic regions, other than the organizer, are necessary for head induction in vertebrates other than the mouse. The search for AVE equivalents and the study of their involvement in head induction has been pursued by several laboratories. The chick anterior hypoblast, the *Xenopus* anterior endoderm and the zebrafish dorsal yolk syncytial layer (YSL) have been proposed to be the mouse AVE equivalents. These regions share with the mouse AVE some features, such as marker gene expression, pre-gastrulation movements and location relative to the prospective neuroectoderm. Removal and transplantation experiments, however, do not support a direct role for chick anterior hypoblast and *Xenopus* anterior endoderm in head induction (Knoetgen et al., 1999; Schneider and Mercola, 1999; Jones et al., 1999).

Removal and transplantation experiments of the zebrafish dorsal YSL have never been performed because of the technical difficulties associated with such a manipulation. Nevertheless, the experiments described in Chapter 3 show that the zebrafish organizer can induce secondary axes possessing head and trunk/tail regions. Moreover, these experiments also show that distinct fate domains within the zebrafish organizer have different axis-inducing abilities. The domain of the zebrafish organizer fated to became prechordal plate works as a head inducer, while the domain fated to became notochord acts as a trunk inducer. The presumptive prechordal plate domain appears to have a more conserved role in vertebrate head induction. For example, the presumptive prechordal plate is a potent head inducer for both *Xenopus* and chick embryos. In addition, mouse node-derived axial endomesoderm seems also to be necessary for head induction.

Several zebrafish experiments suggest that neural specification has occurred by the onset of gastrulation. Several genes are expressed in the epiblast that will form the future neural plate (Grinblat et al., 1998; Koshida et al., 1998). The fact that the zebrafish organizer can induce complete secondary axes in transplantation experiments does not necessarily mean that the zebrafish organizer contains all the information required for neural specification. It could well be that prior to or at the onset of gastrulation signals coming from the YSL or other regions are required to predispose the epiblast to receive signals from the organizer. Therefore, it would be interesting to investigate the axis-inducing abilities of the zebrafish organizer when transplanted to host embryos lacking genes, such as *hex, squint, otx1, anf, axial* and *lim1*. The function of homologous genes in the AVE was shown to be required for head formation in the mouse embryo. Generation of zebrafish embryos without a particular gene function is now possible through the use of morpholino antisense oligonucleotides. These reagents effectively knockdown protein production from specific mRNAs (Nasevicius and Ekker, 2000; Summerton and Weller, 1997).

Transplantation experiments in zebrafish have identified an additional centre required for forebrain patterning (Houart et al., 1998). Cells located at the border between non-neural and neural ectoderm, the row1 cells, possess neural patterning activity. Removing the row1 cells at the mid-gastrula stages, but not more posterior rows, leads to forebrain defects, namely loss of telencephalic gene expression and expansion of the ventral diencephalon. Transplantation of row1 cells to a more posterior region of the neural plate, at mid-gastrula stages, leads to induction of forebrain markers in the surrounding cells. Whether signals from the organizer or other embryonic regions are involved in the specification of the row1 cells is not known at present. The row1 cells seem to be equivalent to a region called the anterior neural ridge (ANR) in the mouse embryo. This region is located between the anterior neural plate and the non-neural ectoderm and was shown to be a signalling centre for forebrain development. Ablation and transplantation experiments have shown that the ANR is important for the anterior-lateral neural plate expression of *BF1*, a gene encoding a transcription factor essential for the normal growth and differentiation of the telencephalon (Shimamura and

Rubenstein, 1997; Ye et al., 1998). The *hesx1* and *hex* mutant embryos show forebrain defects and a detailed analysis of these mutants revealed a loss in the *fgf8* expression in the ANR (Martinez-Barbera et al., 2000; Martinez-Barbera et al., 2000).

7.2. Development without the dorsal organizer

The expression domain of *gsc* defines the region within the zebrafish organizer that will give rise to prechordal plate and the expression domain of *flh* defines the region that will give rise to notochord (Gritsman et al., 2000). The results presented in Chapter 4 show that the domains of expression of *gsc* and *flh* extend beyond the morphological shield. For this reason it was proposed in Chapter 4 that the organizer region in zebrafish comprises the morphological shield and the adjacent marginal tissue. As a consequence of this, when the morphological shield is removed, shield derivatives form, but when the morphological shield and the adjacent marginal cells are removed, the embryos develop with no shield derivatives.

Embryos in which the entire organizer region was removed developed with no shield derivatives, however, these embryos do not show a loss of neural fates along the AP axis. These results, presented in Chapter 4, suggest that neural induction begins prior to the onset of gastrulation, implying that planar signals have a role in early induction of the nervous system. In addition, it seems that the organizer derivatives are important for patterning the neural tube, since complete shield-removed embryos show dorsal-ventral and anterior-posterior defects. It was shown that genetic removal of the zebrafish organizer also fails to disrupt neural induction. Mutant embryos that lack the Nodal molecules, Squint and Cyclops and embryos lacking maternal and zygotic functions of *one-eyed pinhead (MZoep)* lack all organizer derivatives, yet have a patterned nervous system. Despite the lack of dorsal mesoderm, *MZoep* mutant embryos express *chordino*, indicating that some organizer activity remains in the absence of organizer-derived

124

tissues (Gritsman et al., 1999). *squint/cyclops* double mutants also continue to express *chordino* (Feldman, Rennebeck and Talbot, personal communication).

Organizer regeneration has been proposed to explain the fact that embryos develop with normal neural tissues after organizer removal. Although this type of regulative organizer behaviour has been reported in chick embryos (Joubin and Stern, 1999), the results presented in Chapter 4 reveal that the zebrafish organizer is not regenerated *de novo*. In contrast with chick embryos, when the zebrafish organizer region is completely removed the embryos do not form any of the normal shield derivatives. However, in Chapter 5, I describe experiments that give some evidence for the existence of a regulative process that can compensate for the loss of the majority of axial mesoderm precursors after morphological shield removal. This regulative process seems to involve homeogenetic induction. It is possible that signals released from the marginal cells adjacent to the morphological shield convert surrounding non-shield cells into shield fates, such as notochord.

Results presented in Chapter 5 suggest that the morphological shield itself can not convert ventral cells into shield derivatives due to the presence of inhibitor molecules, such as zADMP and Leftys. Hence, it is possible that marginal cells adjacent to the morphological shield convert ventral cells into shield derivatives because of the absence or reduction of such inhibitor molecules. This type of interaction between inducers and inhibitors in a normal embryo would help to confine the organizer region to a specific location in the dorsal side of the zebrafish embryo. The same kind of molecular interactions that position the organizer during gastrulation were found to occur in the chick embryo (Joubin and Stern, 1999). It has been proposed that a Nieuwkoop-like centre located in the middle of the primitive streak releases inducers like Vg1 and Wnt8C that induce the organizer at later gastrulation stages. However, this does not happen if the organizer is not removed, suggesting that the inhibitor cADMP is part of a feedback mechanism that represses induction by the Nieuwkoop-like centre and prevents cells adjacent to the chick node from becoming organizer, once it is induced.

Understanding the molecular mechanism that leads to homeogenetic induction of shield derivatives and the role of zADMP and Leftys in preventing this type of induction will help us to understand the interactions that define the organizer region in zebrafish embryos. To test these hypothesis, it will be interesting to investigate whether the morphological shield from an embryo injected with *zADMP* or *Leftys* morpholinos can convert ventral cells into a notochord fate. In addition, it will also be important to test whether adjacent marginal cells from embryos injected with *zADMP* or *Leftys* RNAs lose their ability to convert ventral cells into notochord.

References

Acampora, D., Avantaggiato, V., Tuorto, F., Briata, P., Corte, G., and Simeone, A. (1998). Visceral endoderm restricted translation of *Otx1* mediates recovery of *Otx2* requirements for specification of anterior neural plate and normal gastrulation. Development *125*, 5091-5104.

Acampora, D., Mazan, S., Lallemand, Y., Avantaggiato, V., Maury, M., Simeone, A., and Brulet, P. (1995). Forebrain and midbrain regions are delected in Otx2-/- mutants due to a defective anterior neuroectoderm specification during gastrulation. Development *121*, 3279-90.

Agius, E., Oelgeschlager, M., Wessely, O., Kemp, C., and De Robertis, E. M. (2000). Endodermal Nodal-related signals and mesoderm induction in *Xenopus*. Development *127*, 1173-83.

Akimenko, M. A., Ekker, M., Wegner, J., Lin, W., and Westerfield, M. (1994). Combinatorial expression of three zebrafish genes related to distal-less: part of a homeobox gene code for the head. J. Neurosci. *14*, 3475-86.

Albano, R. M., Arkell, R., Beddington, R. S., and Smith, J. C. (1994). Expression of inhibin and follistatin during postimplantation mouse development; decidual expression of activin and expression of follistatin in primitive streak, somites and hindbrain. Development *120*, 803-13.

Albers, B. (1987). Competence as the main factor determining the size of the neural plate. Dev. Growth Differ. *29*, 535-45.

Alvarez, I. S., Araujo, M., and Nieto, M. A. (1998). Neural induction in whole chick embryos cultures by FGF. Dev. Biol. *199*, 42-54.

Ang, S. L., and Rossant, J. (1993). Anterior mesendoderm induces mouse Engrailed genes in explant cultures. Development *118*, 139-49.

Ang, S. L., and Rossant, J. (1994). HNF-3 beta is essential for node and notochord formation in mouse development. Cell *78*, 561-74.

Arendt, D., and Nubler-Jung, K. (1999). Rearranging gastrulation in the name of yolk: evolution in yolk-rich amniote eggs. Mech. Dev. *81*, 3-22.

Axelrod, J. D., Miller, J. R., Shulman, J. M., Moon, R. T., and Perrimon, N. (1998). Differential recruitment of Dishevelled provides signalling specificity in the planar cell polarity and Wingless signaling pathways. Genes Dev. *12*, 2610-22.

Bachiller, D., Klingensmith, J., Kemp, C., Belo, J. A., Anderson, R. M., May, S. R., McMahon, J. A., McMahon, A. P., Harland, R. M., Rossant, J., and De Robertis, E. M. (2000). The organizer factors Chordin and Noggin are required for mouse forebrain development. Nature *403*, 658-61.

Baker, J. C., Beddington, R. S. P., and Harland, R. M. (1999). Wnt signaling in *Xenopus* embryos inhibits *Bmp4* expression and activates neural development. Genes Dev. *13*, 3149-59.

Bally-Cuif, L., Gulisano, M., Broccoli, V., and Boncinelli, E. (1995). c-otx2 is expressed in two different phases of gastrulation and is sensitive to retinoic acid treatment in chick embryo, Mech Dev *49*, 49-63.

Bang, A. G., Papalopulu, N., Kintner, C., and Goulding, M. D. (1997). Expression of Pax-3 is initiated in the early neural plate by posteriorizing signals produced by the organizer and by posterior non- axial mesoderm. Development *124*, 2075-85.

Baranski, M., Berdougo, E., Sandler, J. S., K., D. D., and Burrus, L. W. (2000). The dynamic expression pattern of frzb-1 suggests multiple roles inchick development, Dev Biol *217*, 25-41.

Barnes, J. D., Crosby, J. L., Jones, C. M., Wright, C. V., and Hogan, B. L. (1994). Embryonic expression of Lim-1, the mouse homolog of Xenopus Xlim-1, suggests a role in lateral mesoderm differentiation and neurogenesis, Dev Biol *161*, 168-78.

Barr, P. J. (1991). Mammalian subtilisins: the long-sought dibasic processing endoproteases. Cell *66*, 1-3.

Bauer, H., Meier, A., Hild, M., Stachel, S., Economides, A., Hazelett, D., Harland, R. M., and Hammerschmidt, M. (1998). Follistatin and noggin are excluded from the zebrafish organizer. Dev. Biol. *204*, 488-507.

Beddington, R. S. (1994). Induction of a second neural axis by the mouse node. Development *120*, 613-20.

Beddington, R. S., and Robertson, E. J. (1999). Axis development and early asymmetry in mammals. Cell *96*, 195-209.

Beddington, R. S. P., and Robertson, E. J. (1998). Anterior patterning in the mouse. TIG *14*, 277-84.

Beddington, R. S. P., and Robertson, E. J. (1989). An assessment of the developmental potential of embryonic stem cells in the midgestation mouse embryo. Development *105*, 733-37.

Bellairs, R., and Osmond, M. (1998). The atlas of chick development. Academic Press.

Belo, J. A., Bouwmeester, T., Leyns, L., Kertesz, N., Gallo, M., Follettie, M., and De Robertis, E. M. (1997). Cerberus-like is a secreted factor with neuralizing activity expressed in the anterior primitive endoderm of the mouse gastrula. Mech. Dev. *68*, 45-57.

Blader, P., Rastegar, S., Fischer, N., and Strahle, U. (1997). Cleavage of the BMP-4 antagonist chordin by zebrafish tolloid. Science *278*, 1937-40.

Blum, M., Gaunt, S. J., Cho, K. W., Steinbeisser, H., Blumberg, B., Bittner, D., and De Robertis, E. M. (1992). Gastrulation in the mouse: the role of the homeobox gene goosecoid. Cell *69*, 1097-106.

Blumberg, B., Bolado, J., Moreno, T. A., Kintner, C., Evans, R. M., and Papalopulu, N. (1997). An essential role for retinoid signaling in anteriorposterior neural patterning. Development *124*, 373-9.

Boutros, M., Paricio, N., Strutt, D. I., and Mlodzik, M. (1998). Dishevelled activates JNK and discriminates between JNK pathways in planar polarity and wingless signaling. Cell *94*, 109-18.

Bouwmeester, T., Kim, S., Sasai, Y., Lu, B., and De Robertis, E. M. (1996). Cerberus is a head-inducing secreted factor expressed in the anterior endoderm of Spemann's organizer. Nature *382*, 595-601.

Brannon, M., and Kimelman, D. (1996). Activation of Siamois by the Wnt pathway. Dev. Biol. *180*, 344-7.

Brickman, J. M., Jones, C. M., Clements, M., Smith, J. C., and Beddington, R. S. (2000). Hex is a transcriptional repressor that contributes to anterior identity and supresses Spemann organizer function. Development *127*, 2303-15.

Brummett, A. R. (1969). Deletion-transplantation experiments on embryos of Fundulus heteroclitus. I. The posterior embryonic shield. J. Exp. Zool. *169*, 315-334.

Brummett, A. R. (1972). Deletion-transplantation experiments on embryos of Fundulus heteroclitus. II. The anterior embryonic shield. J. Exp. Zool. *172*, 443-464.

Camus, A., and Tam, P. P. L. (1999). The organizer of the gastrulating mouse embryo. Curr. Top. Dev. Biol. *45*, 117-53.

Chang, C., and Hemmati-Brivanlou, A. (1999). *Xenopus* GDF6, a new antagonist of noggin and a partner of BMPs. Development *126*, 3347-57.

Chen, S.-R., and Kimelman, D. (2000). The role of the yolk syncytial layer in germ layer patterning in zebrafish. Development. *127*, 4681-89.

Cho, K. W., Blumberg, B., Steinbeisser, H., and De Robertis, E. M. (1991). Molecular nature of Spemann's organizer: the role of the Xenopus homeobox gene goosecoid. Cell *67*, 1111-20.

Connolly, D. J., Patel, K., and Cooke, J. (1997). Chick noggin is expressed in the organizer and neural plate during axial development, but offers no evidence of involvement in primary axis formation. Int. J. Dev. Biol. *41*, 389-96.

Connors, S., Trout, J., Ekker, M., and Mullins, M. (1999). The role of tolloid/mini fin in dorsoventral pattern formation of the zebrafish embryo. Development *126*, 3119-30.

Cooke, J. (1985). Dynamics of the control of body pattern in the development of Xenopus laevis. III. Timing and pattern after u.v. irradiation of the egg and after excision of presumptive head endo-mesoderm. J. Embryol. Exp. Morphol. *88*, 135-50.

Cooke, J., Smith, J. C., Smith, E. J., and Yaqoob, M. (1987). The organization of mesodermal pattern in Xenopus laevis: experiments using a Xenopus mesoderm-inducing factor. Development *101*, 893-908.

Cox, W. G., and Hemmati-Brivanlou, A. (1995). Caudalization of neural fate by tissue recombination and bFGF. Development *121*, 4349-58.

Crease, D. J., Dyson, S., and Gurdon, J. B. (1998). Cooperation between the activin and Wnt pathways in the spatial control of organizer gene expression. Proc. Natl. Acad. Sci. USA *95*, 4398-403.

Dale, J. K., Vesque, C., Lints, T. J., Sampath, T. K., Furley, A., Dodd, J., and Placzek, M. (1997). Cooperation of BMP7 and SHH in the induction of forebrain ventral midline cells by prechordal mesoderm. Cell *90*, 257-69.

Davidson, B. P., Kinder, S. J., Steiner, K., Schoenwolf, G. C., and Tam, P. P. L. (1999). Impact of node ablation on the morphogenesis of the body axis and the lateral asymmetry of the mouse embryo during early organogenesis. Dev. Biol. *211*, 11-26.

Dick, A., Hild, M., Bauer, H., Imai, Y., Maifeld, H., Schier, A. F., Talbot, W. S., Bouwmeester, T., and Hammerschmidt, M. (2000). Essential role of Bmp7 (snailhouse) and its prodomain in dorsal ventral patterning of the zebrafish embryo. Development *127*.

Ding, J., Yang, L., Yan, Y. T., Chen, A., Desai, N., Wynshaw-Boris, A., and Shen, M. M. (1998). Cripto is required for correct orientation of the anterior-posterior axis in the mouse embryo. Nature *395*, 702-7.

Ding, X., Hausen, P., and Steinbeisser, H. (1998). Pre-mid-blastula-transition patterning of early gene regulation in *Xenopus*; the role of the cortical rotation and mesoderm induction. Mech. Dev. *70*, 15-24.

Dixon, J. E., and Kintner, C. R. (1989). Cellular contacts required for neural induction in *Xenopus* embryos: evidence for two signals. Development *106*, 749-57.

Dominguez, I., Itoh, K., and Sokol, S. Y. (1995). Role of glycogen synthase kinase 3-beta as a negative regulator of dorsalventral axis formation in *Xenopus* embryos. Proc. Natl. Acad. Sci. USA *92*, 8498-8502.

Doniach, T. (1993). Planar and vertical induction of anteroposterior pattern during the development of the amphibian central nervous system. J. Neurobiol. *24*, 1256-75.

Doniach, T., and Musci, T. J. (1995). Induction of anteroposterior neural pattern in Xenopus: evidence for a quantitative mechanism. Mech. Dev. *53*, 403-13.

Du, S. J., Devoto, S. H., Westerfield, M., and Moon, R. T. (1997). Positive and negative regulation of muscle cell identity by members of the hedgehog and TGF-beta gene families. J. Cell Biol. *139*, 145-156.

Dudley, A. T., Lyons, K. M., and Robertson, E. J. (1995). A requirement for bone morphogenetic protein-7 during development of the mammalian kidney and eye. Genes Dev. *9*, 2795-807.

Dufort, D., Schwartz, L., Harpal, K., and Rossant, J. (1998). The transcription factor HNF3beta is required in visceral endoderm for normal primitive streak morphogenesis. Development *125*, 3015-25.

Durston, A. J., Timmermans, J. P., Hage, W. J., F., H. H., de Vries, N. J., Heideveld, M., and Nieuwkoop, P. D. (1989). Retinoic acid causes an anteriorposterior transformation in the developing central nervous system. Nature *340*, 140-4.

Ekker, M., Wegner, J., Akimenko, M. A., and Westerfield, M. (1992). Coordinate embryonic expression of three zebrafish engrailed genes. Development *116*, 1001-1010.

Ekker, S. C., Ungar, A. R., Greenstein, P., von Kessler, D. P., Porter, J. A., Moon, R. T., and Beachy, P. A. (1995). Patterning activities of vertebrate hedgehog proteins in the developing eye and brain. Curr. Biol. *5*, 944-55.

Elul, T., Koehl, M. A., and Keller, R. E. (1997). Cellular mechanisms underlying neural convergent extension in Xenopus laevis embryos. Dev. Biol. *191*, 243-76.

Erter, C. E., Solnica-Krezel, L., and Wright, C. V. (1998). Zebrafish nodal-related 2 encodes an early mesendodermal inducer signaling from the extraembryonic yolk syncytial layer. Dev. Biol. *204*, 361-72.

Eyal-Giladi, H., Debby, A., and Harel, N. (1992). The posterior section of the chick's area pellucida and its involvement in hypoblast and primitive streak formation. Development *116*, 819-30.

Fagotto, F., Guger, K., and Gumbiner, B. M. (1997). Induction of the primary dorsalizing center in *Xenopus* by the Wnt/GSK/beta-catenin signaling pathway but not Vg1, activin and noggin. Development *124*, 453-60.

Fainsod, A., Deissler, K., Yelin, R., Marom, K., Epstein, M., Pillemer, G., Steinbeisser, H., and Blum, M. (1997). The dorsalizing and neural inducing gene follistatin is an antagonist of BMP-4. Mech. Dev. *63*, 39-50.

Fan, M. J., and Sokol, S. Y. (1997). A role for Siamois in Spemann organizer formation. Development *124*, 2581-9.

Fekany, K., Yamanaka, Y., Leung, T., Sirotkin, H. I., Topczewski, J., Gates, M. A., Hibi, M., Renucci, A., Stemple, D., Radbill, A., Schier, A. F., Driever, W., Hirano, T., Talbot, W. S., and Solnica-Krezel, L. (1999). The zebrafish bozozok locus encodes Dharma, a homeodomain protein essential for induction of gastrula organizer and dorsoanterior embryonic structures. Development *126*, 1427-1438.

Fekany-Lee, K., Gonzalez, E., Miller-Bertoglio, V., and Solnica-Krezel, L. (2000). The homeobox gene bozozok promotes anterior neuroectoderm formation in zebrafish through negative regulation of BMP2/4 and Wnt pathways. Development *127*, 2333-45.

Feldman, B., Gates, M. A., Egan, E. S., Dougan, S. T., Rennebeck, G., Sirotkin, H. I., Schier, A. F., and Talbot, W. S. (1998). Zebrafish organizer development and germ-layer formation require nodal- related signals. Nature *395*, 181-5.

Fjose, A., Izpisua-Belmonte, J. C., Fromental-Ramain, C., and Duboule, D. (1994). Expression of the zebrafish gene hlx-1 in the prechordal plate and during CNS development. Development *120*, 71-81.

Foley, A. C., Skromne, I., and Stern, C. D. (2000). Reconciling different models of forebrain induction and patterning: a dual role for the hypoblast. Development *127*, 3839-54.

Foley, A. C., Storey, K. G., and Stern, C. D. (1997). The prechordal region lacks neural inducing ability, but can confer anterior character to more posterior neuroepithelium. Development *124*, 2983-96.

Fredieu, J. R., Cui, Y., Maier, D., Danilchik, M. V., and Christian, J. L. (1997). Xwnt-8 and lithium can act upon either dorsal mesodermal or neurectodermal cells to cause a loss of forebrain in *Xenopus* embryos. Dev. Biol. *186*, 100-14.

Furthauer, M., Thisse, B., and Thisse, C. (1999). Three different *noggin* genes antagonize the activity of bone morphogenetic proteins in the zebrafish embryo. Dev. Biol. *214*, 181-96.

Gamse, J., and Sive, H. (2000). Vertebrate anteroposterior patterning: the *Xenopus* neurectoderm as a paradigm. BioEssays *22*, 976-86.

Gerhart, J., Doniach, T., and Stewart, R. (1991). Organizing the *Xenopus* organizer. In Gastrulation: movements, patterns and molecules, R. E. Keller, W. J. Clark and F. Griffin, eds. (New York: Plenum), pp. 57-77.

Gilbert, S. F. (2000). Developmental Biology, 6th edition. Sinauer Associates, Inc., Sunderland, Massachussetts.

Gimlich, R. L. (1986). Acquisition of developmental autonomy in the equatorial region of the *Xenopus* embryo. Dev. Biol. *115*, 340-52.

Gimlich, R. L., and Cooke, J. (1983). Cell lineage and the induction of secondary system in amphibian development. Nature *306*, 471-73.

Glinka, A., Wu, W., Delius, H., Monaghan, A. P., Blumenstock, C., and Niehrs, C. (1998). Dickkopf-1 is a member of a new family of secreted proteins and functions in head induction. Nature *391*, 357-62.

Glinka, A., Wu, W., Onichtchouk, D., Blumenstock, C., and Niehrs, C. (1997). Head induction by simultaneous repression of Bmp and Wnt signalling in Xenopus. Nature *389*, 517-9.

Godsave, S. F., and Slack, J. M. (1989). Clonal analysis of mesoderm induction in Xenopus laevis. Dev. Biol. *134*, 486-90.

Gont, L. K., Fainsod, A., Kim, S. H., and De Robertis, E. M. (1996). Overexpression of the homeobox gene Xnot-2 leads to notochord formation in Xenopus, Dev Biol *174*, 174-8.

Griffin, K. J., Amacher, S. L., Kimmel, C. B., and Kimelman, D. (1998). Molecular identification of spadetail: regulation of zebrafish trunk and tail mesoderm formation by T-box genes. Development *125*, 3379-88.

Grinblat, Y., Gamse, J., Patel, M., and Sive, H. (1998). Determination of the zebrafish forebrain: induction and patterning. Development *125*, 4403-16.

Gritsman, K., Talbot, W. S., and Schier, A. F. (2000). Nodal signaling patterns the organizer. Development *127*, 921-32.

Gritsman, K., Zhang, J., Cheng, S., Heckscher, E., Talbot, W. S., and Schier, A. F. (1999). The EGF-CFC protein one-eyed pinhead is essential for nodal signaling. Cell *97*, 121-32.

Guger, K. A., and Gumbiner, B. M. (1995). beta-Catenin has Wnt-like activity and mimics the Nieuwkoop centre in *Xenopus* dorsal-ventral patterning. Dev. Biol. *172*, 115-25.

Gunz, H., and Tacke, L. (1989). Neural differentiation of *Xenopus laevis* ectoderm takes place after disaggregation and delayed reaggregation without inducer. Cell Diff. Dev. *28*, 211-18.

Hamburger, V. (1988). The heritage of experimental embryology: Hans Spemann and the organizer. Oxford University Press, Oxford.

Hamburger, V., and Hamilton, H. L. (1951). A series of normal stages in the development of the chick. J. Morph. *88*, 49-92.

Hammerschmidt, M., Pelegri, F., Mullins, M. C., Kane, D. A., van Eeden, F. J., Granato, M., Brand, M., Furutani-Seiki, M., Haffter, P., Heisenberg, C. P., Jiang, Y. J., Kelsh, R. N., Odenthal, J., Warga, R. M., and Nusslein-Volhard, C. (1996). dino and mercedes, two genes regulating dorsal development in the zebrafish embryo. Development *123*, 95-102.

Hammerschmidt, M., Serbedzija, G. N., and McMahon, A. P. (1996). Genetic analysis of dorsoventral pattern formation in the zebrafish: requirement of a BMP-like ventralizing activity and its dorsal repressor. Genes Dev. *10*, 2452-61.

Hansen, C. S., Marion, C. D., Steele, K., George, S., and Smith, W. C. (1997). Direct neural induction and selective inhibition of mesoderm and epidermis inducers by Xnr3. Development *124*, 483-92.

Harland, R., and Gerhart, J. (1997). Formation and function of Spemann's organizer. Ann. Rev. Cell. Dev. Biol. *13*, 611-67.

Hashimoto, H., Itoh, M., Yamanaka, Y., Yamashita, S., Shimizu, T., Solnica-Krezel, L., Hibi, M., and Hirano, T. (2000). Zebrafish Dkk1 functions in forebrain specification and axial mesendoderm formation. Dev. Biol. *217*, 138-52.

Hatta, K., Kimmel, C. B., Ho, R. K., and Walker, C. (1991). The cyclops mutation blocks specification of the floor plate of the zebrafish central nervous system. Nature *350*, 339-41.

Hatta, K., and Takahashi, Y. (1996). Secondary axis induction by heterospecific organizers in zebrafish. Dev. Dyn. *205*, 183-95.

Hawley, S. H. B., Wunnenberg-Stapleton, K., Hashimoto, C., Laurent, M. N., Watabe, T., Blumberg, B. W., and Cho, K. W. (1995). Disruption of BMP signals in embryonic *Xenopus* ectoderm leads to direct neural induction. Genes Dev. *9*, 2923-35.

He, X., Saint Jeanne, J. P., Woodgett, J. R., Varmus, H. E., and Dawid, I. B. (1995). Glycogen Synthase kinase-3 and dorsalventral patterning in *Xenopus* embryos. Nature *374*, 617-22.

Heasman, J., Crawford, A., Goldstone, K., Garner Hamrick, P., Gumbiner, B., McCrea, P., Kintner, C., Noro, C. Y., and Wylie, C. (1994). Overexpression of cadherins and underexpression of b-catenin inhibit dorsal mesoderm induction in early *Xenopus* embryos. Cell *79*, 791-803.

Heisenberg, C.-P., Tada, M., Rauch, G.-J., Saude, L., Concha, M. L., Geisler, R., Stemple, D. L., Smith, J. C., and Wilson, S. W. (2000). Silberblick/Wnt11 mediates convergent extension movements during zebrafish gastrulation. Nature *405*, 76-81.

Heisenberg, C. P., Brand, M., Jiang, Y. J., Warga, R. M., Beuchle, D., van Eeden, F. J., Furutani-Seiki, M., Granato, M., Haffter, P., Hammerschmidt, M., Kane, D. A., Kelsh, R. N., Mullins, M. C., Odenthal, J., and Nusslein-Volhard, C. (1996). Genes involved in forebrain development in the zebrafish, Danio rerio. Development *123*, 191-203.

Heisenberg, C. P., and Nusslein-Volhard, C. (1997). The function of silberblick in the positioning of the eye anlage in the zebrafish embryo. Dev. Biol. *184*, 85-94.

Hemmati-Brivanlou, A., Kelly, O. G., and Melton, D. A. (1994). Follistatin, an antagonist of activin, is expressed in the Spemann organizer and displays direct neuralizing activity. Cell *77*, 283-95.

Hemmati-Brivanlou, A., and Melton, D. A. (1992). A truncated activin receptor inhibits mesoderm induction and formation of axial structures in Xenopus embryos. Nature *359*, 609-14.

Hemmati-Brivanlou, A., and Thomsen, G. A. (1995). Ventral mesodermal patterning in Xenopus embryos: expression patterns and activities of BMP-2 and BMP-4. Dev. Genet. *17*, 78-89.

Hendzel, M. J., Wei, Y., Mancini, M. A., van Hooser, A., Ranalli, T., Brinkley, B. R., Brazett-Jones, D. P., and Allis, C. D. (1997). Mitosis-specific phosphorylation of histone H3 initiates primarily within pericentromeric heterochromatin during G2 and spreads in an ordered fashion coincident with mitotic chromosome condensation. Chromosoma *106*, 348-60.

Herrmann, B. G., Labeit, S., Poustka, A., King, T. R., and Lehrach, H. (1990). Cloning of the T gene required in mesoderm formation in the mouse, Nature *343*, 617-22.

Hill, J., Clarke, J. D., Vargesson, N., Jowett, T., and Holder, N. (1995). Exogenous retinoic acid causes specific alterations in the development of the midbrain and hindbrain of the zebrafish embryo including positional respecification of the Mauthner neuron. Mech. Dev. *50*, 3-16.

Ho, C.-Y., Houart, C., Wilson, S. W., and Stainier, D. Y. R. (1999). A role for the extraembryonic yolk syncytial layer in patterning the zebrafish embryo suggested by properties of the hex gene. Curr. Biol. *9*, 1131-34.

Ho, R. K., and Kane, D. A. (1990). Cell-autonomous action of zebrafish spt-1 mutation in specific mesodermal precursors. Nature *348*, 728-30.

Ho, R. K., and Kimmel, C. B. (1993). Commitment of cell fate in the early zebrafish embryo. Science *261*, 109-11.

Hoang, B. H., Thomas, J. T., Abdul-Karim, F. W., Correia, K. M., Conlon, R. A., Luyten, F. P., and T., B. R. (1998). Expression pattern of two Frizzled-related genes, Frzb-1 and Sfrp-1, during mouse embryogenesis suggest a role for modulating action of Wnt family members, Dev Dyn *212*, 364-72.

Hogan, H., Beddington, R., Costantini, F., and Lacy, E. (1994). Manipulating the mouse embryo. A laboratory manual (2nd edition). Cold Spring Harbor Laboratory Press, New York.

Holley, S. A., and Nusslein-Volhard, C. (2000). Somitogenesis in zebrafish. Curr. Top. Dev. Biol. *47*, 247-77.

Holowacz, T., and Sokol, S. (1999). FGF is required for posterior neural patterning but not for neural induction. Dev. Biol. *205*, 296-308.

Hoppler, S., Brown, J. D., and Moon, R. T. (1996). Expression of a dominant-negative Wnt blocks induction of MyoD in Xenopus embryos. Genes Dev. *10*, 2805-17.

Houart, C., Westerfield, M., and Wilson, S. W. (1998). A small population of anterior cells patterns the forebrain during zebrafish gastrulation. Nature *391*, 788-92.

Inoue, A., Takahashi, M., Hatta, K., Hotta, Y., and Okamoto, H. (1994). Developmental regulation of islet-1 mRNA expression during neuronal differentiation in embryonic zebrafish. Dev. Dyn. *199*, 1-11.

Izpisua-Belmonte, J. C., De Robertis, E. M., Storey, K. G., and Stern, C. D. (1993). The homeobox gene goosecoid and the origin of organizer cells in the early chick blastoderm, Cell *74*, 645-59.

Jones, C. M., Broadbent, J., Thomas, P. Q., Smith, J. C., and Beddington, R. S. (1999). An anterior signalling centre in Xenopus revealed by the homeobox gene XHex. Curr. Biol. *9*, 946-54.

Jones, C. M., Kuehn, M. R., Hogan, B. L., Smith, J. C., and Wright, C. V. (1995). Nodal-related signals induce axial mesoderm and dorsalize mesoderm during gastrulation, Development *121*, 3651-62.

Joubin, K., and Stern, C. D. (1999). Molecular Interactions continuously define the organizer during the cell movements of gastrulation. Cell *98*, 559-571.

Kageura, H. (1995). Three regions of the 32-cell embryo of *Xenopus laevis* essential for formation of a complete tadpole. Dev. Biol. *170*, 376-86.

Karnovsky, M. J. (1965). A formaldehyde-glutaraldehyde fixative of high osmolarity for use in electron microscopy. J. Cell Biol., 137-138.

Kazanskaya, O. V., Severtzova, E. A., Barth, K. A., Ermakova, G. V., Lukyanov, S. A., Benyumov, A. O., Pannese, M., Boncinelli, E., Wilson, S. W., and Zaraisky, A. G. (1997). Anf: a novel class of vertebrate homeobox genes expressed at the anterior end of the main embryonic axis. Gene *200*, 25-34.

Keller, R., Shih, J., and Domingo, C. (1992). The patterning and functioning of protrusive activity during convergence and extension of the Xenopus organiser. Dev. Suppl, 81-91.

Keller, R. E., and Daniltchick, M. (1988). Regional expression, pattern and timing of convergence and extension during gastrulation of *Xenopus laevis*. Development *103*, 193-209.

Kelly, G. M., Erezyilmaz, D. F., and Moon, R. T. (1995). Induction of a secondary embryonic axis in zebrafish occurs following the overexpression of beta-catenin. Mech. Dev. *53*, 261-73.

Kelly, G. M., Greenstein, P., Erezyilmaz, D. F., and Moon, R. T. (1995). Zebrafish wnt8 and wnt8b share a common activity but are involved in distinct developmental pathways. Development *121*, 1787-99.

Kengaku, M., and Okamoto, H. (1995). bFGF as a possible morphogen for the anteroposterior axis of the central nervous system in Xenopus. Development *121*, 3121-30.

Kessler, D. S. (1997). Siamois is required for formation of Spemann's organizer. Proc. Natl. Acad. Sci. USA *94*, 13017-22.

Kim, C. H., Oda, T., Itoh, M., Jiang, D., Artinger, K. B., Chandrasekharappa, S. C., Driever, W., and Chitnis, A. B. (2000). Repressor activity of Headless/Tcf3 is essential for vertebrate head formation. Nature *407*, 913-6.

Kimelman, D., and Griffin, K. J. P. (2000). Vertebrate mesendoderm induction and patterning. Curr. Opin. Gen. Dev. *10*, 350-356.

Kimmel, C. B., Ballard, W. W., Kimmel, S. R., Ullmann, B., and Schilling, T. F. (1995). Stages of embryonic development of the zebrafish. Dev. Dyn. *203*, 253-310.

Kimmel, C. B., and Warga, R. M. (1987). Indeterminate cell lineage of the zebrafish embryo. Dev. Biol. *124*, 269-80.

Kimmel, C. B., Warga, R. M., and Kane, D. A. (1994). Cell cycles and clonal strings during formation of the zebrafish central nervous system. Development *120*, 265-76.

Kimmel, C. B., Warga, R. M., and Schilling, T. F. (1990). Origin and organization of the zebrafish fate map. Development 108, 581-94.

Kingsley, D. M. (1994). The TGF-beta superfamily: new members, new receptors and new genetic test of function in different organisms. Genes Dev. 8, 133-46.

Kintner, C. R., and Dodd, J. (1991). Hensen's node induces neural tissue in Xenopus ectoderm. Implications for the action of the organizer in neural induction. Development 113, 1495-505.

Kintner, C. R., and Melton, D. A. (1987). Expression of Xenopus N-CAM RNA in ectoderm is an early response to neural induction. Development 99, 311-25.

Kishimoto, Y., Lee, K. H., Zon, L., Hammerschmidt, M., and Schulte-Merker, S. (1997). The molecular nature of zebrafish swirl: BMP2 function is essential during early dorsoventral patterning. Development 124, 4457-66.

Kispert, A., Ortner, H., Cooke, J., and Herrmann, B. G. (1995). The chick Brachyury gene: developmental expression pattern and response to axial induction by localized activin, Dev Biol 168, 406-15.

Klingensmith, J., Ang, S. L., Bachiller, D., and Rossant, J. (1999). Neural induction and patterning in the mouse in the absence of the node and its derivatives. Dev. Biol. 216, 535-49.

Knoetgen, H., Teichmann, U., Wittler, L., Viebahn, C., and Kessel, M. (2000). Anterior neural induction by nodes from rabbits and mice. Dev. Biol. 225, 370-80.

Knoetgen, H., Viebahn, C., and Kessel, M. (1999). Head induction in the chick by primitive endoderm of mammalian, but not avian origin. Development 126, 815-825.

Kodjabachian, L., Dawid, I. B., and Toyama, R. (1999). Gastrulation in zebrafish: what mutants teach us. Dev. Biol. *213*, 231-45.

Kodjabachian, L., and Lemaire, P. (1998). Embryonic induction: is the Nieuwkoop centre a useful concept? Curr. Biol. *8*, R918-21.

Kofron, M., Demel, T., Xanthos, J., Lohr, J., Sun, B., Sive, H., Osada, S., Wright, C., Wylie, C., and Heasman, J. (1999). Mesoderm induction in *Xenopus* is a zygotic event regulated by maternal VegT via TGFbeta growth factors. Development *126*, 5759-70.

Koos, D. S., and Ho, R. K. (1998). The nieuwkoid gene characterizes and mediates a Nieuwkoop-center-like activity in the zebrafish. Curr. Biol. *8*, 1199-206.

Koos, D. S., and Ho, R. K. (1999). The *nieuwkoid/dharma* homeobox gene is essential for bmp2b repression in the zebrafish pregastrula. Dev. Biol. *215*, 190-207.

Koshida, S., Shinya, M., Mizuno, T., Kuroiwa, A., and Takeda, H. (1998). Initial anteroposterior pattern of the zebrafish central nervous system is determined by differential competence of the epiblast. Development *125*, 1957-66.

Krauss, S., Concordet, J. P., and Ingham, P. W. (1993). A functionally conserved homolog of the Drosophila segment polarity gene hh is expressed in tissues with polarizing activity in zebrafish embryos. Cell *75*, 4905-16.

Kroll, K. L., and Amaya, E. (1996). Transgenic *Xenopus* embryos from sperm nuclear transplantations reveal FGF signaling requirements during gastrulation. Development *122*, 3173-83.

Lamb, T. M., and Harland, R. M. (1995). Fibroblast growth factor is a direct neural inducer, which combined with noggin generates anterior-posterior neural pattern. Development *121*, 3627-36.

Lamb, T. M., Knecht, A. K., Smith, W. C., Stachel, S. E., Economides, A. N., Stahl, N., Yancopolous, G. D., and Harland, R. M. (1993). Neural induction by the secreted polypeptide noggin. Science 262, 713-8.

Larabell, C. A., Torres, M., Rowning, B. A., Yost, C., Miller, J. R., Wu, M., Kimelman, D., and Moon, R. T. (1997). Establishment of the dorsal-ventral axis in Xenopus embryos is presaged by early asymmetries in b-catenin that are modulated by the Wnt signalling pathway. J. Cell Biol. 136, 1123-1136.

Launay, C., Fromentoux, V., Shi, D. L., and Boucaut, J. C. (1996). A truncated FGF receptor blocks neural induction by endogenous Xenopus inducers. Development 122, 869-80.

Laurent, M. N., Blitz, I. L., Hashimoto, C., Rothbacher, U., and Cho, K. W. (1997). The Xenopus homeobox gene twin mediates Wnt induction of goosecoid in establishment of Spemann's organizer. Development 124, 4905-16.

Lemaire, P., Garrett, N., and Gurdon, J. B. (1995). Expression cloning of Siamois, a Xenopus homeobox gene expressed in dorsal-vegetal cells of blastulae and able to induce a complete secondary axis. Cell 81, 85-94.

Levin, M. (1998). The roles of activin and follistatin signaling in chick gastrulation. Int. J. Dev. Biol. 42, 553-9.

Levin, M., Johnson, R. L., Stern, C. D., Kuehn, M., and Tabin, C. (1995). A molecular pathway determining left-right asymmetry in chick embryogenesis, Cell 82, 803-14.

Leyns, L., Bouwmeester, T., Kim, S. H., Piccolo, S., and De Robertis, E. M. (1997). Frzb-1 is a secreted antagonist of Wnt signaling expressed in the Spemann organizer. Cell 88, 747-56.

Li, Y., Allende, M. L., Finkelstein, R., and Weinberg, E. S. (1994). Expression of two zebrafish orthodenticle-related genes in the embryonic brain, Mech Dev *48*, 229-44.

Liu, P., Wakamiya, M., Shea, M. J., Albrecht, U., Behringer, R. R., and Bradley, A. (1999). Requirement for Wnt3 in vertebrate axis formation. Nat. Genet. *22*, 361-5.

Long, W. L. (1983). The role of the yolk syncytial layer in determination of the plane of bilateral symmetry in rainbow trout, *Salmo gairdneri*. J. Exp. Zool. *228*, 91-97.

Martinez-Barbera, J. P., Clements, M., Thomas, P., Rodriguez, T., Meloy, D., Kioussis, D., and Beddington, R. S. (2000). The homeobox gene Hex is required in definitive endodermal tissues for normal forebrain, liver and thyroid formation. Development *127*, 2433-45.

Martinez-Barbera, J. P., Rodriguez, T. A., and Beddington, R. S. (2000). The homeobox gene Hesx1 is required in the anterior neural ectoderm for normal forebrain formation. Dev. Biol. *223*, 422-30.

Martinez-Barbera, J. P., Toresson, H., Da Rocha, S., and Krauss, S. (1997). Cloning and expression of three members of the zebrafish Bmp family: Bmp2a, Bmp2b and Bmp4. Gene *198*, 53-9.

Matzuk, M. M., Lu, N., Vogel, H., Sellheyer, K., Roop, D. R., and Bradley, A. (1995). Multiple defects and perinatal death in mice deficient in follistatin. Nature *374*, 360-3.

McGrew, L. L., Hoppler, S., and Moon, R. T. (1997). Wnt and FGF pathways cooperatively pattern anteroposterior neural ectoderm in *Xenopus*. Mech. Dev. *69*, 105-114.

McGrew, L. L., Lai, C. J., and Moon, R. T. (1995). Specification of the anteriorposterior neural axis through synergistic interaction of the Wnt signaling cascade with noggin and follistatin. Dev. Biol. *172*, 337-42.

McMahon, J. A., Takada, S., Zimmerman, L. B., Fan, C. M., Harland, R. M., and McMahon, A. P. (1998). Noggin-mediated antagonism of BMP signaling is required for growth and patterning of the neural tube and somite. Genes Dev. *12*, 1438-52.

Melby, A. E., Warga, R. M., and Kimmel, C. B. (1996). Specification of cell fates at the dorsal margin of the zebrafish gastrula. Development *122*, 2225-37.

Meno, C., Gritsman, K., Ohishi, S., Ohfuji, Y., Heckscher, E., Mochida, K., Shimono, A., Kondoh, H., Talbot, W. S., Robertson, E. J., Schier, A. F., and Hamada, H. (1999). Mouse lefty2 and zebrafish antivin are feedback inhibitors of nodal signaling during vertebrate gastrulation. Molecular Cell *4*, 287-98.

Miller, J. R., Rowning, B. A., Larabell, C. A., Yang-Schneider, J. A., Bates, R. L., and Moon, R. T. (1999). Establishment of the dorsal-ventral axis in *Xenopus* embryos coincides with the dorsal enrichment of dishevelled that is dependent on cortical rotation. J. Cell Biol. *146*, 427-37.

Miller-Bertoglio, V., Carmany-Rampey, A., Furthauer, M., Gonzalez, E. M., Thisse, C., Thisse, B., Halpern, M. E., and Solnica-Krezel, L. (1999). Maternal and zygotic activity of the zebrafish ogon locus antagonizes BMP signaling. Dev. Biol. *214*, 72-86.

Mizuno, T., Yamaha, E., Wakahara, M., Kuriwa, A., and Takeda, H. (1996). Mesoderm induction in zebrafish. Nature *383*, 131-132.

Moens, C. B., Cordes, S. P., Giorgianni, M. W., Barsh, G. S., and Kimmel, C. B. (1998). Equivalence in the genetic control of hindbrain segmentation in fish and mouse. Development *125*, 381-91.

Moens, C. B., and Fritz, A. (1999). Techniques in neural development. Methods Cell Biol. *59*, 253-72.

Moens, C. B., Yan, Y. L., Appel, B., Force, A. G., and Kimmel, C. B. (1996). valentino: a zebrafish gene required for normal hindbrain segmentation. Development *122*, 3981-90.

Molenaar, M., van de Wetering, M., Oosterwegel, M., Peterson-Maduro, J., Godsave, S., Korinek, V., Roose, J., Destree, O., and Clevers, H. (1996). XTcf-3 transcription factor mediates beta-catenin-induced axis formation in *Xenopus* embryos. Cell *86*, 391-99.

Moon, R. T., Brown, J. D., and Torres, M. (1997). WNTs modulate cell fate and behaviour during vertebrate development. Trends Genet. *13*, 157-62.

Moon, R. T., and Kimelman, D. (1998). From cortical rotation to organizer gene expression: toward a molecular explanation of axis specification in Xenopus. Bioessays *20*, 536-45.

Moos, M., Jr., Wang, S., and Krinks, M. (1995). Anti-dorsalizing morphogenetic protein is a novel TGF-beta homolog expressed in the Spemann organizer. Development *121*, 4293-301.

Morita, T., Nitta, H., Kiyama, Y., Mori, H., and Mishina, M. (1995). Differential expression of two zebrafish emx homeoprotein mRNA in the developing brain. Neurosciences Lett. *198*, 131-4.

Muhr, J., Jessell, T. M., and Edlund, T. (1997). Assignment of early caudal identity to neural plate cells by a signal from caudal paraxial mesoderm. Neuron *19*, 487-502.

Mullins, M. C., Hammerschmidt, M., Kane, D. A., Odenthal, J., Brand, M., van Eeden, F. J., Furutani-Seiki, M., Granato, M., Haffter, P., Heisenberg, C. P., Jiang, Y. J., Kelsh, R. N., and Nusslein-Volhard, C. (1996). Genes establishing dorsoventral pattern formation in the zebrafish embryo: the ventral specifying genes. Development *123*, 81-93.

Nasevicius, A., and Ekker, S. C. (2000). Effective targeted gene 'knockdown' in zebrafish. Nat. Genet. *26*, 216-20.

Niehrs, C. (1999). Head in the WNT: the molecular nature of Spemann's head organizer. Trends Genet. *15*, 314-9.

Niehrs, C. (2001). The spemann organizer and embryonic head induction. Embo J. *20*, 631-37.

Nieuwkoop, P. D. (1952). Activation and organization of the central nervous system in amphibians. J. Exp. Zool. *120*, 1-108.

Nieuwkoop, P. D. (1985). Inductive interactions in early amphibian development and their general nature. J. Embryol. Exp. Morphol. *89*, 333-47.

Nikaido, M., Tada, M., Saji, T., and Ueno, N. (1997). Conservation of BMP signaling in zebrafish mesoderm patterning. Mech. Dev. *61*, 75-88.

Ober, E. A., and Schulte-Merker, S. (1999). Signals from the yolk cell induce mesoderm, neuroectoderm, the trunk organizer, and the notochord in zebrafish. Dev. Biol. *215*, 167-81.

Onichtchouk, D., Glinka, A., and Niehrs, C. (1998). Requirement for *Xvent-1* and *Xvent-2* gene function in dorsalventral patterning of *Xenopus* mesoderm. Development *125*, 1447-56.

Oppenheimer, J. (1936). Transplantation experiments on developing teleosts (Fundulus and Perca). J. Exp. Zool. *72*, 409-37.

Oppenheimer, J. M. (1953). The development of transplanted fragments of *Fundulus* gastrulae. Proc.Natl.Acad. Sci. *39*, 1149-1152.

Oppenheimer, J. M. (1936). Structures developed in amphibians by implantation of living fish organizer. Proc. Soc. Exp. Med. *34*, 461-3.

Pannese, M., Polo, C., Andreazzoli, M., Vignali, R., Kablar, B., Barsacchi, G., and Boncinelli, E. (1995). The Xenopus homologue of Otx2 is a maternal homeobox gene that demarcates and specifies anterior body regions, Development *121*, 707-20.

Papalopulu, N., Clarke, J. D., Bradley, L., Wilkinson, D., Krumlauf, R., and Holder, N. (1991). Retinoic acid causes abnormal development and segmental patterning of the anterior hindbrain in Xenopus embryos. Development *113*, 1145-58.

Pasteels, J. (1945). On the formation of the primitive entoderm of the duck (*Anas domestica*) and on the significance of the bilaminar embryo in birds. Anat. Rec. *93*, 5-21.

Pera, E. M., and Kessel, M. (1997). Patterning of the chick forebrain anlage by the prechordal plate. Development *124*, 4153-62.

Piccolo, S., Agius, E., Leyns, L., Bhattacharyya, S., Grunz, H., Bouwmeester, T., and De Robertis, E. M. (1999). The head inducer Cerberus is a multifunctional antagonist of Nodal, BMP and Wnt signals. Nature *397*, 707-10.

Piccolo, S., Agius, E., Lu, B., Goodman, S., Dale, L., and De Robertis, E. M. (1997). Cleavage of Chordin by Xolloid metalloprotease suggests a role for proteolytic processing in the regulation of Spemann organizer activity. Cell *91*, 407-16.

Piccolo, S., Sasai, Y., Lu, B., and De Robertis, E. M. (1996). Dorsoventral patterning in Xenopus: inhibition of ventral signals by direct binding of chordin to BMP-4. Cell 86, 589-98.

Pierce, S. B., and Kimelman, D. (1995). Regulation of Spemann organizer formation by the intracellular kinase Xgsk-3. Development 121, 755-65.

Placzek, M. (1995). The role of the notochord and floorplate in inductive interactions. Curr. Opin. Genet. Dev. 5, 499-506.

Placzek, M., Jessell, T. M., and Dodd, J. (1993). Induction of floor plate differentiation by contact-dependent, homeogenetic signals. Development 117, 205-18.

Psychoyos, D., and Stern, C. D. (1996). Restoration of the organizer after radical ablation of Hensen's node and the anterior primitive streak in the chick embryo. Development 122, 3263-73.

Rebagliati, M. R., Toyama, R., Fricke, C., Haffter, P., and Dawid, I. B. (1998). Zebrafish nodal-related genes are implicated in axial patterning and establishing left-right asymmetry. Dev. Biol. 199, 261-72.

Reddi, A. H. (1992). Regulation of cartilage and bone differentiation by bone morphogenetic proteins. Curr. Opin. Cell Biol. 4, 850-55.

Rivera-Perez, J. A., Mallo, M., Gendron-Maguire, M., Gridley, T., and Behringer, R. R. (1995). Goosecoid is not an essential component of the mouse gastrula organizer but is required for craniofacial and rib development, Development 121, 3005-12.

Rhinn, M., Dierich, A., Shawlot, W., Behringer, R. R., Le Meur, M., and Ang, S. L. (1998). Sequential roles for *Otx2* in visceral endoderm and neuroectoderm for forebrain and midbrain induction and specification. Development *125*, 845-56.

Rodaway, A., Takeda, H., Koshida, S., Broadbent, J., Price, B., Smith, J., C, Patient, R., and Holder, N. (1999). Induction of the mesendoderm in the zebrafish germ ring by yolk-derived TGF-beta family signals and discrimination of mesoderm and endoderm by FGF. Development *126*, 3067-78.

Rodriguez-Esteban, C., Capdevilla, J., Economides, A. N., Pascual, J., Ortiz, A., and Izpisua-Belmonte, J. C. (1999). The novel Cer-like protein Caronte mediates the establishment of embryonic left-right asymmetry. Nature *401*, 243-51.

Rossant, J., Spence, A., and Rossant, J. (1998). Chimeras and mosaics in mouse mutant analysis. Trends Genet. *14*, 358-63.

Ruiz i Albata, A. (1992). Planar and vertical signals in the induction and patterning of the *Xenopus* nervous system. Development *115*, 67-80.

Ruiz i Altaba, A., and Jessell, T. M. (1992). Pintallavis, a gene expressed in the organizer and midline cells of frog embryos: involvement in the development of the neural axis, Development *116*, 81-93.

Ryu, S.-L., Fujii, R., Yamanaka, Y., Shimizu, T., Yabe, T., Hirata, T., Hibi, M., and Hirano, T. (2001). Regulation of *dharma/bozozok* by the Wnt pathway. Dev. Biol. *231*, 397-409.

Sagerstrom, C. G., Grinbalt, Y., and Sive, H. (1996). Anteroposterior patterning in the zebrafish, Danio rerio: an explant assay reveals inductive and suppressive cell interactions. Development *122*, 1873-83.

Sampath, K., Rubinstein, A. L., Cheng, A. M., Liang, J. O., Fekany, K., Solnica-Krezel, L., Korzh, V., Halpern, M. E., and Wright, C. V. (1998). Induction of the zebrafish ventral brain and floorplate requires cyclops/nodal signalling, Nature *395*, 185-9.

Sasai, Y., and De Robertis, E. M. (1997). Ectodermal patterning in vertebrate embryos. Dev. Biol. *182*, 5-20.

Sasai, Y., Lu, B., Piccolo, S., and De Robertis, E. M. (1996). Endoderm induction by the organizer-secreted factors chordin and noggin in Xenopus animal caps. Embo J. *15*, 4547-55.

Sasai, Y., Lu, B., Steinbeisser, H., and De Robertis, E. M. (1995). Regulation of neural induction by the Chd and Bmp-4 antagonistic patterning signals in Xenopus. Nature *376*, 333-6.

Sasai, Y., Lu, B., Steinbeisser, H., Geissert, D., Gont, L. K., and De Robertis, E. M. (1994). Xenopus chordin: a novel dorsalizing factor activated by organizer- specific homeobox genes, Cell *79*, 779-90.

Sato, S. M., and Sargent, T. M. (1989). Development of neural inducing capacity in dissociated *Xenopus* embryos. Dev. Biol. *134*, 263-66.

Schier, A. F., Neuhauss, S. C., Helde, K. A., Talbot, W. S., and Driever, W. (1997). The one-eyed pinhead gene functions in mesoderm and endoderm formation in zebrafish and interacts with no tail. Development *124*, 327-42.

Schneider, S., Steinbeisser, H., Warga, R. M., and Hausen, P. (1996). Beta-catenin translocation into nuclei demarcates the dorsalizing centers in frog and fish embryos. Mech. Dev. *57*, 191-8.

Schneider, V. A., and Mercola, M. (1999). Spatially distinct head and heart inducers within the Xenopus organizer region. Curr. Biol. *9*, 800-9.

Schulte-Merker, S., Ho, R. K., Herrmann, B. G., and Nusslein-Volhard, C. (1992). The protein product of the zebrafish homologue of the mouse T gene is expressed in nuclei of the germ ring and the notochord of the early embryo. Development *116*, 1021-32.

Schulte-Merker, S., Lee, K. J., McMahon, A. P., and Hammerschmidt, M. (1997). The zebrafish organizer requires chordino. Nature *387*, 862-3.

Schulte-Merker, S., van Eeden, F. J., Halpern, M. E., Kimmel, C. B., and Nusslein-Volhard, C. (1994). no tail (ntl) is the zebrafish homologue of the mouse T (Brachyury) gene. Development *120*, 1009-15.

Schultheiss, T. M., Burch, J. B., and Lassar, A. B. (1997). A role for morphogenetic proteins in the induction of cardiac myogenesis. Genes Dev. *11*, 451-62.

Servetnick, M., and Grainger, R. M. (1991). Homeogenetic neural induction in Xenopus. Dev. Biol. *147*, 73-82.

Shawlot, W., and Behringer, R. R. (1995). Requirement for Lim1 in head-organizer function. Nature *374*, 425-30.

Shawlot, W., Deng, J. M., and Behringer, R. R. (1998). Expression of the mouse *cerberus*-related gene *Cerr1*, suggests a role in anterior neural induction and somitogenesis. Proc. Natl. Acad. Sci. USA *95*, 6198-6203.

Shawlot, W., Wakamiya, M., Kwan, K. M., Kania, A., Jessell, T. M., and Behringer, R. R. (1999). *Lim1* is required in both primitive streak-derived tissues and visceral endoderm for head formation in the mouse. Development *126*, 4925-32.

Shih, J., and Fraser, S. E. (1996). Characterizing the zebrafish organizer: microsurgical analysis at the early-shield stage. Development *122*, 1313-22.

Shimamura, K., and Rubenstein, J. L. (1997). Inductive interactions direct early regionalization of the mouse forebrain. Development *124*, 2709-18.

Shinya, M., Eschbach, C., Clark, M., Lehrach, H., and Furutani-Seiki, M. (2000). Zebrafish dkk-1, induced by the pre-MBT wnt signaling, is secreted from the prechordal plate and patterns the anterior neural plate. Mech. Dev. *98*, 3-17.

Simeone, A., Acampora, D., Gulisano, M., Stornaiuolo, A., and Boncinelli, E. (1992). Nested expression domains of four homeobox genes in developing rostral brain, Nature *358*, 687-90.

Simpson, E. H., Johnson, D. K., Hunsicker, P., Suffolk, R., Jordan, S. A., and Jackson, I. J. (1999). The mouse *Cerl* (*Cerberus* related or homologue) gene is not required for anterior pattern formation. Dev. Biol. *213*, 202-206.

Sive, H. L., Draper, B. W., Harland, R. M., and Weintraub, H. (1990). Identification of a retinoic acid-sensitive period during primary axis formation in Xenopus laevis. Genes Dev. *4*, 932-42.

Sive, H. L., Grainger, R. M., and M., H. R. (2000). Early development of *Xenopus laevis*: a laboratory manual. Cold Spring Harbor Laboratory Press, New York.

Slack, J. M., Isaacs, H. V., and Darlington, B. G. (1988). Inductive effects of fibroblast growth factor and lithium ion on Xenopus blastula ectoderm. Development *103*, 581-90.

Smith, J. C., Price, B. M., Green, J. B., Weigel, D., and Herrmann, B. G. (1991). Expression of a Xenopus homolog of Brachyury (T) is an immediate-early response to mesoderm induction, Cell *67*, 79-87.

Smith, W. C., and Harland, R. M. (1992). Expression cloning of noggin, a new dorsalizing factor localized to the Spemann organizer in Xenopus embryos, Cell 70, 829-40.

Smith, J. C., and Slack, J. M. (1983). Dorsalization and neural induction: properties of the organizer in Xenopus laevis. J. Embryol. Exp. Morphol. 78, 299-317.

Smith, J. L., and Schoenwolf, G. C. (1998). Getting organized: new insights into the organizer of higher vertebrates. Curr. Top. Dev. Biol. 40, 79-110.

Sokol, S. Y. (1996). Analysis of Dishevelled signalling pathways during Xenopus development. Curr. Biol. 6, 1456-67.

Sokol, S. Y., Klingensmith, J., Perrimon, N., and Itoh, K. (1995). Dorsalizing and neuralizing properties od Xdsh, a maternally expressed Xenopus homologue of dishevelled. Development 121, 1637-47.

Solnica-Krezel, L., Stemple, D. L., and Driever, W. (1995). Transparent things: cell fates and cell movements during early embryogenesis of zebrafish. Bioessays 17, 931-9.

Stachel, S. E., Grunwald, D. J., and Myers, P. Z. (1993). Lithium perturbation and goosecoid expression identify a dorsal specification pathway in the pregastrula zebrafish. Development 117, 1261-74.

Stein, S., and Kessel, M. (1995). A homeobox gene involved in node, notochord and neural plate formation of chick embryos, Mech Dev 49, 37-48.

Stemple, D. L., Solnica-Krezel, L., Zwartkruis, F., Neuhauss, S. C., Schier, A. F., Malicki, J., Stainier, D. Y., Abdelilah, S., Rangini, Z., Mountcastle-Shah, E., and Driever, W. (1996). Mutations affecting development of the notochord in zebrafish. Development *123*, 117-28.

Storey, K. G., Crossley, J. M., De Robertis, E. M., Norris, W. E., and Stern, C. D. (1992). Neural induction and regionalisation in the chick embryo. Development *114*, 729-41.

Storey, K. G., Goriely, C. M., Sargent, C. M., Brown, J. M., Burns, H. D., Abud, H. M., and Heath, J. K. (1998). Early posterior neural tissue is induced by FGF in the chick embryo. Development *125*, 473-84.

Storey, K. G., Selleck, M. A., and Stern, C. D. (1995). Neural induction and regionalisation by different subpopulations of cells in Hensen's node. Development *121*, 417-28.

Strahle, U., Blader, P., Henrique, D., and Ingham, P. W. (1993). Axial, a zebrafish gene expressed along the developing body axis, shows altered expression in cyclops mutant embryos. Genes Dev. *7*, 1436-46.

Streit, A., Berliner, A. J., Papanayotou, C., Sirulnik, A., and Stern, C. D. (2000). Initiation of neural induction by FGF signalling before gastrulation. Nature *406*, 74-8.

Streit, A., Lee, K. J., Woo, I., Roberts, C., Jessell, T. M., and Stern, C. D. (1998). Chordin regulates primitive streak development and the stability of induced neural cells, but is not sufficient for neural induction in the chick embryo. Development *125*, 507-19.

Streit, A., and Stern, C. D. (1999). Establishment and maintenance of the border of the neural plate in the chick: involvement of FGF and BMP activity. Mech. Dev. *82*, 51-66.

Streit, A., and Stern, C. D. (1999). Neural induction. A bird's eye view. Trends Genet 15, 20-4.

Summerton, J., and Weller, D. (1997). Morpholino antisense oligomers: design, preparation, and properties. Antisense Nucleic Acid Drug Dev. 7, 187-95.

Sun, X., Meyers, E. N., Lewandoski, M., and Martin, G. R. (1999). Targeted disruption of Fgf8 causes failure of cell migration in the gastrulating mouse embryo. 1999 13, 1834-46.

Suzuki, A., Kanedo, E., Ueno, N., and Hemmati-Brivanlou, A. (1997). Regulation of epidermal induction by BMP2 and BMP7 signaling. Dev. Biol. 189, 112-22.

Suzuki, A., Shioda, N., and Ueno, N. (1995). Bone morphogenetic protein acts as a ventral mesoderm modifier in early Xenopus embryos. Dev. Growth Differ. 37, 581-88.

Tada, M., and Smith, J. C. (2000). Xwnt11, a target of Xenopus Brachyury, regulates gastrulation movements via Dishevelled, but not through the canonical Wnt pathway. Development 127, 2227-38.

Taira, M., Jamrich, M., Good, P. J., and Dawid, I. B. (1992). The LIM domain-containing homeo box gene Xlim-1 is expressed specifically in the organizer region of Xenopus gastrula embryos, Genes Dev 6, 356-66.

Talbot, W. S., Trevarrow, B., Halpern, M. E., Melby, A. E., Farr, G., Postlethwait, J. H., Jowett, T., Kimmel, C. B., and Kimelman, D. (1995). A homeobox gene essential for zebrafish notochord development. Nature 378, 150-7.

Tam, P. P., and Steiner, K. A. (1999). Anterior patterning by synergistic activity of th early gastrula organizer and the anterior germ layer tissues of the mouse embryo. Development 126, 5171-9.

Tam, P. P., Steiner, K. A., Zhou, S. X., and Quinlan, G. A. (1997). Lineage and functional analyses of the mouse organizer. Cold Spring Harb. Symp. Quant. Biol. *62*, 135-44.

Tam, P. P. L., and Quilan, G. A. (1996). Mapping vertebrate embryos. Curr. Biol. *6*, 104-6.

Thisse, C., and Thisse, B. (1999). Antivin, a novel and divergent member of the TGFbeta superfamily, negatively regulates mesoderm induction. Development *126*, 229-40.

Thisse, C., and Thisse, B. (1998). High resolution whole-mount in situ hybridization. Zebrafish Sci. Mon. *5*, 8-9.

Thisse, C., Thisse, B., Halpern, M. E., and Postlethwait, J. H. (1994). Goosecoid expression in neurectoderm and mesendoderm is disrupted in zebrafish cyclops gastrulas. Dev. Biol. *164*, 420-9.

Thomas, P., and Beddington, R. (1996). Anterior primitive endoderm may be responsible for patterning the anterior neural plate in the mouse embryo. Curr. Biol. *11*, 1487-1496.

Thomas, P. Q., Brown, A., and Beddington, R. S. (1998). Hex: a homeobox gene revealing peri-implantation asymmetry in the mouse embryo and an early transient marker of endothelial cell precursors. Development *125*, 85-94.

Toyama, R., O'Connell, M. L., Wright, C. V., Kuehn, M. R., and Dawid, I. B. (1995). Nodal induces ectopic goosecoid and lim1 expression and axis duplication in zebrafish. Development *121*, 383-91.

Trevarrow, B., Marks, D. L., and Kimmel, C. B. (1990). Organization of hindbrain segments in the zebrafish embryo. Neuron *4*, 669-79.

van Straaten, H. W., Hekking, J. W., Wiertz-Hoessels, E. J., Thors, F., and Drukker, J. (1988). Effect of the notochord on the differentiation of a floor plate area in the neural tube of the chick embryo. Anat. Embryol. *177*, 317-24.

Varlet, I., Collignon, J., and Robertson, E. J. (1997). *nodal* expression in the primitive endoderm is required for specification of the anterior axis during mouse gastrulation. Development *124*, 1033-44.

Vesque, C., Ellis, S., Lee, A., Szabo, M., Thomas, P., Beddington, R., and Placzek, M. (2000). Development of chick axial mesoderm: specification of prechordal mesoderm by anterior endoderm-derived TGFb family signalling. Development *127*, 2795-2809.

Viebahn, C. (1999). The anterior margin of the mammalian gastrula: comparative and phylogenetic aspects of its role in axis formation and head induction. Curr. Top. Dev. Biol. *46*, 63-103.

von Dassow, G., Schmidt, J. E., and Kimelman, D. (1993). Induction of the Xenopus organizer: expression and regulation of Xnot, a novel FGF and activin-regulated homeo box gene. Genes Dev. *7*, 355-66.

Waddington, C. H. (1932). Experiments on the development of the chick and the duck embryo cultivated in vitro. Proc. Trans. R. Soc. Lond. (B) *211*, 179-230.

Wallingford, J. B., Rowning, B. A., Vogeli, K. M., U., R., Fraser, S. E., and Harland, R. M. (2000). Dishevelled controls cell polarity during Xenopus gastrulation. Nature *405*, 81-5.

Wang, S., Krinks, M., Lin, K., Luyten, F. P., and Moos, M., Jr. (1997). Frzb, a secreted protein expressed in the Spemann organizer, binds and inhibits Wnt-8. Cell *88*, 757-66.

Warga, R. M., and Kimmel, C. B. (1990). Cell movements during epiboly and gastrulation in zebrafish. Development *108*, 569-80.

Watabe, T., Kim, S., Candia, A., Rothbacher, U., Hashimoto, C., Inoue, K., and Cho, K. W. (1995). Molecular mechanisms of Spemann's organizer formation: conserved growth factor synergy between Xenopus and mouse. Genes Dev. *9*, 3038-50.

Weinstein, D. C., and Hemmati-Brivanlou, A. (1999). Neural induction. Annu. Rev. Cell Dev. Biol. *15*, 411-33.

Wilson, E. T., Cretekos, C. J., and Helde, K. A. (1995). Cell mixing during early epiboly in the zebrafish embryo. Dev. Genet. *17*, 6-15.

Wilson, P. A., and Hemmati-Brivanlou, A. (1995). Induction of epidermis and inhibition of neural fate by Bmp-4. Nature *376*, 331-3.

Wilson, P. A., Oster, G., and Keller, R. (1989). Cell rearrangement and segmentation in Xenopus; direct observation of cultured explants. Development *105*, 155-66.

Wilson, S. I., Graziano, E., Harland, R., Jessell, T. M., and Edlund, T. (2000). An early requirement for FGF signalling in the acquisition of neural cell fate in the chick embryo. Curr. Biol. *10*, 421-29.

Winnier, G., Blessing, M., Labosky, P. A., and Hogan, B. L. (1995). Bone morphogenetic protein-4 is required for mesoderm formation and patterning in the mouse. Genes Dev. *9*, 2105-16.

Wodarz, A. (1998). Mechanisms of Wnt signaling in development. Annu. Rev. Dev. Biol. *14*, 59-88.

Wolpert, L. (1998). Principle of Development, 1st edition. Current Biology, Ldt, London.

Woo, K., and Fraser, S. E. (1997). Specification of the zebrafish nervous system by nonaxial signals. Science *277*, 254-7.

Xu, Q., Alldus, G., Holder, N., and Wilkinson, D. G. (1995). Expression of truncated Sek-1 receptor tyrosine kinase disrupts the segmental restriction of gene expression in the Xenopus and zebrafish hindbrain. Development *121*, 4005-16.

Xu, Q., Holder, N., Patient, R., and Wilson, S. W. (1994). Spatially regulated expression of three receptor tyrosine kinase genes during gastrulation in the zebrafish. Development *120*, 287-99.

Xu, R. H., Kim, J., Taira, M., Zhan, S., Sredni, D., and Kung, H. F. (1995). A dominant negative bone morphogenetic protein 4 receptor causes neuralization in *Xenopus* ectoderm. Biochem. Biophys. Res. Commun. *212*, 212-9.

Yamada, T., Placzek, M., Tanaka, H., Dodd, J., and Jessell, T. M. (1991). Control of cell pattern in the developing nervous system: polarizing activity of the floor plate and notochord. Cell *64*, 635-47.

Yamanaka, Y., Mizuno, T., Sasai, Y., Kishi, M., Takeda, H., Kim, C. H., Hibi, M., and Hirano, T. (1998). A novel homeobox gene, dharma, can induce the organizer in a non-cell- autonomous manner. Genes Dev. *12*, 2345-53.

Yan, Y.-L., Hatta, K., Riggleman, B., and Postlethwait, J. H. (1995). Expression of a type II collagen gene in zebrafish embryonic axis. Dev. Dyn. *203*, 363-76.

Yatskievych, T. A., Pascoe, S., and Antin, P. B. (1999). Expression of the homeobox gene Hex during early stages of chick embryo development. Mech. Dev. *80*, 107-9.

Ye, W., Shimamura, K., Rubenstein, J. L., Hynes, M. A., and Rosenthal, A. (1998). FGF and Shh signals control dopaminergic and serotonergic cell fate in the anterior naural plate. Cell *93*, 755-66.

Yost, C., Torres, M., Miller, J. R., Huang, E., Kimelman, D., and Moon, R. T. (1996). The axis inducing activity, stability and subcellular distribuition of b-catenin is regulated in *Xenopus* by glycogen synthase kinase 3. Genes Dev. *10*, 1443-54.

Yuan, S., and Schoenwolf, G. C. (1998). De novo induction of the organizer and formation of the primitive streak in an experimental model of notochord reconstitution in avian embryos. Development *125*, 201-13.

Zhang, H., and Bradley, A. (1996). Mice deficient for BMP2 are nonviable and have defects in amnion/chorion and cardiac development. Development *122*, 2977-86.

Zhang, J., Houston, D. W., King, M. L., Payne, C., Wylie, C., and Heasman, J. (1998). The role of maternal VegT in establishing the primary germ layers in *Xenopus* embryos. Cell *94*, 515-24.

Zhou, X., Sasaki, H., Lowe, L., Hogan, B. L., and Kuehn, M. R. (1993). Nodal is a novel TGF-beta-like gene expressed in the mouse node during gastrulation, Nature *361*, 543-7.

Zimmerman, L. B., De Jesus-Escobar, J. M., and Harland, R. M. (1996). The Spemann organizer signal noggin binds and inactivates bone morphogenetic protein 4. Cell *86*, 599-606.

Zoltewicz, J. S., and Gerhart, J. C. (1997). The Spemann organizer of Xenopus is patterned along its anteroposterior axis at the earliest gastrula stage. Dev. Biol. *192*, 482-91.

Zorn, A. M., Butler, K., and Gurdon, J. B. (1999). Anterior endomesoderm specification in Xenopus by Wnt/beta-catenin and TGF-beta signalling pathways. Dev. Biol. *209*, 282-97.